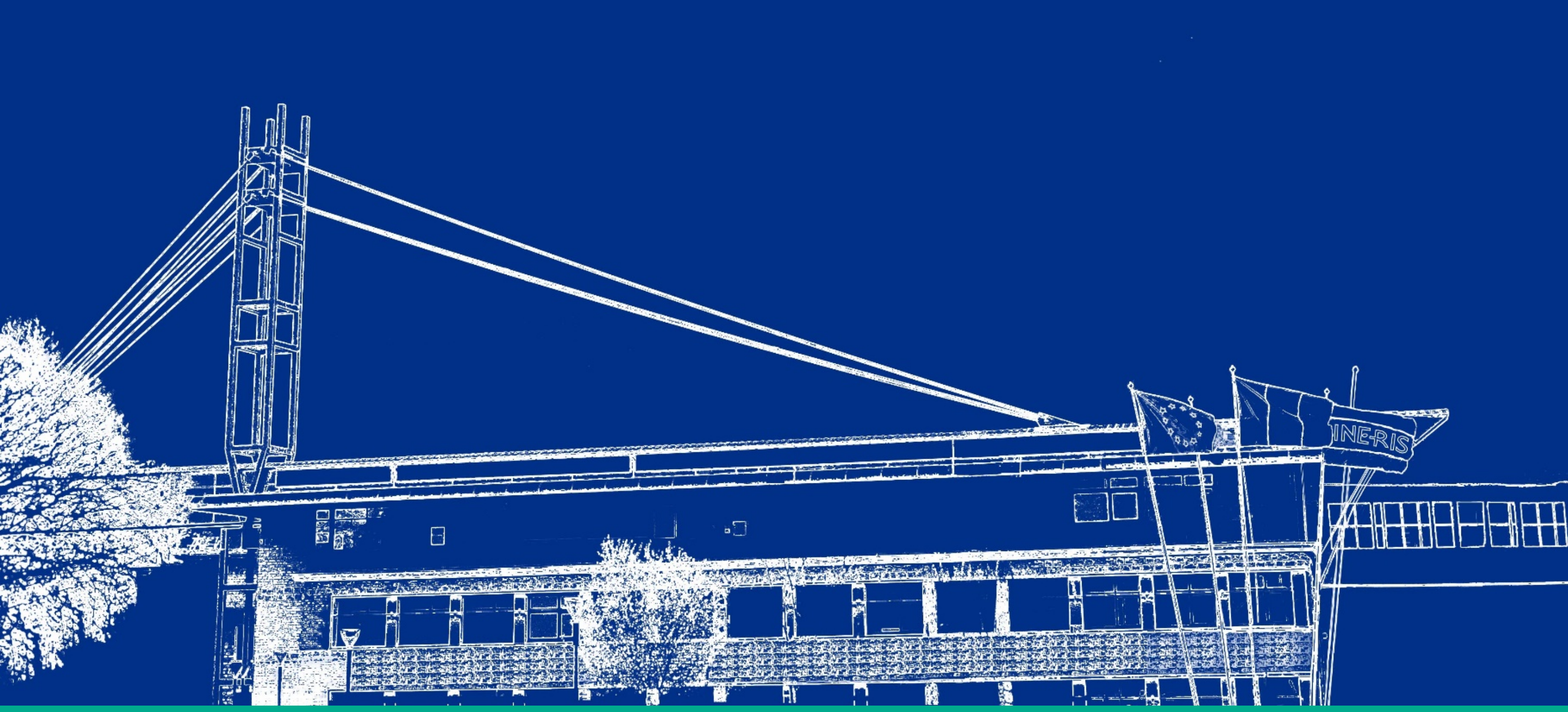

(ID Model = 454913)

Ineris - 204910 - 2727405 - v1.0

25/01/2022

Mine tailings dam failures: review and assessment of the phenomenon

maîtriser le risque
pour un développement durable

PREAMBLE

This document has been drafted for the purpose of supporting the public powers entrusted to Ineris, by virtue of the provisions of Article R131-36 of the Environmental Code.

Ineris shall not be liable, whether directly or indirectly, for any inaccuracies, omissions or errors or any similar occurrences relating to the information used.

The accuracy of this document must be determined on the basis of the objective knowledge available and, where appropriate, of the current regulations at the date of the drafting of the document. As a result, Ineris cannot be held responsible for any changes in these elements after this date. The mission shall not entail any obligation for Ineris to update this document after this date.

Given the missions incumbent upon it, Ineris is not a decision-maker. The opinions, advice, recommendations or equivalent that will be provided by Ineris as part of the missions entrusted to it are solely aimed at aiding the decision-making process. As a result, the responsibility of Ineris cannot replace that of the decision-maker that is therefore, notably, solely responsible for any interpretations made on the basis of this document. Any recipient of the document should use the results included therein in full, or otherwise objectively. Its use in the form of extracts or summary notes will be the sole and entire responsibility of the recipient. He/she will also be responsible for all other amendments made to it. Ineris declines all responsibility for any use of the document outside the purpose of the mission.

Name of the manager in charge of the report: Direction Sites et Territoires

Editor: FRANCK Christian

Verification: GOUZY AURELIEN

Approval: BIGARRE PASCAL - on (date) 25/01/2022

External proofreading: the author would like to thank Isabelle VUIDART, GEODERIS, and Yann GUNZBURGER, Georessources, for their invaluable proofreading of both content and form

Table of Contents

LIST OF FIGURES

LIST OF TABLES

LIST OF PHOTOGRAPHS

Summary

There are more than 20,000 mine tailings dams around the world, which contain tailings from ore exploitation, processing and washing. The failure of these structures is one of the most recorded and destructive ground movement phenomena, both in terms of the number of victims and the environmental impact generated. Since the beginning of the twentieth century, there have been more than one hundred and thirty cases of failure resulting in victims (nearly 2,800) and/or significant or even major pollution. More than fifty cases of failure have been recorded since the beginning of the twenty-first century.

Since the initial construction work, progress has been made in controlling this risk, particularly in the light of feedback from historical accidents. Nevertheless, many of these structures do not offer sufficient safety guarantees when exceptional or abnormal events (heavy rainfall, earthquakes) or structural or man-made failures (faulty design or construction, deterioration or failure of associated structures, inadequate monitoring) occur. However, the risk could be controlled when the mine is in operation and managed by an operator, in particular when best available techniques for design, construction, maintenance, monitoring and control are followed.

On the other hand, when the mine is closed and then abandoned, and returned to the natural environment, these structures remain and are likely to be affected by failures, the most destructive of which may, under certain conditions, generate a flow phenomenon that may impact the downstream part of the structure. Given the relatively recent date of construction of most mine tailings dams, feedback on their internal evolution until their potential failure after their operational period remains limited to date. Furthermore, the change in climate conditions in the future constitutes a host of factors which can increase the conditions of failure of the structure, whose environment can undergo a progressive anthropization increasing the risk.

This report is therefore part of the assessment of the ground movement hazard that may be generated by these dams. More specifically, the aim is to put forward the main principles and tools for assessing the flow-type phenomenon linked to their failure. It is based on feedback from recorded accidents, as well as on consultation of the bibliography and failure and propagation models relating to this subject.

A number of factors for assessing the phenomenon and simple models are put forward, which aim to support the assessment work on a specific site. The document reflects that the assessment of the intensity of the phenomenon is not easy to determine, as it combines multiple factors relating to the tailings, their water content, the rheology of the phenomenon and the morphology of the terrain downstream. A site with a potentially high hazard with the issues outlined should be subject to specific investigations to further assess the phenomenon.

On the other hand, when the mine is closed and then abandoned, returned to the natural environment, these structures remain and are likely to be affected by ruptures, the most destructive of them causing, under certain conditions, a mud flow phenomenon that can impact downstream of the dam. But, due to quite recent construction date of most tailings dams, experience feedback on their internal evolution until their potential failure after their operational period remains limited to this day. The evolution of climatic conditions in the future constitutes a sum of factors that may increase the failure conditions of the dam, the environment of which may be subjected to progressive anthropization, increasing the risk.

This report deals with the evaluation of the hazard of ground movement that these dams can generate. It particularly proposes main principles and tools for evaluating the flow-type phenomenon which can be associated to their failure. It is based on this experience feedback from the identified accidentology, as well as a consultation of the bibliography and models of failure and propagation relating to this subject.

A number of criteria to assess the phenomenon, and simple models, are proposed, the objective of which is to accompany the assessment work on a specific dam site. The document shows in particular that the evaluation of the intensity of the phenomenon is not easy to determine, because it combines multiple factors relating to the residues, their water content, the rheology of the phenomenon and the morphology of the ground downstream. A dam site presenting a potentially high hazard with exposed stakes must be the subject of specific investigations in order to complete the assessment of the phenomenon.

To cite this document, use the link provided hereinafter:

French National Institute for Industrial Environment and Risks, , Verneuil-en-Halatte : Ineris - 204910 - v1.0, 25/01/2022.

Key words: Accident, hazard, dam, flow, mine, phenomenon, mine tailings, slope stability

1 Introduction and challenge

There are more than 20,000 mine tailings dams around the world, which delineate deposits of tailings from the washing, processing and exploitation of ore.

The failure of these structures is one of the most recorded and destructive ground movement phenomena, both in terms of the number of victims and the environmental impact generated. Since the beginning of the twentieth century, there have been more than 130 cases of failures resulting in casualties (nearly 2,800 in total) and/or significant environmental impacts. More than fifty cases of failure have been recorded since the beginning of the twenty-first century.

Figure 1: Merriespruit disaster, Harmony, South Africa, 1994, (ICME,[53])

Relative to the number of structures built, the number of mine tailings dam failures has tended to decrease over time (Bowker and Chambers, 2015, reported in UNEP [98]), but major failures in terms of severity have increased, with this trend continuing for several decades (Figure 2).

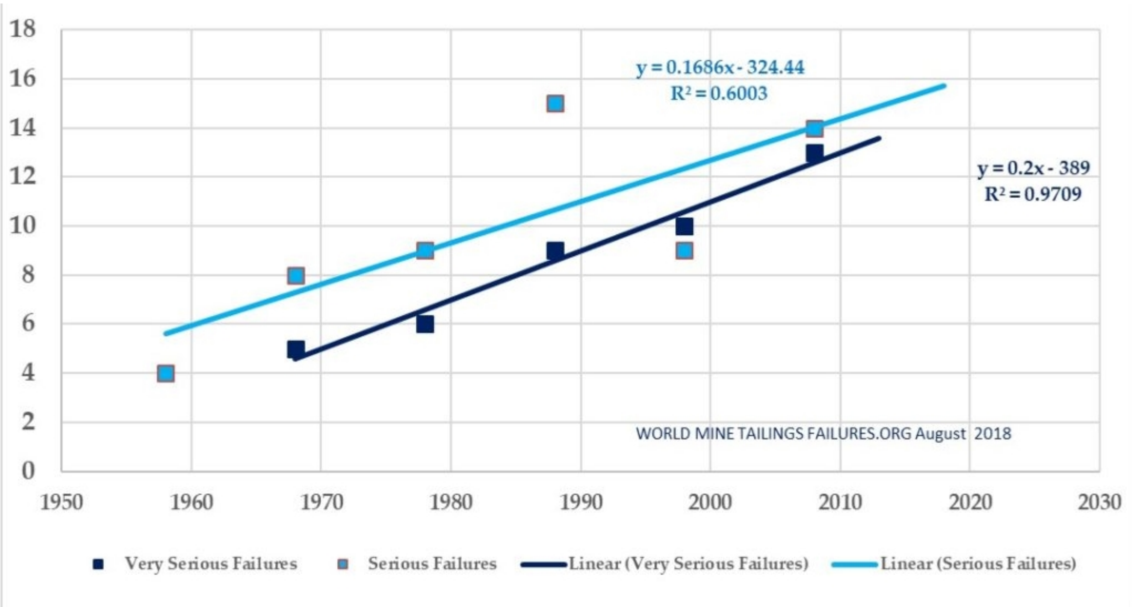

Figure 2: Evolution of the number of "serious" (light blue) and "very serious" (dark blue) cases of failure, between 1958 and 2017, according to www.https://worldminetailingsfailures.org/,[105]

Since the initial construction work, progress has been made in controlling this risk, particularly in the light of feedback from historical events. Nevertheless, as the recent Brumadinho disaster in Brazil on 25 January 2019 (270 dead and missing) reminds us, many of these structures do not offer sufficient safety guarantees when exceptional or abnormal events (heavy rainfall, earthquakes) occur or when structural or human failures (faulty design or construction, deterioration or failure of related structures, inadequate monitoring) are involved.

However, the risk could be better controlled when the mine is in operation and managed by an operator, in particular when best available techniques for design, construction, maintenance, monitoring and control are followed.

On the other hand, when the mine is closed and then abandoned, and returned to the natural environment, these structures remain and are likely to be affected by failures, the most destructive of which may, under certain conditions, generate a flow phenomenon that may impact the downstream part of the structure. Given the relatively recent date of construction of most mine tailings dams, feedback on their potential failure after their operational period remains limited to date.

This report is part of the assessment of the flow-type hazard that can be generated by former dams. Following on from the mining hazard assessment guide drawn up by Ineris in 2018 [49], which dealt succinctly with this type of ground movement, the aim is more specifically to recommend the main principles and tools for assessing the flow-type phenomenon associated with the failure of these structures.

It is based on feedback from the accidents recorded, both in terms of causes and consequences, as well as on consultation of the literature on the subject[1].

This document presents the geotechnical aspects relating to this phenomenon. The chapter on the ecological impact was the subject of a specific documentary research report drawn up by Ineris [51].

[1]The numbers refer to the bibliographic references consulted or quoted, detailed in chapter 10

2 Some concepts and definitions used in the report

Dam: a dam is a structure designed to temporarily or permanently hold back a greater or lesser quantity of water for different uses (hydroelectric power generation; drinking water supply; irrigation; regulation of river flows; tourist activities, etc.). The structures are most often built across a river, but some of them are built outside the major river bed and fed by diverting part of the flow of nearby rivers; this is the case of hill dams and dams forming part of pumping stations (STEP) (source www.ecologie-solidaire.gouv.fr).

Mine tailings dam: This term will be used in this report to refer to any man-made structure that retains at least a mixture of mine tailings and water. The term ***dyke*** is very often used by mine operators and even in regulatory texts (Directive 2006/21/EC, Order of 19 April 2010). However, it should be noted that dams are intended to retain effluents and are very often located across a watercourse. Some dams can retain mine waste rock and not tailings (see below). Dykes do not have a retention function but are intended to prevent effluent from overflowing the river bed and are therefore longitudinal to the river in most cases.

Pond: in the context of the issue covered by this report, a natural or constructed site designed to receive fine-grained waste, normally tailings, and variable quantities of free water from the treatment of mining resources, as well as from the purification and recycling of process water (text taken from Directive 2006/21/EC [29]).

Flow: a ground movement where the material constituting a slope is completely unstructured and re-mobilised due to the strong presence of water. It is then transformed into a more or less viscous fluid that flows at a generally high speed. This flow is sometimes made up of blocks of material and various debris that have been swept away or torn off.

Extraction waste: as defined in Directive 2006/21/EC [29], all waste resulting from the prospecting, extraction, processing and storage of resources exploited by mines and quarries. Mine tailings fall into this category.

Mine tailings: This term refers to the solid or sludgy wastes remaining after the treatment of minerals by separation processes (e.g. crushing, grinding, screening, flotation and other physico-chemical techniques) to extract valuable minerals from the rock.

Mining waste: This term refers to a mixture of loose rock from mining operations, which is considered to be of no economic value to the operator (lack of or insufficient ore content) and therefore not processed and deposited. The English term "waste" or "waste rock" is often used.

3 Regulatory framework in Europe and France

Each country has its own regulations governing mining and extractive industries in terms of mine tailings dam safety. Changes in regulations are based in particular on local or international knowledge and feedback. The International Commission on Large Dams (ICOLD)[2] is an international non-governmental organisation that promotes the exchange of knowledge and experience in the field of dam engineering.

As international regulations are extensive, we have limited ourselves here to referring to the main texts in Europe and in France concerning the subject of mine tailings dams.

The ***European Decision 2000/532/EC of 3 May 2000*** [26] establishes the list of wastes, including those classified as hazardous. In French law, this list is defined and appears in articles ***R541-7 and R541-8 of the Environmental Code.*** Category 1 includes "wastes from the exploration and exploitation of mines and quarries and from the physical and chemical processing of minerals", including waste from extraction and waste rock. In particular, acid-generating waste rock from or leading to the conversion of sulphide, waste rock containing dangerous substances, and waste containing dangerous substances from the physical and chemical processing of minerals, whether or not they are metalliferous, are classified as hazardous in all cases. Other wastes may be classified as hazardous if they possess at least one of the fifteen properties[3] set out in Regulation EU1357/2014, replacing Annex III of Directive 2008/98/EC.

The ***European Directive 2006/21/EC of 15 March 2006*** [29] concerns the management of waste from the extractive industries. It applies to so-called "extractive waste" resulting from "*the prospecting, extraction, treatment and storage of mineral resources and the working of quarries*" (Article 2), and "*aims to prevent or reduce, as far as possible, adverse effects on the environment, in particular on water, air, soil, fauna and flora, and the landscape, as well as risks to human health arising from the management of waste from extractive industries*" (Article 1).

Article 5 of the Directive requires Member States to ensure that the operator draws up a waste management plan (WMP). Among the objectives is to "*take into account, during the design phase, the management during operation and after closure of the waste facility, by choosing a design which:*

i. requires minimal and, if possible, ultimately no monitoring, control or management of the closed waste facility, ...,

iii. ensures the long-term geotechnical stability of dykes or slag heaps rising above the pre-existing ground surface."

Annex III defines a category A waste which, in addition to the hazard classification of the waste, substance or preparation, includes the condition that "*a failure or malfunction, such as the collapse of a heap or the breach of a dyke, could lead to a major accident, based on a risk assessment taking into account factors such as the current or future size, location and environmental impact of the facility*".

Therefore the concepts of dyke stability and dyke failure appear explicitly in the European Directive.

For this category A, Article 5 requires the operator to "*document that a major-accident prevention policy, a safety management system to implement it and an internal emergency plan will be put in place*".

This WMP is "*reviewed/amended every five years, if necessary, in the event of substantial changes in the operation of the installation or the waste deposited*".

Article 6 is dedicated to "major accident prevention and information". Member States must ensure that major-accident hazards are identified and that the necessary measures are taken from the design stage through to post-closure monitoring of the waste facility. The operator must define a major-accident prevention policy, put in place a safety management system and an internal

---

[2] Or CIGB (Commission Internationale des Grands Barrages) in French

[3] HP1 "Explosive", HP2 "Oxidising", HP3 "Flammable", HP4 "Irritant", HP5 "Specific target organ toxicity (STOT)/aspiration toxicity", HP6 "Acute toxicity", HP7 "Carcinogenic", HP8 "Corrosive", HP9 "Infectious", HP10 "Reproductive toxicity", HP11 "Mutagenic HP12 "Release of acutely toxic gas", HP13 "Sensitising", HP14 "Ecotoxic", HP15 "Waste capable of exhibiting any of the above hazardous properties not directly exhibited by the original waste"

emergency plan in the event of an accident. The competent authority shall draw up an external emergency plan for off-site measures in the event of an accident.

In 2018, in relation to this directive, the European Commission established a reference report on Best Available Techniques (BAT) for the management of waste from the extractive industries [32].

Decree no. 2010-369 of 13 April 2010 amending the nomenclature of classified installations [27] introduces, as part of the transposition of European Directive 2006/21/EC, the heading 2720 "*Installation for the storage of waste resulting from the prospecting, extraction, treatment and storage of mineral resources and from the operation of quarries (site chosen to accumulate or deposit solid, liquid, dissolved or suspended waste)*". Hazardous waste storage facilities, or non-hazardous non-inert waste storage facilities, are subject to authorisation[4].

The ***Order of 19 April 2010*** [8]on the management of waste from the extractive industries sets out, in accordance with the requirements of European Directive 2006/21/EC, the general requirements applicable to installations under heading 2720 of the nomenclature of classified installations. In particular, it includes the provisions relating to the definition and classification of the different types of waste, and the implementation of a WMP.

The provisions of this decree concern "*installations consisting of a dyke or a retaining or confining structure or any other useful structure, slag heaps, stockpiles and ponds, slopes, all waste rock storage and, more generally, extraction waste, as well as excavation holes in which the waste is put back, after extraction of the mineral, for the purposes of restoration and construction*" (Article 1).

The Order stipulates in Article 5 that the WMP shall include, among other things, in relation to this topic, "*a description of the technical measures ... and the relevant organisational and management measures to reduce the probability and effects of the hazardous phenomena ... and to act on their kinetics*", "*a study of the condition of the land likely to be damaged by the waste management facility*", the control and monitoring procedures throughout the life of the facility and after closure/restoration.

The Order defines in its Annex VII a category A of waste management facility, whose short or long term effects of a failure (loss of structural integrity, operational or functional failure) may lead to *a/ serious consequences on natural persons b/ serious damage to human health and the environment.* Three classification criteria are adopted by the Order: *the level of risk of loss of integrity of the storage facilities, the quantity of hazardous waste in the storage facilities, the quantity of hazardous substances and preparations present in the tailings ponds.*

In article 7, the operator must, in the case of a category A facility, define a major risk prevention policy and the resources dedicated to its management and present a summary of the safety management system that he intends to apply, annexed to the WMP.

The internal operation plan stipulated in Article 9 is the transcription of the internal emergency plan of the European Directive. It is annexed to the WMP and updated at each of its revisions.

Annex VI of the order details the resources and objectives of the safety management system.

Annex VII, in point 3 relating to the assessment of the risk of loss of integrity of storage facilities, stipulates that, in the event of loss of integrity of the tailings ponds, "***human lives are considered to be at risk when the water or sludge levels are at least seventy centimetres above the ground or when the velocity of the water or sludge exceeds 50 centimetres/second***".

Decree no. 2010-1394 of 12 November 2010 on the requirements applicable to certain mining operations and to facilities for the management of ***inert waste*** and ***unpolluted soil*** resulting from their operation sets out the minimum technical requirements to be met by the extractive industries in order to limit the impact of their waste on the environment and to comply with the requirements of Directive 2006-21 of 15 March 2006.

---

[4]The scope of this heading does not include storage facilities for inert extraction waste or unpolluted soil resulting from the exploration, extraction, treatment and storage of mineral resources or quarries, as these facilities are managed by connection via the mining code for mines, or regulated by heading 2510 for the storage of inert waste and unpolluted soil resulting from the working of quarries

4 Different types of mine tailings dams

4.1 Geometry and construction methods

The construction of mine tailings dams is largely dependent on the topographical constraints of the extraction site or the mining process. There are several configurations (ICOLD[5], [41]):

- across a valley. Most of the major dams are in this configuration;
- on a hillside;
- at the top of a hill (the dam does not stretch around the whole perimeter);
- at the top in a stacked configuration (the dam stretches all around).

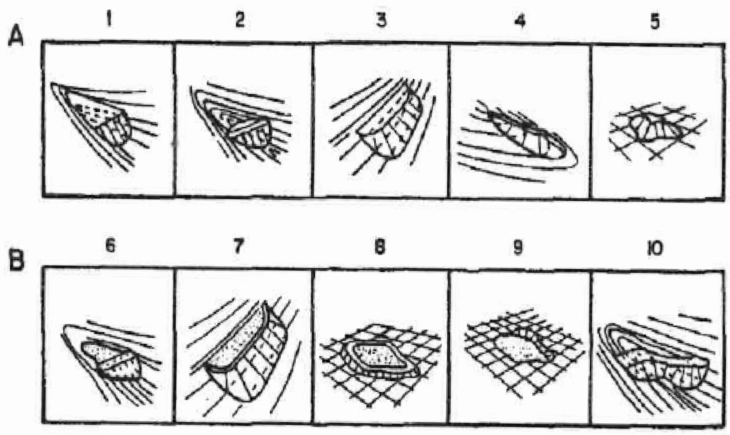

Fig. 1-1

Types de remblais de résidus miniers.

(A) Type de décharge des matériaux de rebuts miniers.
(B) Type de retenue.

(1) Remblai de comblement en val.
(2) Remblai en travers de val.
(3) A flanc de coteau.
(4) Sur sommet.
(5) Empilement

(6) Remblai en travers de val
(7) A flanc de coteau.
(8) Entouré d'une digue simple.
(9) Incisé.
(10) Système complexe : en travers de val A flanc de coteau.

Types of refuse disposal structures.

(A) Type of dump.
(B) Type of impoundment.

(1) Valley-fill
(2) Cross-valley.
(3) Side-hill.
(4) Ridge.
(5) Pile.

(6) Cross-valley
(7) Side-hill.
(8) Diked.
(9) Incised.
(10) Complex : cross-valley, side-hill.

Figure 3: Different dam configurations or layouts (ICOLD, [41])

[5] International Commission On Large Dams

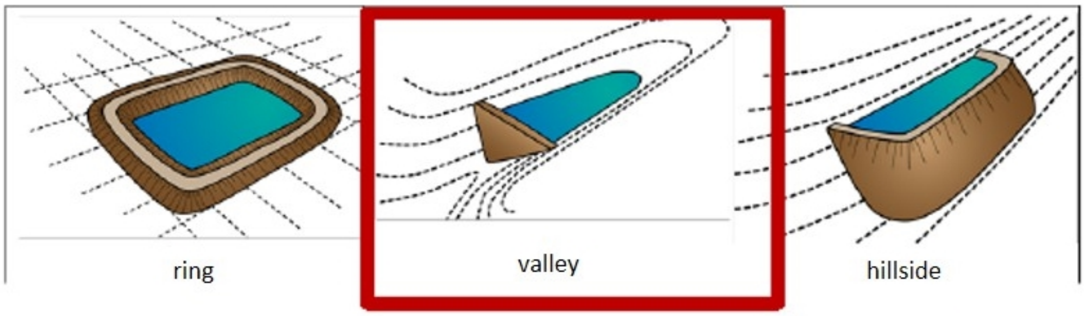

Figure 4: The main dam layouts.
The valley layout is the most widely used

There are four main methods of construction and raising: the upstream method, the downstream method, the central method and the conventional method.

For the first three methods, the mine tailings can be reused for part of the structure. The material is then processed by cycloning, separating the sandy fraction, which is used for dam construction, and the sludge, which is discharged into the impoundment (ICOLD, [42]).

The ***upstream method*** is by far the most widely used. It consists first of all of the construction of a low basal starter embankment. The mine tailings are then removed either by 'spigoting' (progressive percolation of the tailings from orifices in the lower part of the adduction pipes) or from the crest of the starter embankment or the raised embankments. During mining, the dam is raised using material taken from nearby tailings (where the sand fraction is high) and/or waste rock and resting on the surface of the lower-layer tailings, and this cycle is repeated, with the embankments and the axis of the structure moving upstream (ICOLD, [42], Spence, [95]).

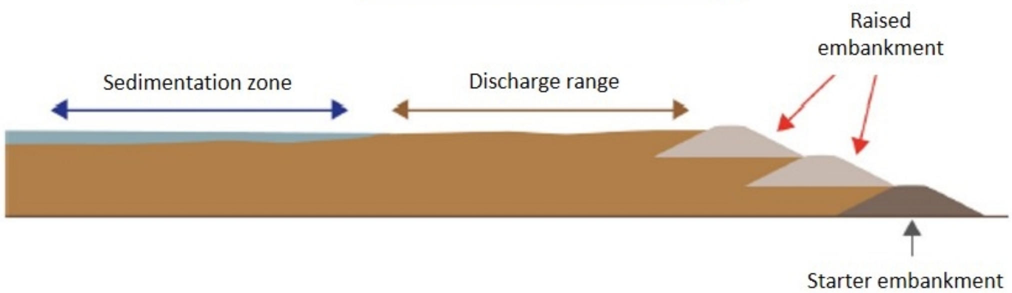

Figure 5: Schematic cross-section of an industrial retention structure built using the upstream method, with a discharge area (after Vick, [100]).

Prior to the 1980s, virtually all mine tailings dams were constructed using this method (ICOLD, [42]). Taking the example of China, where there are more than 12,000 mine tailings dams, 95% of them are constructed using this method (Yin et al., [109]). These dams are indeed the most economical, as the tailings are reused to build them, the input of other materials (local or imported rock, backfill, mine waste rock, ...) is limited, and the volumes required for raising are small. In addition, they allow for rapid operation, as the tailings can be dumped next to them as soon as the starter embankment is created.

Such dams have been used successfully in dry and arid climates where a minimum amount of water is stored in the dam. These methods have also been used successfully when careful spigoting combined with effective drainage is carried out in wetter climates (ICOLD, [42]).

Feedback shows that the stability of this type of dam is inversely proportional to its height (ICOLD, [41]), as the height increases, so do the potential areas of weakness (Jeyapalan et al., [56]).

This method is also the most prone to failure due to the raising and lack of groundwater drainage within the tailings, or due to excessive permeability of the dykes which can lead to low-compacted dams failing, or due to liquefaction of saturated materials (ICOLD, [42]). It is recommended that this type of dam not be built at speeds greater than 5-10 m per year to allow time for interstitial pressures to dissipate (Spence, [95]).

Finally, this method is not recommended in seismic regions and has been banned in Chile and Peru since the 1990s (in Agurto-Detzel et al., [1]).

The so-called ***'semi-aerial' method*** is a variable of the upstream method, with the placement of waste rock in thin layers (10 to 15 cm, in Ginige, [36]) and by spigotage (ICOLD, [42]).

The ***downstream method*** consists of building a dam in the downstream direction from the starter embankment. The dam is therefore built on carefully prepared and compacted material, compared to the upstream method where the dam is built progressively on the tailings. The construction of impermeable cores and drainage systems provides greater control of the water table in the structure (Spence, [95]). This is one of the most common methods used in areas of high seismic risk (ICOLD, [42]).

The disadvantage is mainly economic, as much larger volumes of material are used to build the dam. Caldwell and Smith, 1985, calculated the cost to be 9 to 16 times higher than the upstream method (in Halmann et al., [37]).

The ***central or centreline method*** involves building a starter embankment and raising the structure along a vertical axis, with the embankment dumped both upstream and on the outside (ICOLD, [41]) - variant 1 of Figure 6, or more on the outside to use less material (Spence, [95]) - variant 2 of Figure 6. The latter method is a compromise between the two previous methods, between controlling stability and moisture content, and the volume of material to be used.

The ***conventional method*** is not to use tailings, but to place borrow material, or waste rock, of better geo-mechanical quality. This method is sometimes used when the tailings are very fine and their rate of rise is not compatible with the three previous construction methods. In this case, the dam can be built in advance to the required height (ICOLD, [41]).

Regardless of the methods chosen, a so-called starter embankment is constructed as a starting point for the construction of the final dam. This starter embankment can be watertight if the upstream method is used, or draining if the downstream method is used.

4.2 Other classifications

Many classifications exist, including storage (volume of effluent retained) and height of the dam.

Table 1: Dam size classification, from US Army Corps of Engineers, taken from ICOLD, [41]. Values are transformed and rounded in the metric system

Name	Pond capacity (m^3)	Height (m)
Small	Between 60,000 and 1.2M	Between 7 and 12
Average	Between 1.2M and 62M	Between 12 and 30
Large	Over 62M	Over 30

Regarding the height of the building, Mei [75] identified 26 dams in China with a height of more than 100 m and 10 dams with a storage capacity of more than 100 million cubic metres. In China, 80% of the deposits are with dams less than 30m high (Mei [75], Ju et al., [60]).

There are also rankings for potential danger (loss of life and economic loss, according to the US Army Corps of Engineers (ICOLD, [41]).

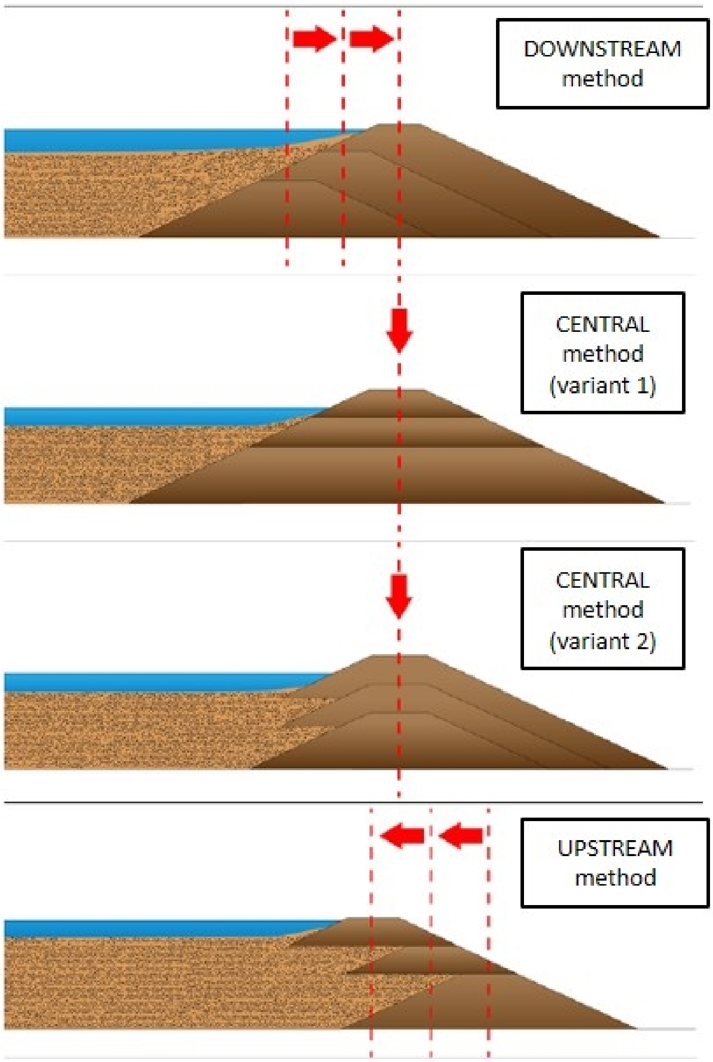

Figure 6: The different methods for raising mine dams

4.3 Nature and characteristics of dam and tailings materials

Dams are mostly made up of mine waste rock, the composition of which varies according to the substance extracted and its geology. For example, coal mine waste rock has a shale and sandstone component, polymetallic mines have sulphide-rich materials, gold mine materials depend on the method of extraction (alluvial or in the rock mass) but can also be sulphide-rich (ICOLD, [41]).

The materials used have, due to their intrinsic stability and dam effluent retention function, a wide range of grain sizes, from clays and silts to stones and even boulders. Generally speaking, the conditions of layer deposition lead to horizontal permeability that is ten to one hundred times greater than the vertical permeability. The angle of friction of waste rock deposits varies according to the nature of the structure: between 22° and 32° for coal mines, between 30° and 36° for other mines (ICOLD, [41]).

In chapter 4.1 we saw that dams can be partly made of mine tailings (especially their sandy fraction).

The ***mine tailings*** retained by the dams are generally predominantly sandy-silty and are placed, generally in the form of sludge, by hydraulic gravity or forced hydro-cycloning[6] (Lucia et al., [66]). The sludge is discharged into the storage area, where the solid particles settle in suspension, and

[6]Process that uses centrifugal force to separate heavier-than-water particles

the fluid is conveyed to a storage tank, where it is usually returned to the treatment plant (Ginige, [36]). The particles are angular and elongated, due to the different processes, including the crushing of the rock (Spence, [95], Kossoff et al., [61]).

The size of the grains is very variable, but we can note the predominance of sands, then silts, to the detriment of coarser elements (gravels) or fine elements (clays) (Sarsby, [125], cited in Kossoff et al., [61]).

Depending on the sedimentation conditions of these tailings, there may or may not be segregation by grain size, with heavier grains settling faster and therefore further upstream than finer grains.

Within tailings, there is an increase in density with depth, due to compaction, water loss and chemical diagenesis of the material (Sarsby, 2000 [125], cited in Kossoff et al. [61]).

Table 2: Main characteristics of tailings according to their origin (Vick, 1983, in Spence, [95]).

Category	General character
Soft-rock tailings	
Fine coal refuse Trona insols Potash	Contain both sand and slime fractions, but slimes may dominate overall properties because of presence of clay.
Hard-rock tailings	
Lead-zinc Copper Gold-silver Molybdenum Nickel (sulphide)	May contain both sand and slime fractions, but slimes are usually of low plasticity to nonplastic. Sands usually control overall properties for engineering purposes.
Fine tailings	
Phosphatic clays Bauxite red muds Fine taconite tailings Slimes from tar sands tailings	Sand fraction generally small or absent. Behaviour of material, particularly sedimentation-consolidation characteristics, dominated by silt or clay sized particles and may pose disposal volume problems.
Coarse tailings	
Tar sands tailings Uranium tailings Gypsum tailings Coarse taconite tailings Phosphate sand	Contain either principally sands or nonplastic silt sized particles exhibiting sand-like behaviour and generally favourable engineering characteristics.

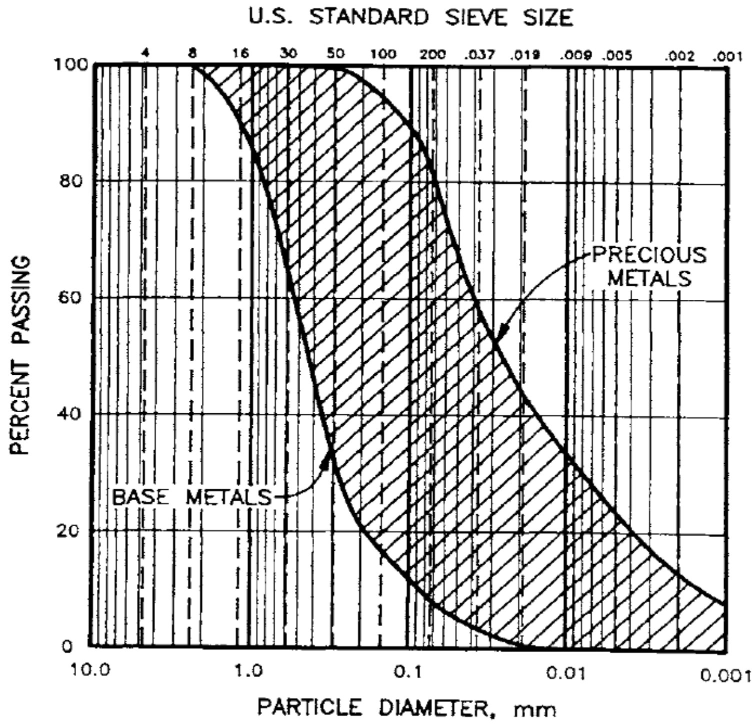

Figure 7: Tailings size distribution (Hallman et al., [37])

Ozcan et al, [81], present the tailings size distribution of the Lahanos copper-zinc mine in Turkey, and compare it to other mines.

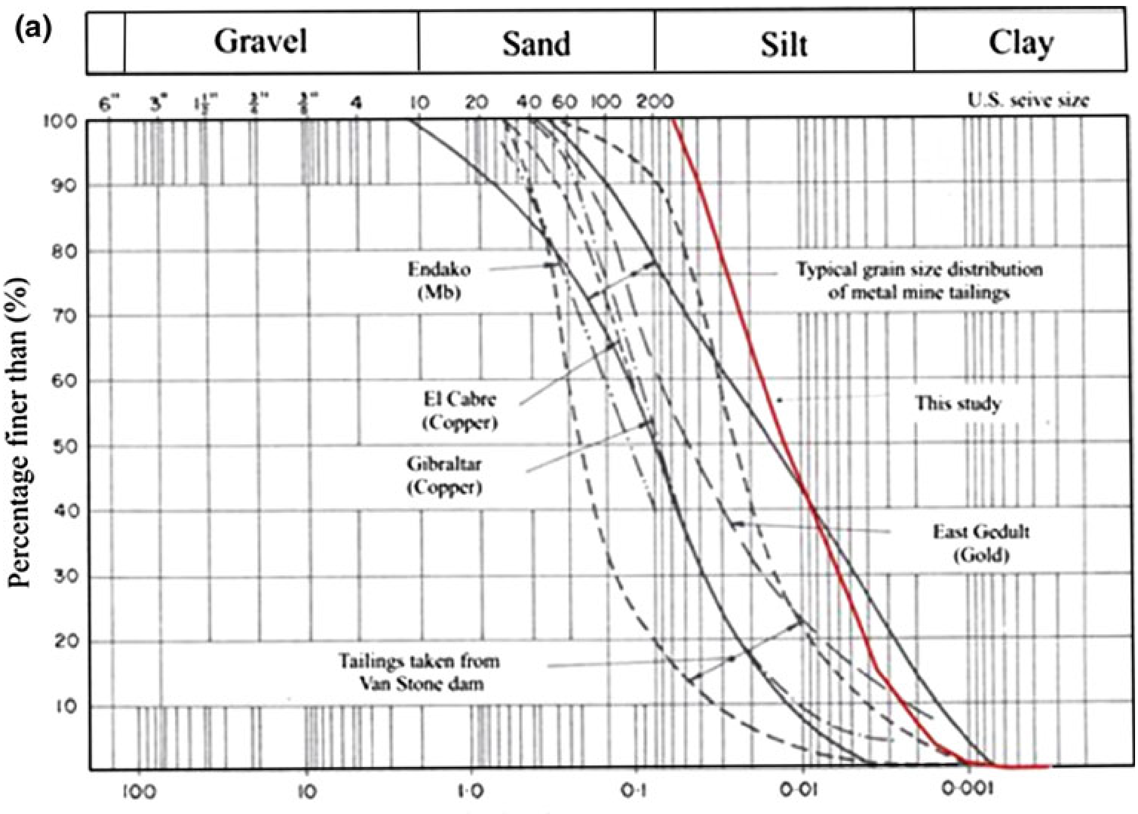

Figure 8: Comparison of size classes of Lahanos mine tailings (red) and those of other mines (Ozcan et al., [81] and CANMET, [114])

Phosphate mine tailings are known to contain a much higher clay fraction, or even greater than the silt-sand component (Lucia et al., [66]).

Table 3 lists the characteristics of tailings found in the literature, both in general and by mined substance.

4.4 Stage of life

ICOLD (1989, [42]) suggests three distinct successive periods:

- the operational phase, where the operator ensures the safety of the building and meets the requirements of the supervisory authorities
- the so-called "restructuring" phase, after operation, according to procedures and facilitation work subject to the approval of the supervisory authorities. During this phase, the characteristics of the materials, tailings and associated effluents evolve, reaching a certain condition of mechanical and even physico-chemical equilibrium;
- the long-term phase, which depends on the duration of chemical reactions in the rock waste mass and in the effluents. This period can be very long, in some cases several hundred years.

Table 3: Elements for characterising mine tailings, taken from the literature

Mines	Grain size	Dry density (kN/m³)	Void index	Degree of saturation (%)	Plasticity: Atterberg limits	Compressibility	Effective cohesion (kPa)	Angle of friction (°)	Permeability (m/s)
General [37]	See Figure 7		0.6-1.0 1.0-1.6 for very fine material in some mines						1. 10^{-5} for sandy-silt material
General [75]		19 for coarse sands, 20 for fine sands, 19.5 for silty sands, 14.6 for clayey materials					11 for coarse sands, 9.8 for fine sands, 10.8 for silty sands, 13.7 for clayey materials	32 for coarse sands, 29 for fine sands, 28 for silty sands, 26 for clayey materials	Vertical permeability: 6.4. 10^{-3} for coarse sands, 4.2. 10^{-3} for fine sands, 9.5. 10^{-4} for silty sands, 1.6. 10^{-5} for clayey materials
Copper, Chile [103]		17.5-20.1 (average)							
Copper, China [109]	D20: 0.018-D80: 0,125	19-20			W_P [13.8-15.7], W_L [21.3-23.6], I_p [7.5-7.9]		6,5-11	28-31	Vertical permeability: 1,26.10^{-4} for coarse sands, 3,3.10^{-6} for the finest materials
Copper, lead, zinc, Greece [65]	39-60% sand, 31-53% silt, 8-9% clay	17-17,7				Compression index [0.032-0.080] Initial void index [0.522-0.57]	72-90	28-31	
Copper-zinc, Turkey [81]	D20: 0.004-D80: 0.03				W_P [9.3-10.3], W_L [12.3-14.6], I_p [2.9-4.3]		5	35	
Fluorine, France [14]	Large fraction [0.1-0.4 mm]. CU = 5	15-18.1						32-37	1.10^{-6} - 1.10^{-5}
Graphite, Chine [39]		15.9-17.0	0.71-1.87				0.3-5.1	7 (silty sludge) -35	
Gold, China		13.9-19.5	0.57-1.16				0	31.8	9.10^{-6}
Gold, France [14]	90% <0.21mm, 70% <0.1mm								
Gold, Zimbabwe [93]		13-16	0.63-1.05						
Phosphorus, China [70]: characteristics of phosphogypsum		16					0.3	30	5,6.10^{-6}
Lead zinc, France [14], data from three sites	67% <0.04mm, 84% <0.08mm 38% <0.04mm, D50 = 0.08mm	14.5							1.10^{-6} - 1.10^{-5}
Lead zinc, Italy [76]		16.9-18.4	0.61-1.09	86-100	W_P [139-17.3], W_L [17.2-25.2], I_p [2.1-8.0]	Compression index [0.058-0.225] Consolidation coefficient [3.2.10^{-2}-6.9.10^{-3}]cm²/s	5-28	33-37	
Tungsten, France [14]		16.4-21.3						40-45	
Zinc, France [14]		15.4						34-37	1.10^{-6}

5 Feedback on mine tailings dam failures and their consequences

5.1 Some statistics on the failure of embankment dams

There is a multitude of hydraulic dams in the world known as "embankment dams", i.e. made of loose materials, which can be fine to very coarse (riprap). This family of structures includes several categories according to their function, the type of material used and the method used to ensure watertightness (homogeneous dams, impermeable core dams, watertight central wall dams, upstream mask dams, etc.).

As mine tailings dams are also made of loose materials (i.e. tailings and mine waste rock and/or local borrow materials), it is useful to acquire some statistical information on the disturbances observed or recorded on this type of structure.

Davies, 2001 [24], indicates that in the last thirty years, two to five 'major' failures per year are recorded on embankment dams. In relation to the number of dams recorded at that time, this leads to a statistical probability of failure of 1/1750 to 1/700, which is comparable to the 1/10000 probability of so-called conventional dams.

The ICOLD set out statistics in its 1983 report [52]. From 107 identified dam failures, the following details were extracted:

- 77% of dam failures affect embankment structures;
- 89% of embankment dam failures are related to earthen structures, 11% to rockfill structures;
- 33% of embankment dam failures are related to the body of the structure, 9% to its foundation, 11% to both the foundation and the body. 47% of failures are related to associated structures.

The four most frequent causes of failure of embankment dams (several causes can be listed for a failure), linked to a failure of the body and/or the foundation, are, in decreasing order, internal erosion, percolation, differential movements and failure of the embankment/dam connections.

The highest percentage of failures is found for structures between 15m and 30m in height (Figure 9). Furthermore, these failures are mostly observed during the filling phase and after five years of life (Figure 10).

The United States Department of the Interior Geological Survey, in 1985 (Costa, [23]), reported, for embankment dam failures, causes related to internal erosion for 38% of cases, overflow for 35%, and foundation problems for 21% of cases. These last disturbances appeared less than ten years after the construction of the dam, the other causes are spread over a longer period of time. Between 1963-1983, in the United States, dams less than 15 m high accounted for 90% of the disasters, partly linked, according to the author, to the lack of monitoring and alarm systems.

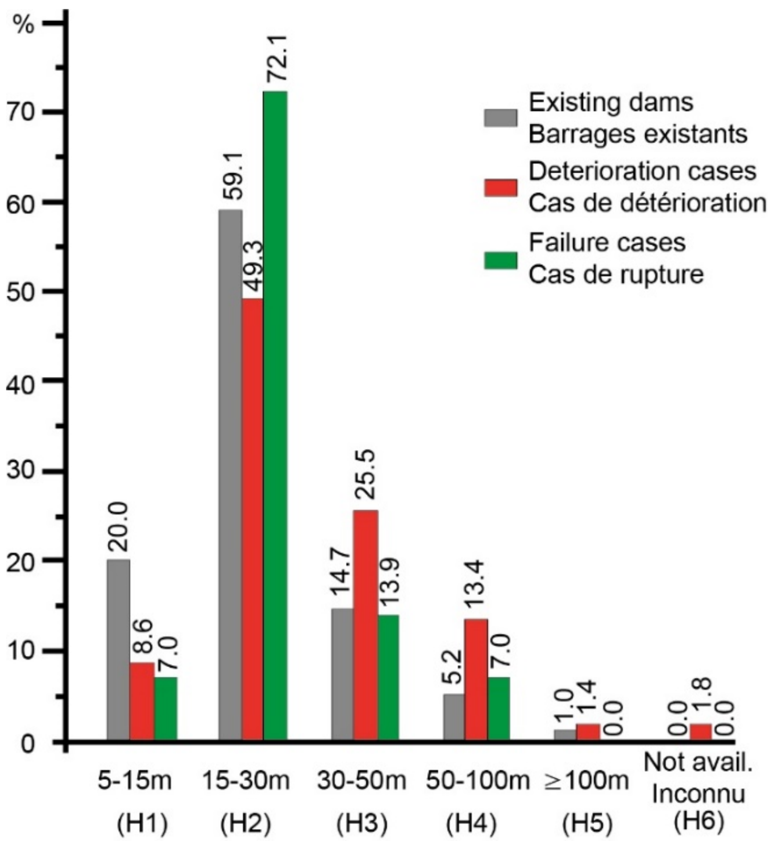

Figure 9: Percentage distribution of deterioration and failure cases affecting the foundation and/or the body of the dam according to the height of the structure (according to ICOLD, [52])

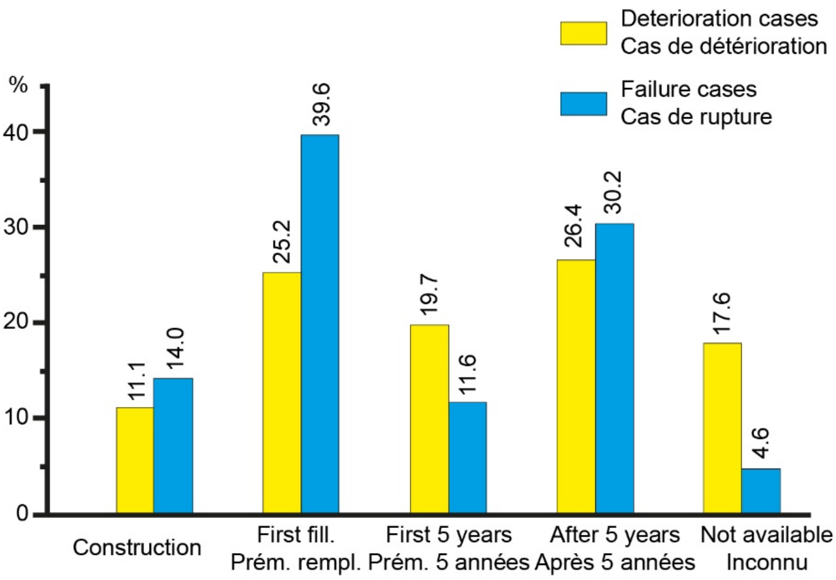

Figure 10: Percentage distribution of cases of deterioration and failure affecting the foundation and/or the body of the dam according to the life stage of the structure (from ICOLD, [52])

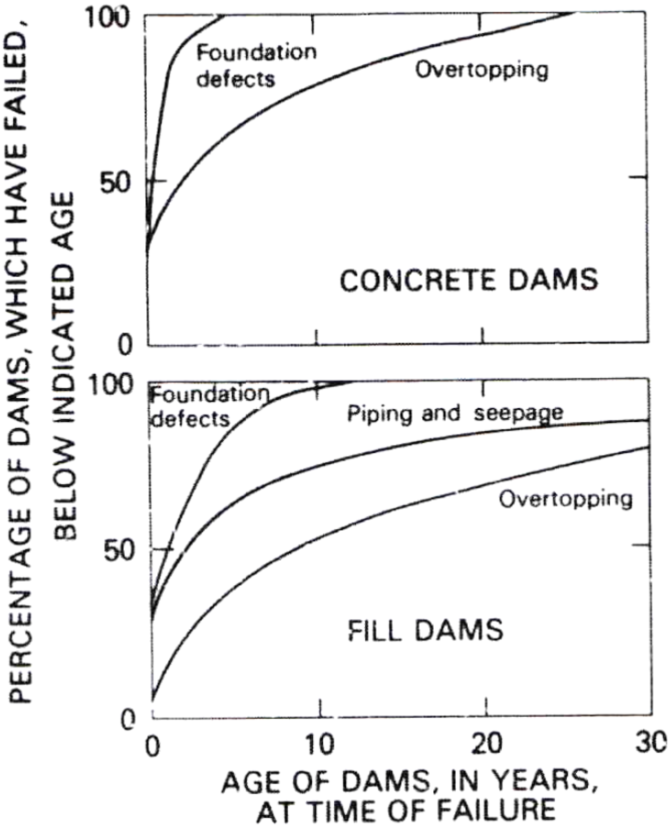

Figure 11: Percentage of dam failures according to age and main causes. The lower graph represents embankment dams (ICOLD, 1973, in Costa [23])

5.2 The case of mine tailings dams: some statistical evidence

5.2.1 Databases consulted and compiled

First of all, we should clarify the terminology used hereafter: dam *incidents* include *failures* and *accidents* (significant movements and/or malfunctions noted, without the structure breaking).

As of 2007, a database in the framework of a European project *(e-EcoRisk database - A Regional Enterprise Network Decision - Support System for Environmental Risk and Disaster Management of Large-Scale Industrial Spills)* including, in particular, mine tailings dam failures, listed 250 cases, many of which contained little information [86].

At the end of 2009, there were 218 cases of tailings dam failures since the beginning of the twentieth century, of which 147 cases had sufficient information to allow analysis (Azam and Li, [9]).

The website https://worldminetailingsfailures.org/, (WMTF) established by the Center for Science in Public Participation (CSP2), lists failures since 1915. It is regularly updated (last update March 2019 at the time of writing). The core of the database corresponds to the work of ICOLD/UNEP[7], published in 2001 in its bulletin n°121 [43]. It is completed by data acquired by the WISE website [8], and by the CSP2's own data. This database is quantitatively and qualitatively very important, and it has enabled this organisation to establish severity criteria, which we will refer back to below.

Ineris has drawn up a table of the main known accidents, based on the WISE site, to which data from documents and websites consulted for this report have been added. This table, which can be found in Annex 1, is based on the headings in Figure 12.

---

[7] United Nations Environment Program

[8] World Information Service on Energy Uranium Project, https://www.wise-uranium.org/, [104]

Name of the accident	Continent	Country, Region	Year	Substance	Characteristics of the dam	Deposit properties	Downstream properties

Fault properties	Main causes mentioned	Consequences	Comments	Sources consulted	Details online

Figure 12: Headings in the table of main accidents drawn up by Ineris (Annex 1)

5.2.2 Distribution over time

Of the 218 dam failures recorded at the end of 2009, a clear majority occurred during the 1960s (22% of failures), 1970s (26%) and 1980s (23%). This peak is linked to the demand for metals following the Second World War, but also to the mining boom in emerging countries. The 1990s (19 cases, 9%) and 2000 (20 cases, 9%) are relatively similar, reflecting a fairly clear reduction in the number of cases, in relation to the implementation of prevention and safety policies. On the other hand, there is no evidence of a continuing decline over the last two decades (Azam, Li [9]). The table of main failures in Appendix 1 shows 34 cases between 2010 and July 2020.

5.2.3 Geographical distribution

Also based on this sample of 218 cases, the majority of failures take place in North America (38%), Europe (27%) and South America (18%). It should be noted that of the 20 cases in the decade of 2000, 6 came from Europe and 6 from Asia (Azam, Li [9]).

The table of failures in Appendix 1 shows, between 2010 and July 2020, 17 cases in America (including 6 in Brazil), 12 cases in Asia, 3 cases in Europe (including the Echassières case in France, discussed in Chapter 6.1), 1 case in Africa and 1 case in Oceania (Australia).

Rico et al. [88] also established in 2007 that, out of 147 cases with sufficient information, 50 (34%) were from countries without binding environmental policies or laws on the prevention of mining risks.

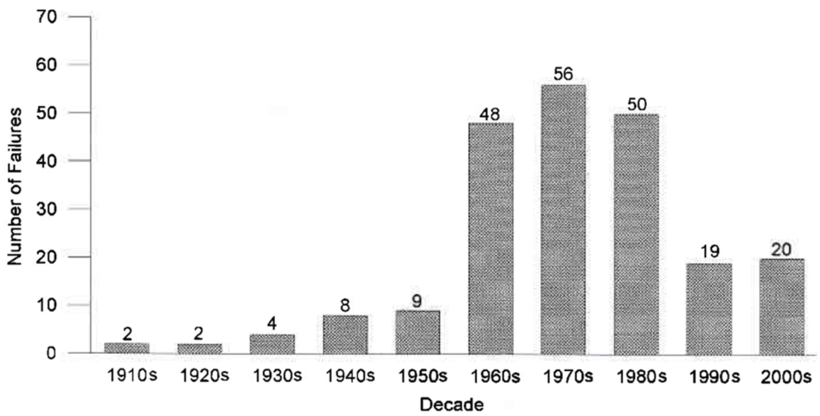

Figure 13: Number of mine tailings dam failures per decade (Azam, Li [9])

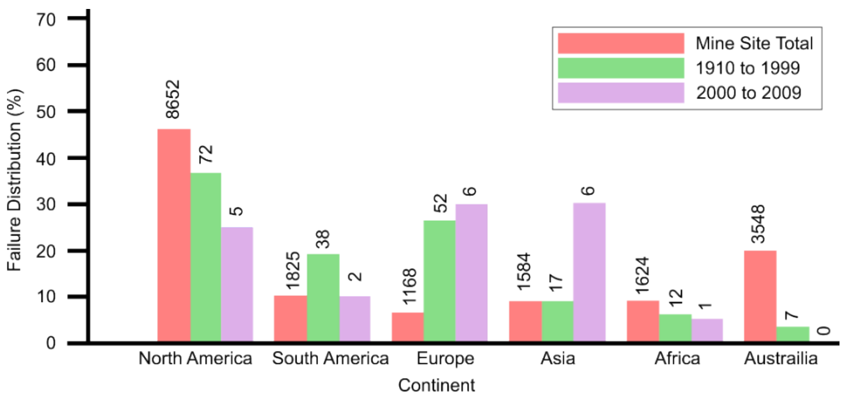

Figure 14: Number of mine tailings dam failures by continent - subcontinent (after Azam, Li [9])

5.2.4 Distribution by dam life stage

According to Rico et al. [88], 83% of failures involve structures that are active at the time of failure (in the operational phase in ICOLD terminology [42]), and 15% of cases involve so-called inactive structures (no longer in the operational phase and not monitored by the operator) or abandoned structures (in restructuring or long-term phases according to the ICOLD terminology [42]). The causes of the latter category are not known according to the authors.

In 2001, ICOLD [43] also reported that few dam incidents (about 25 cases) occur during the "inactive" stage (after the dam has been completely filled, or when the tailings-generating activity stops).

5.2.5 Distribution by dam height

Rico et al. provide a breakdown of the failure cases according to the height of the dam, as shown in Table 4 [88]. We can see that the majority of cases concern dam heights below 15m.

Table 4: Distribution of tailings dam failures by dam height, worldwide and in Europe (from Rico et al. [88])

Height of the dam	Percentage of dam failures (World)	Percentage of dam failures (Europe)
Less than 15 m	44%	52%
15-30 m	33%	42%
Over 30 m	23%	2 cases

ICOLD, 2001 [43], states that **almost 63% of the failure cases correspond to a dam height below 20m.**

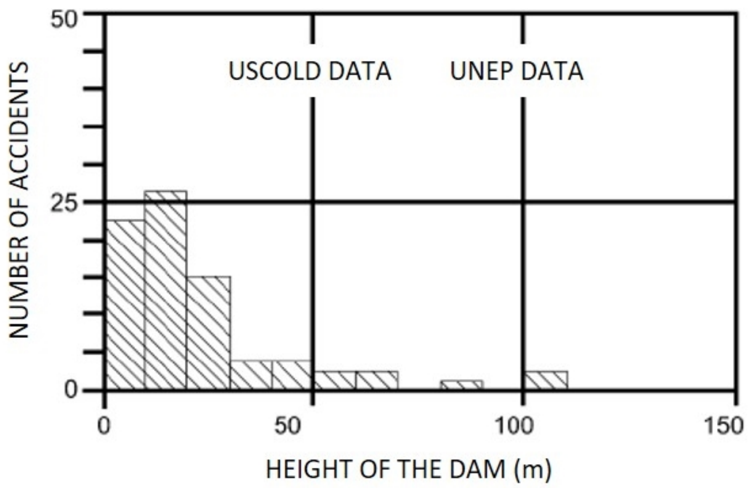

Figure 15: Comparison of the number of dam failures and their height (from ICOLD, [43])

5.2.6 Distribution by construction method

Davies et al, 2000 [25] provide a review of the failures and show that **67% of the cases (58 cases in 2000) concern dams built by the upstream method.** But these authors indicate that these are the most numerous (about 50% of the 3500 known dams).

ICOLD, in 2001 [43], illustrates the share of accidents and failures for each construction method, including water retention dams, reflecting, all other things being equal, a lesser control of the structure for dams built by the upstream method.

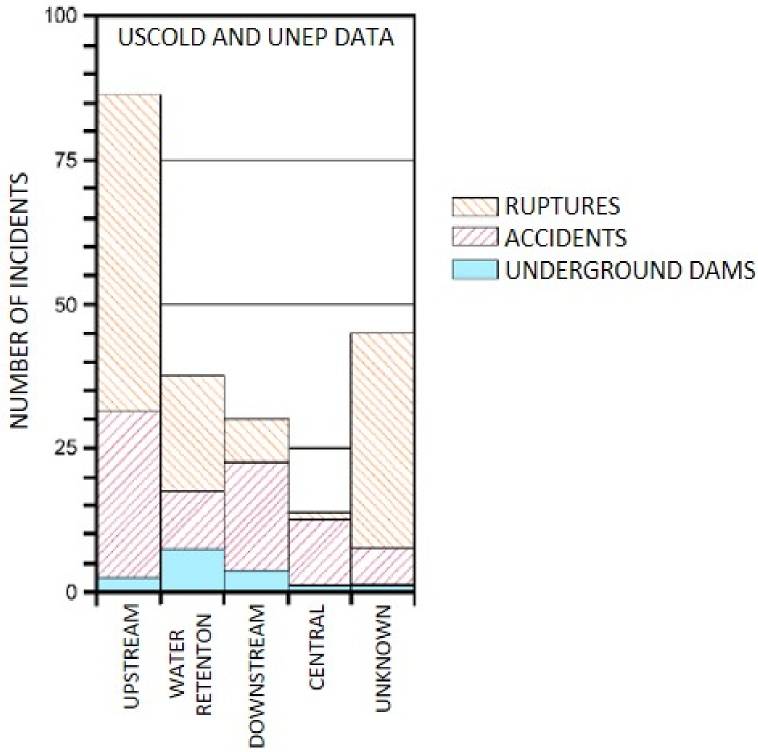

Figure 16: Comparison of the number of dam incidents and their construction method (from ICOLD, [43])

This proportion is even more pronounced in 2007 (Rico et al. [88]) after examining 147 failure cases, as **76% of them concern dams built using the upstream method.** This proportion is lower for European cases (47%).

5.2.7 Distribution by cause

As reported in Davies et al. 2000 [25], the failure cases for upstream dams are related to slope (34%) and seismicity (24%). The remaining cases are divided into foundation, overflow, percolation or structural problems. All cases of material liquefaction are related to dams built using the upstream method.

The main cause of failure of dams not built by the upstream method is related to seepage problems and in particular to the poor design of drainage systems. For these dams, the seismic cause is much less significant (Davies et al. [25]).

Rico et al. [88] established, on the basis of the 147 cases of failure identified, eleven main causes, both external and internal. It appears that 39% of them have multiple causes. Referring to the single cause or the one considered most relevant when there are multiple causes:

- 25% of global cases are caused by abnormal/exceptional rainfall;
- 14% of cases are related to seismic liquefaction (no such cases in Europe);
- 18% of cases are related to internal erosion, seepage, overflow or slope stability problems. It should be noted that, since only one leading cause is highlighted in these statistics, these internal factors may be underestimated, as they are masked by the initial external cause of heavy rainfall;
- 10% of cases are linked to insufficient or inadequate human management of the site (retention, drainage, raising, overloading, etc.);
- 9% of cases are related to a structural problem, and 6% are related to a problem with the dam's foundation;
- 15% of cases have an unknown cause.

Davies et al. 2000 [25] report that for so-called "inactive dams" (which could be assumed to include inactive structures not monitored by the operator and abandoned structures, or, as ICOLD [42] calls them, structures in the restructuring or long-term phase), the main mode of failure is due to overflow in

50% of cases. ICOLD [43] states that for inactive dams, the main causes of incidents are overflow and seismicity.

ICOLD [43] cross-referenced the main causes of incidents in a somewhat different, crude classification (the potential meteoric cause does not appear explicitly). It is noted that the main causes of failure are overflow, slope instability and earthquakes. It can also be seen that overflow and earthquakes generate incidents that lead to the failure of the construction to a much greater extent than accidents without failure.

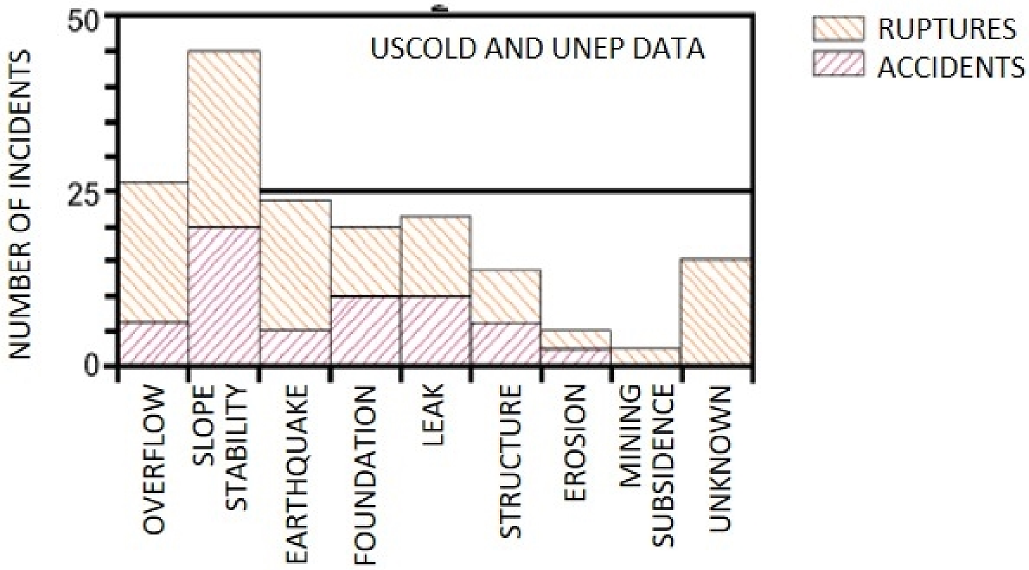

Figure 17: Comparison of the number of dam incidents (failures, accidents) and the cause (from ICOLD, [43])

This prevalence of overflow, slope instability and earthquakes can be seen in the UNEP, 2017 [98] represented in Figure 18, for the period 1915-2016.

Ma et al, 2012 [70], report that surveys in China and other countries indicate that 40% of dam failures are related to infiltration problems.

Villavicencio et al, 2016 [103], report for Chile, where 449 tailings deposits are identified, that seismic liquefaction is the cause of failure in 50% of the cases, on dams built using the upstream method and ranging in height from 5m to 35m.

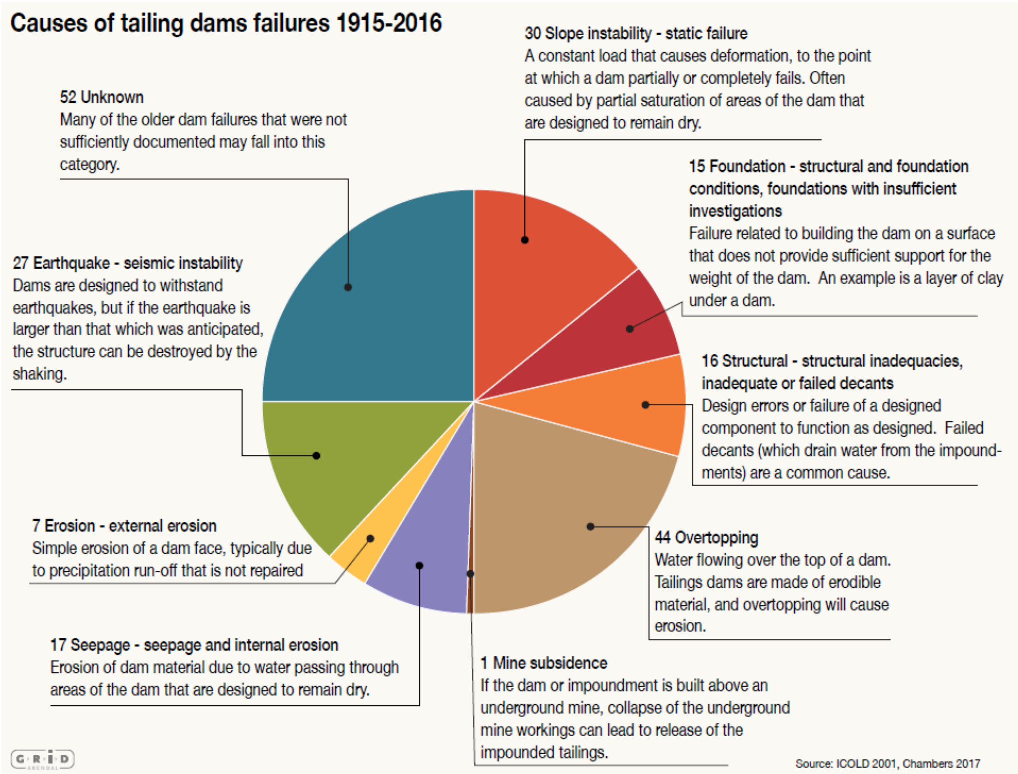

Figure 18: Representation of the number of dam failures by detailed cause (Chambers, 2017, ICOLD, 2001 [43], in UNEP, 2017 [98]

5.2.8 Distribution by consequence

In terms of ***mobilised volume***, Azam and Li, in 2010 [9], indicate that, of the 72 cases with information on the mobilised volume, 70% of them involved a volume of less than 500,000 m^3. 24% of failures mobilised more than 1 million cubic metres. A value of 1/5th of the contained volume that is mobilised is suggested, but not substantiated, in this article.

In terms of the ***final slope*** of the effluent at equilibrium after the failure, case histories indicate that final slopes do not exceed 5° (Lucia et al, 1981 [66]).

In terms of ***severity***, a four-level coding scheme has been developed by WMTF [105], numbered from 1 ("very severe") to 4 ("potential failure", meaning an observed condition that, if left unattended, could develop into a failure over time). This coding is based primarily, but not exclusively, on the three severity variables of volume released, distance travelled and number of dead. But it also relies on feedback on disasters from the scientific community. The WMTF website indicates that only two of the classes, "very severe" and "severe", work well in statistical analysis.

Based on Table 5, we can see that the number of very serious failures (a total of 56 cases since 1908) is increasing (about 5 per decade since 1908, more than 8 per decade since 1958, more than 10 per decade since 1988).

The sum of serious and very serious accidents (a total of 119 cases since 1908) shows the same increase (almost 11 per decade since 1908, over 18 per decade since 1958, over 23 per decade since 1988).

If we look only at the number of deaths, the decade 1958-1967 stands out very clearly with more than 1000 deaths. This is followed by the decade 2008-2017 with more than 400 deaths, and the decades 1978-1987 and 1968-1977 with more than 300 deaths. It should be noted that the Brumadinho disaster of 25 January 2019, which resulted in 270 deaths and missing persons, is not included in this table.

Table 5: Table of failures by level of severity as established by WMTF [105]

FIG 2 TSF DAM FAILURES BY DECADE FROM 1915 As Known 08/01/2018												
	count by severity code					count by severity indicators			facility descriptors			
Decade	Very Serious Failures	Serious Failures	Minor Failures	Potential Failure Condition	All Failures potential failures	Cumulative Release	Cumulative Runout (km)	Deaths	Avg Ht m	Avg Storage (M cum)	# w ht	#w stor cap
	1	2	3	4	count	M Cub m	km	count	m	M cub m		
2008-17	13	14	16	0	43	95,8	832	435	45	40 895 903	13	11
1998-07	10	9	13	0	32	20,9	326	52	22	14 298 571	5	7
1988-97	9	15	29	5	58	56,5	116	88	29	7 526 143	33	14
1978-87	6	9	28	3	46	22,3	60	347	25	9 761 640	36	25
1968-77	5	8	14	0	27	24,2	275	317	25	2 375 000	45	11
1958-67	7	4	16	2	29	25,6	98	1 053	18	1 775 864	30	11
1948-57	1	3	0	0	4	1,7			22	0	5	0
1938-47	1	1	2	0	4	0,2			15	0	2	0
1928-37	2	0	0	0	2	12,8	11	300	61	29 200 000	1	0
1918-27*	0	0	0	0	0	0,0	0	0	0	0	0	0
1908-17	2	0	0	0	2	4,0	0	0	61	0,0	1	0
	=======	=======	=======	=======	=======	=======	=======	=======	=======	=======	=======	=======
TOTAL/AVERAGE	56	63	118	10	247	263,8	1 718	2 157	66	5 697 143	171	79
												WORLD MINE TAILNGS FAILURES.ORG

113 records w ith no information on release runouts or deaths are not given a classicication other than locus of failure as indicated by ICOLD assigned codes

* no records for 1918-1927

5.3 Focus on some iconic cases

5.3.1 Failure of the Stava mine tailings dam, Italy, 1985

Main sources: Aria database [3], Davies et al. [25], Luino, De Graff [67], Pirulli et al. [83], Rico et al. [88], WISE

The failure of the so-called "Stava dam" in the province of Trentino-Alto Adige occurred on 19 July 1985, in the Prestavel mine. The mine had been exploiting lead and silver since the sixteenth century, and then turned to the extraction of fluorite from 1934 [67].

In 1961, the Montecatini mining company (Montedison Group) decided to set up a flotation system to produce 97-98% pure fluorite. This required abundant water as well as the creation of tailings settling and storage areas.

Two slope ponds were built in 1962 (lower pond) and 1970 (upper pond). In 1980, the facility was taken over by Prealpi Mineraria, which reused the two ponds from 1982 [67].

Photograph 1: Stava stacked tailings dams before failure (http://www.fiemmefassa.com)

The ponds are surrounded on the downstream side by dams 25m (lower pond) to 34m (upper pond) high, with an external slope ranging from 1.2H to 1.5H/1 V (i.e. from 33° to 40°), built according to the upstream method.

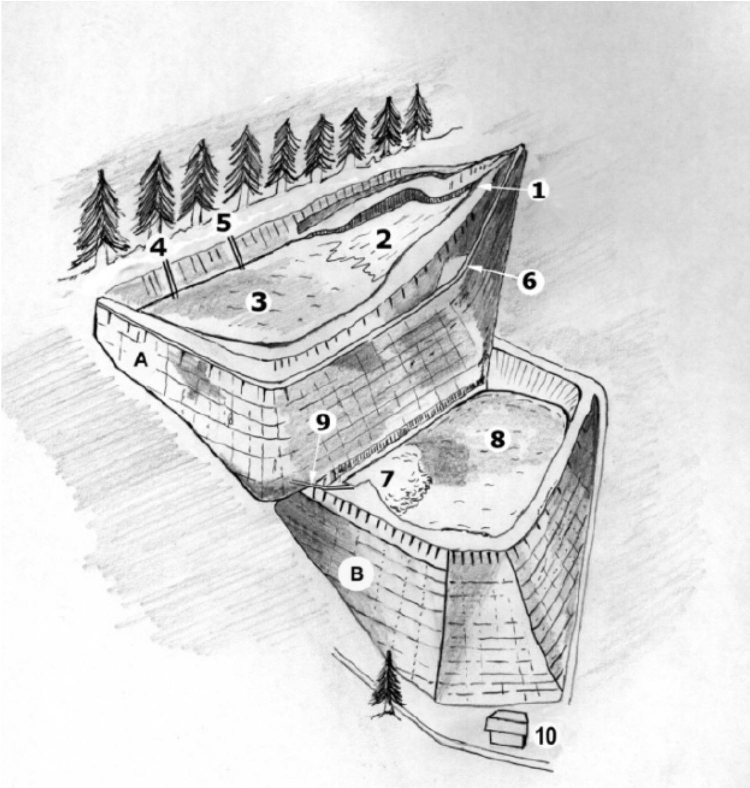

Figure 19: Detail of the two ponds (1: cyclone separation zone, 2 and 7: sand deposits, 3 and 8: silt deposits, 9: drainage of the upper pond) (Luino, De Graff [67])

Around noon on 19 July 1985, a wave of about 185,000m³ of liquefied tailings containing 95% water and with an estimated speed of 60 km/h broke through the valley to the Avisio river, engulfing the villages of Stava and Tesero in a few minutes. 269 people were killed, 62 buildings and 8 bridges were destroyed. More than 4 km downstream was devastated and the residual sludge thickness was 20 to 40cm. The damage was estimated at 155 million euros at the time.

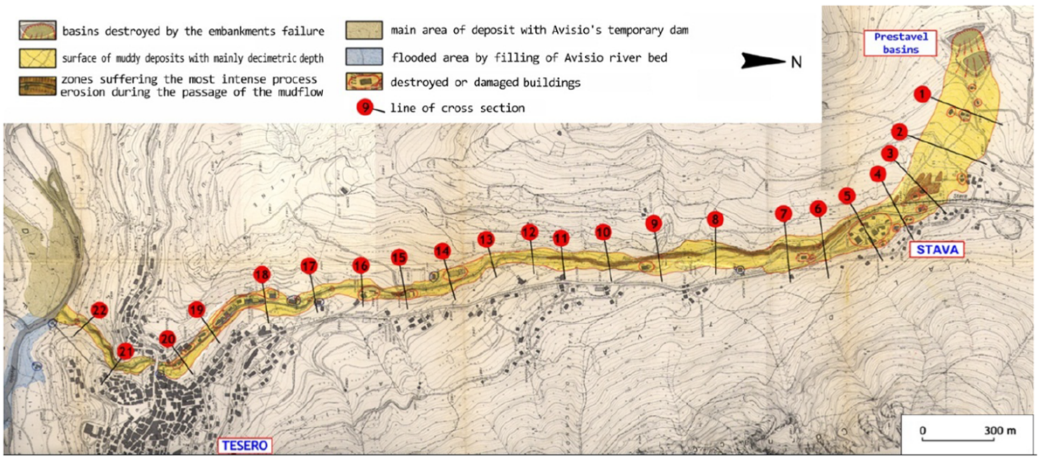

Figure 20: Path of the sludge wave through the Avisio valley (Luino, De Graff [67])

Photograph 2: Before and after shots in the village of Tesero (in Luino, De Graff [67])

A commission of experts commissioned by the courts to establish the causes of the accident studied and rejected the hypotheses that it had been triggered by an earthquake or an explosive blast in one of the many mines in the region.

However, the commission found that subsidence in the upper pond had detached the end of a water pipe at the site of an old repair. This pipe was used to drain the water collected in the centre of the pond and passed through the body of the containment dam. This failure of the drainage system therefore did not allow the water to drain properly and led to a hydraulic surge in the body of the upper containment dam, leading to its collapse, then to the overflow and failure of the lower dam.

The fault probably occurred several months before the accident: a breach had occurred in the side wall of the upper pond in January 1985, leading to a leak that was repaired in March. The ponds were completely emptied in May for repair work and put back into service on 15 July, 4 days before the accident.

The record rainfall that year (+22% compared to the 66 previous years), as well as the two days preceding the rupture, and the very heavy snowfall of the previous winter contributed to the accident. However, they were not the main cause, as damage had already been found in January, before the snow melted and the heaviest rain fell.

The investigation also revealed design errors: the slope of the dams was too steep (up to 40°), and the foundation soil was too marshy to allow proper drainage and consolidation of the materials making up the upper dam. A member of the expert commission states that the structure "was built to the limit of its capacity to remain stable. The slightest disturbance was enough for it to collapse. [...] It is surprising that the dam did not collapse earlier". No stability checks had been carried out in the twenty years prior to the disaster.

Following the accident, Italian legislation on rock waste ponds was tightened and the Prestavel mine was permanently closed.

5.3.2 Fundao mine tailings dam failure, Brazil, 2015

Main sources: Agurto-Detzel et al. [1], Aria database [4], Fundaoinvestigation [34], Morgenstern et al. [78], Roche et al. [90], WISE [104]

The most significant event in Brazil prior to the Brumadinho disaster was the rupture of the Fundão dam, within the Germano iron ore mine, operated by Samarco, in the Minas Gerais mining region. The failure occurred on 5 November 2015, releasing around 33 million cubic metres of saturated tailings, resulting in the death of 19 people and causing considerable environmental damage, with pollution spreading over 650 km from the failure site. An expert panel report on the causes of the accident was published in 2016 (Morgenstern et al. [78]), from which the following conclusions are taken.

Photograph 3: Fundao dam before and after failure (Morgenstern et al. [78])

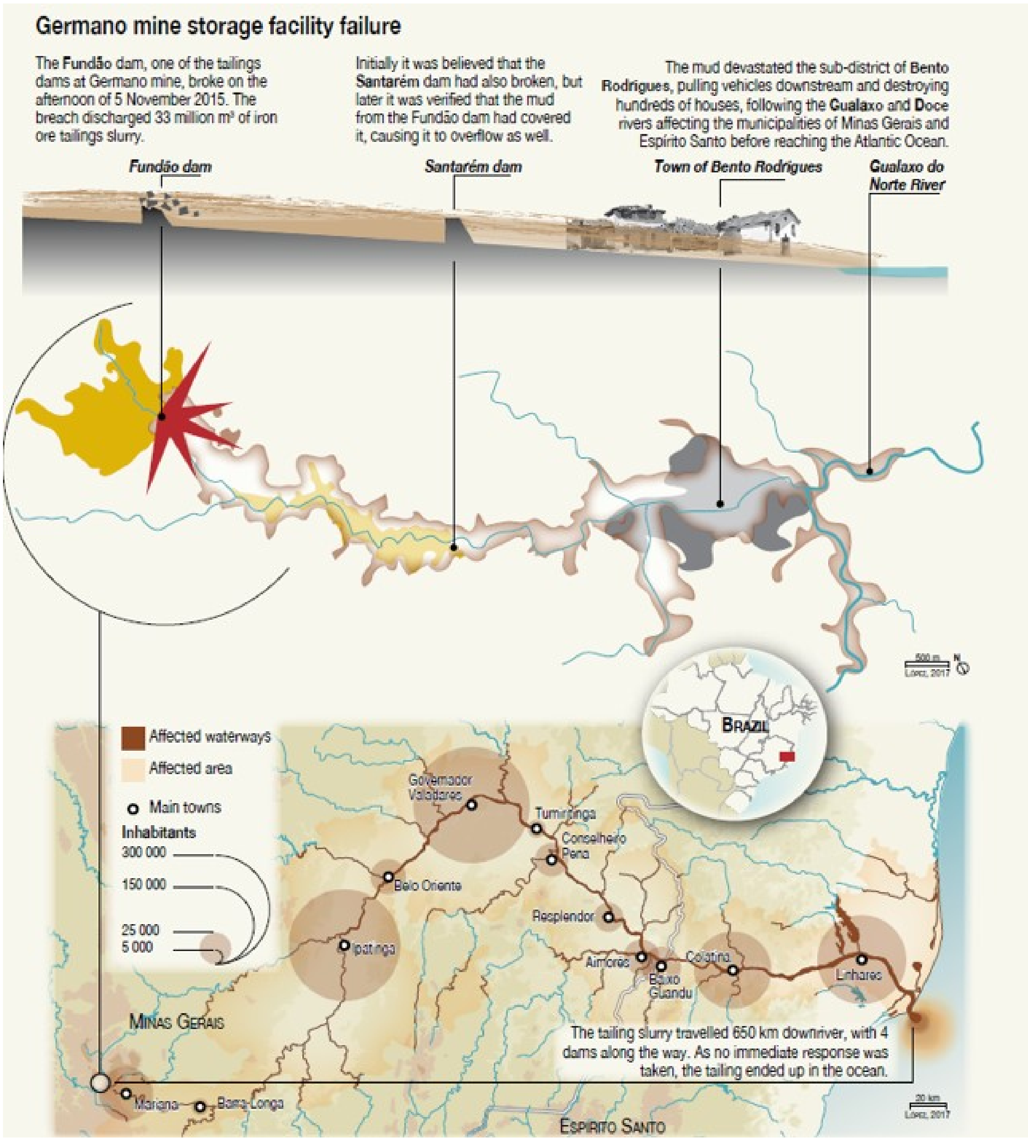

Figure 21: Impacts of the Germano de Samarco mine accident from Roche et al. [90].

The Fundão dam, 500m long and 90m high, was designed between 2004 and 2007 and built, using the upstream method, in 2008 and 2009. The tailings pond had a particular design which involved the establishment of an unsaturated sand buffer zone between the unit dams and the tailings placed.

However, difficulties were encountered at the design phase and construction adaptations were made that could lead to saturated conditions in the sand.

Witnesses revealed that the failure started on the left hand side of the dam, where the dam had been set back from its previous alignment, and where tailings sludge had invaded the sandy buffer zone referred to earlier on numerous occasions. This presence of tailings sludge constituted a barrier to drainage and a potential area of weakness. The setting back of this side of the dam was to allow for the repair of a faulty duct at the base of the deposit and the construction of additional horizontal cover drains to allow the dykes to be subsequently raised. This change in geometry resulted in a significant overload on this part of the sludge-contaminated sandy deposits.

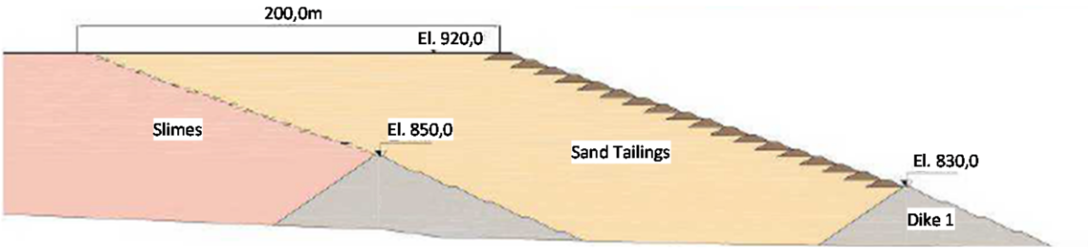

Figure 22: Design of the Fundao tailings pond, consisting of a sand buffer zone (Morgenstern et al. [78])

The causes of the failure reported by the experts are therefore the result of a combination of several adverse factors: 1) a buffer zone for drainage soaked with fine tailings, which reduced the efficiency of drainage and led to saturation of the material, 2) rapid overloading of the material, which made failure and liquefaction possible, and 3) the possible influence of low magnitude earthquakes (1.8-2.6), which occurred just prior to the collapse. The experts consider that these seismic events, whose epicentres are close to each other, probably accelerated the failure which was already well underway.

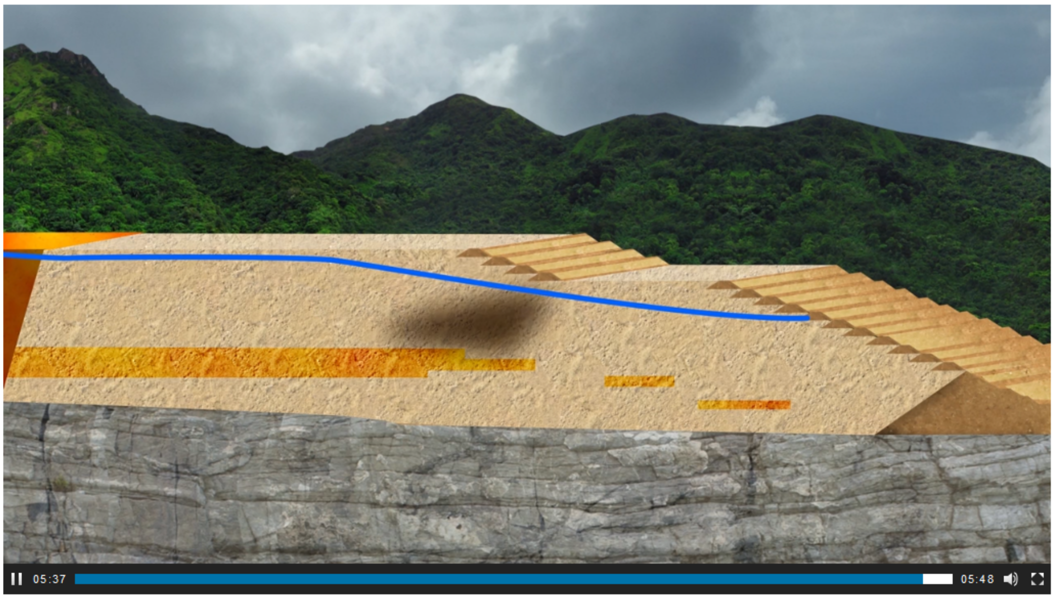

Figure 23: Extract from the animation on the causes of the Fundao dam failure. Beds of orange tailings sludge within the sand zone, leading to the rise of water (blue line) progressively up the height of it, creating conditions for liquefaction of the sand (black spot) (Fundaoinvestigation website [34])

5.3.3 Failure of the Brumadinho mine tailings dam, Brazil, 2019

Main sources: Robertson en al. [89], www.vale.com [99], WISE [104], WMTF [106]

On Friday 25 January 2019, Dam 1 of the Corrego de Feijao mining complex in Brumadinho, Minas Gerais, failed, causing a devastating mudslide of an estimated volume of 12.7 million cubic metres, according to media sources, leaving 270 people dead or missing.

This iron ore mining complex dates back to 1963 and was bought by the Vale mining company in 2001. The dam, built in 1976 using the upstream method, has a height of 87m and a crest length of 720m. It was built in 10 increments, the last one in 2013.

The 18m high starter dam was constructed from fine-grained ore with high drainage capacity, covered with a 4m thick laterite layer on the upstream slope and 1m thick on the downstream slope.

The slope of the structure is 33° upstream and 30° downstream. The slope on the downstream side had an intermediate 5 metre-wide berm. There is no reference to an internal drainage system.

The volume of tailings retained is 11.7 million cubic metres over an area of almost 25 hectares.

The dam was designed for a safety factor of 1.3, which was considered reasonable during the construction period.

According to Vale [99], the dam was inactive and not subject to any operating activity. A project to decommission the structure was even underway. The dam was declared stable by the company TUV SUD, specialised in geotechnics, in publications dated 13 June and 26 September 2018, as part of the periodic review and regular inspection processes for dam safety. These two publications attest, again according to the operator, to the physical and hydraulic safety of the dam.

Figure 24: Aerial view of Corrego de Feijao Dam 1 (in WMTF [106])

Vale also reports that the dam had been subject to field inspections twice a week, all of which are reported to the National Mining Agency (ANM). The last inspection recorded by the ANM was carried out on 21 December 2018. All inspections did not detect any change in the condition of the structure. The dam had 94 piezometers, including 46 automated and 41 water level indicators to monitor its integrity.

According to Vale, the dam had a Mining Dam Emergency Action Plan (PAEBM), which would have defined the flood zone in the event of a failure. In addition, the dam had a video surveillance system, a siren warning system, and the population downstream was registered. A simulation had apparently been carried out on 16/06/2018, under the coordination of the Civil Defence.

In December 2019, a panel of experts produced a report (Robertson et al. [89]) on the circumstances of the disaster and Vale's management of the risk associated with this structure, from which the following key elements have been extracted.

The analysis of the failure was aided by the availability of high quality video footage, which clearly indicates a failure from the crest down to an area just above the berm (corresponding to the starter dam). The lower part of the dam bulges outwards before the dam surface breaks.

Figure 25: Image taken from the video of the failure. You can clearly see the ruptured crest of the dam and the bulging of the lower part (WMTF, [105])

The rupture extended across almost the entire width of the dam, and the structure collapsed in less than 10 seconds, releasing 9.7 million cubic metres of material. The mobilised dam material shows a sudden change in behaviour, turning into liquid and flowing downstream at high speed.

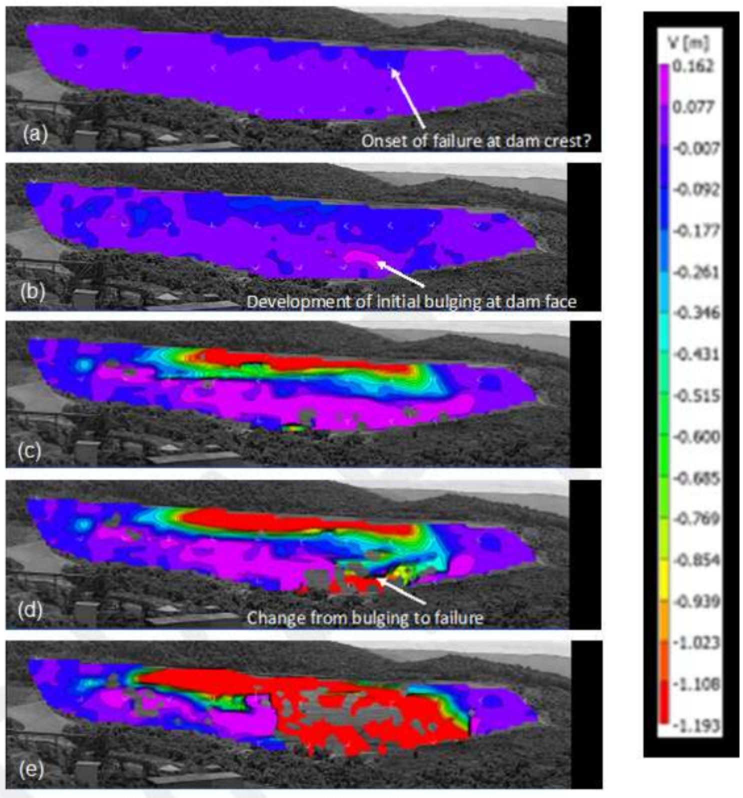

Figure 26: Fracture propagation within the dam (Robertson et al. [89])

The initial fracture is relatively shallow and is followed by a series of shallow, steeply sloping slides in the tailings. Based on these observations, the experts conclude that the failure is the result of (static) liquefaction of the dam materials.

A drone survey of the structure seven days earlier showed, again according to the experts, no signs of failure. The dam was extensively monitored, including with inclinometers, ground-based radar to monitor deformation of the face, and piezometers. No significant distortion or changes were recorded prior to the failure. Analysis of earlier satellite imagery indicated that small deformations had occurred on the face of the dam in the year prior to failure, with the rainy season accelerating the distortion. In the lower part of the dam, deformations measured in the 12 months prior to the failure did not exceed 30 mm. According to the experts, such deformations are consistent with slow, long-term settlement of the dam but are not considered precursors of failure.

The combination of these factors led, according to the experts, to the failure of the structure:

- the structure's too steep a slope;
- management of tailings deposition that sometimes allowed water from the ponds to approach the crest of the dam and bring unaggregated tailings close to the crest;
- construction of the upper dams on top of fine, weaker tailings;
- a lack of significant internal drainage which resulted in a consistently high water level in the dam;
- high iron content within the tailings, making them potentially very brittle in an undrained condition;
- high and intense regional rainfall which prevented the unsaturated material above the water table from acting as a drain.

6 The situation in France

6.1 In mainland France

In mainland France, almost all mining stocks are in a post-operating situation. The last iron ore mine was closed in 1995 and the last uranium mine was closed in 2001. The exploitation “Mines des Potasses d'Alsace” ceased in 2003 and the last coal mine shut down in 2004. Active mining industries in mainland France are now associated with the extraction of salt, by underground mining or dissolution, bauxite, and the exploitation of hydrocarbon and geothermal deposits (Ineris, Cerema, GEODERIS [48]).

At the end of the 1990s, the occurrence of various events or inconveniences in former mining areas led the French government to set up tools to manage the consequences of the shutdown of mining activities in a so-called 'post-mining' phase.

Article 20 of European Directive 2006/21/EC ([29]) requires Member States to draw up an inventory of deposits related to the extractive industries. In the specific context of former mining operations, this inventory for mainland France was established by GEODERIS[9]. It is on the basis of the report summarising the results at national level (GEODERIS, 2012 [35]) that the items, particularly those relating to former mining dams, are reported below.

The GEODERIS report distinguishes between metal mine deposits and coal mine deposits. In terms of deposit typology, the report distinguishes between deposits, ponds and retention structures[10]. Tailings dams can be considered to fall into the latter category, but ponds can be surrounded by enclosure structures[11] of a similar type to those of dams.

For metal mines, 380 of the 2109 deposits recorded are tailings. The proportion increases if we look at deposits of more than 100,000m^3, so 53 deposits out of the 93 inventoried are made up of tailings. The inventory shows only 34 impoundment structures. Of these, 23, or almost 70%, are located in four former regions, Languedoc-Roussillon, Limousin, Midi-Pyrénées and Rhône-Alpes (Table 6).

GEODERIS, with a view to prioritising risks on a national scale, classifies these impoundment structures as high risk for 56% of them, and medium risk for 28% of them.

Table 6: Distribution by region of the French mainland of metal mine deposits, following the inventory established by GEODERIS [35]

[9]Groupement d'Intérêt Public (GIP), formed by the Ministry of Ecological Transition and Solidarity, BRGM and INERIS, the French government's expert (central administrations and decentralised services) in the field of post-mining

[10]GEODERIS defines them as "*linear built structures, involved in the storage of mining waste (among these entities are in particular the main mining dykes, in the ICPE (facilities requiring environmental impact assessment) sense*)". These structures therefore include mine tailings dams *stricto sensu*

[11]Structures, generally built in embankments, delimiting on its perimeter a mining effluent pond

Region	Number of objects						
	Deposits	Ponds	Retention structures[7]	Deposit zones	Challenges	Points observed	Measurements
Alsace	69	4	0	38	92	46	15
Aquitaine	28	0	0	17	27	44	30
Auvergne	222	19	3	92	471	110	368
Basse-Normandie	3	0	1	3	10	3	0
Bourgogne	48	0	1	28	64	43	7
Bretagne	35	2	1	27	27	2	4
Centre	7	0	0	7	10	12	2
Champagne-Ardenne	2	0	0	2	2	4	1
Corsica	72	4	0	26	39	145	213
Franche-Comté	26	0	0	14	33	39	0
Haute-Normandie	Region with no deposit						
Ile-de-France	Region with no deposit						
Languedoc-Roussillon	466	23	8	140	416	469	562
Limousin	51	1	5	48	46		
Lorraine	42	0	0	22	50	57	6
Midi-Pyrénées	355	19	5	145	419	572	201
Nord-Pas-de-Calais	Region with no deposit						
Pays-de-la- Loire	18	0	2	15	20	2	2
Picardie	Region with no deposit						
Poitou - Charentes	6	0	0	6	8	1	2
Provence- Alpes-Côte-D'azur	370	10	3	138	366	323	355
Rhône-Alpes	289	27	5	118	310	574	376

The following sites are particularly noteworthy, according to the risk hierarchy established by GEODERIS [35], using simple criteria based on the characteristics of the structures (dimensions, volume retained). The aim was to identify the impoundment structures that might require a posteriori stability studies:

- in the Auvergne-Rhône-Alpes region, the sites of Montmins (Allier), Largentière (Ardèche) and Barbecot-Roure (Puy-de-Dôme);
- in the Brittany region, the site of Huelgoat (Finistère);
- in the Nouvelle-Aquitaine region, the Bourneix sector (Haute-Vienne);
- in the Occitanie region, the Pic-de-la-Fourque site (Ariège), the La Caunette site (Aude), the La Croix-de-Pallières, Les Malines, Saint-Sauveur and Saint-Sébastien-d'Aigrefeuille sites (Gard), the Bleymard site (Lozère), and the Noailhac and Peyrebrune sites (Tarn);
- in the Provence-Alpes-Côte-d'Azur region, the Fontsante site (Var).

For coal mines, 1057 of the 1274 deposits listed are made up of washing tailings, and 89 of them concern fine washing tailings (schlamms). The inventory only lists 14 deposits with impounding structures. GEODERIS, again as part of its risk prioritisation on a national scale, classes one of these impounding structures as high failure risk, and two of them as a medium risk.

With regard to recent reports of mine tailings dam failures, only one case was identified, that of Montmins, in the commune of Echassières, in the Allier, which occurred on 1 March 2015.

On this former mining site, where tungsten was extracted until 1962, the dam of a former tailings settling pond broke, creating a breach 30 m wide and 20 m high.

This so-called "Bellevue" pond is part of a network of four tailings dams, three upstream and one downstream of a single stream, the Cotillon. The entire water body has emptied, resulting in backfill and sediment containing arsenic and tungsten polluting the Bouble River.

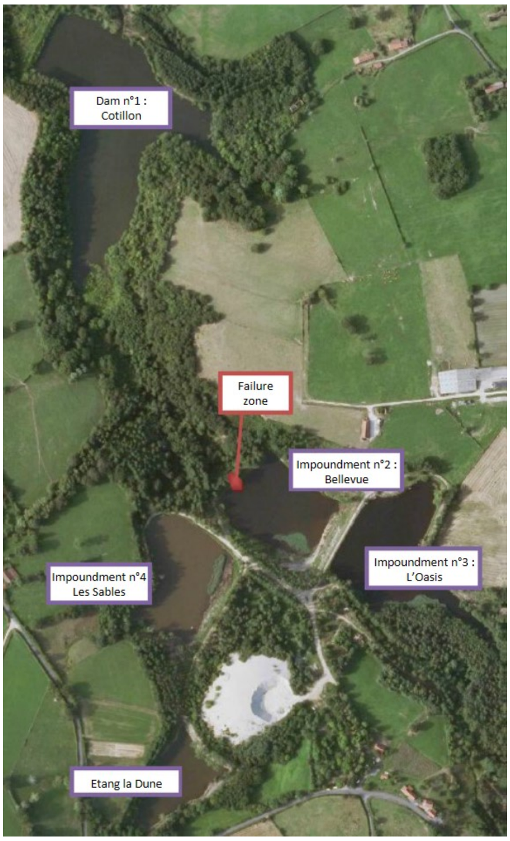

Figure 27: Former Montmins mine, Echassières. The four tailings containment structures and the breach zone (source Somival)

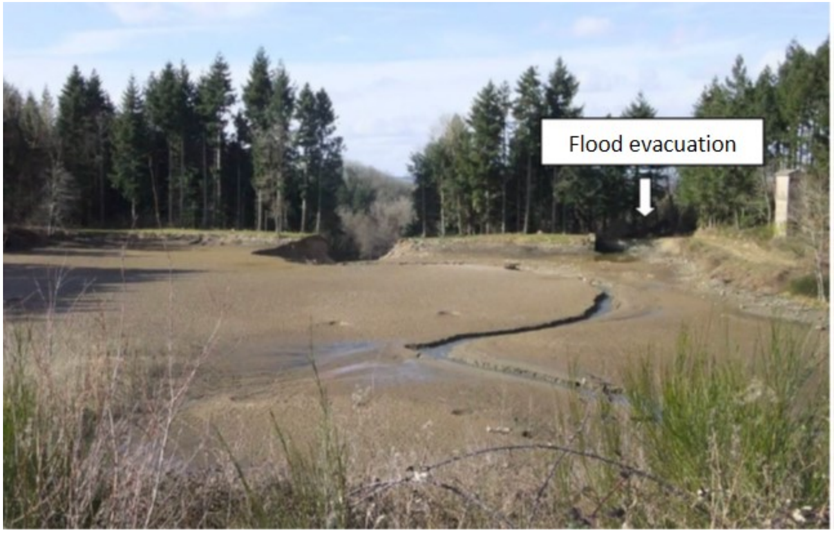

Photograph 4: Breach on 1 March 2015 in the "Bellevue" pond of the former Montmins mine, Echassières, Allier (source Somival)

Following the event, the other tailings impoundment structures were drained in order to reduce the risk of a domino effect causing other dams to rupture.

The causes attributed to this failure are significant rainfall, insufficient sizing of the spillways, but also the presence of burrowing animals, noted during a visit in 2013 to the failure zone, having probably weakened the crest of the dam.

Another rupture, not related to a mine tailings dam but to an enclosure dyke of an industrial pool, deserves mention, particularly with regard to the causes stated. The case concerns the rupture of a lagooning and settling pond (pond no. 2) dyke on 20 March 2004 at the Malvési plant producing uranium tetrafluoride in the Aude department. The rupture created a breach 180 m long and 15 m high and released all the retained liquid. 15,000 m3 of process water and 10,000 m3 of sludge rich in nitrates (ammonium, sodium, calcium) were mobilised in a 10-hectare field, creating a 30-40 cm thick deposit at the foot of the other pools 3, 5 and 6. The nearby Tauran canal was not affected by the effluents (Aria database [6]).

Photographs of ponds B1-B2 before and after the accident (Wise site).

Photograph 5: Malvési pond no. 2 dyke before and after rupture (http://www.criirad.org/actualites/dossiers2006/comurhex/rapportcomurhex_criirad_1.pdf)

The lateral leaks in the dyke body made up of waste rock from a former sulphur mine had been observed since 1980, leading to the installation of a network of drains and piezometers.

The initial cause of the breach of the enclosing dyke was deep cracking of the sludge in this pond due to the intense heat of the summer of 2003. The heavy autumn rains that followed would have led to the infiltration of the water from the pool into the body of the dyke, leading to its saturation and the rise in interstitial pressure, and then the failure of the structure. Five days earlier, the operator had noticed the appearance of a 15 m long longitudinal crack in the crest of the dyke.

6.2 In French Guiana

With a production of 1.8 tonnes in 2014, gold mining is the second largest industrial sector in French Guiana. The ore is currently extracted mainly in the form of secondary deposits (displacement of the ore concentration in alluvial or colluvial materials), and sometimes in the form of primary deposits (concentration within the rock that has undergone oxidation or alteration, with or without preservation of the original structure).

As at 31 December 2015, 39 mining titles (concessions, operating permits and exclusive research permits) were valid in French Guiana, 20% of which were for exploration. Some sixty mining authorisations (AEX), issued by the prefect, complete the range of gold extractions. The report by the Ministry of Economy and Finance, BRGM and the Mine & Société network, drawn up in 2017 ([77]), from which the above data was extracted, refers to the existence of around ten primary gold mining or exploration sites. However, it was alluvial production, particularly through AEX, that revived the activity in the 1990s and maintained it to this day.

Alluvial mining is performed pursuant to the "trenches" principle, i.e. the installation of successive excavations, a few metres deep, near the bed of a river, known locally as a "creek". Once the recoverable material has been extracted, the trenches are used as settling and storage ponds. The waste rock is laid out in the form of earthen embankments of a maximum of 3 to 4 m to separate ponds or to protect against river overflows (BRGM, 2012 [16]).

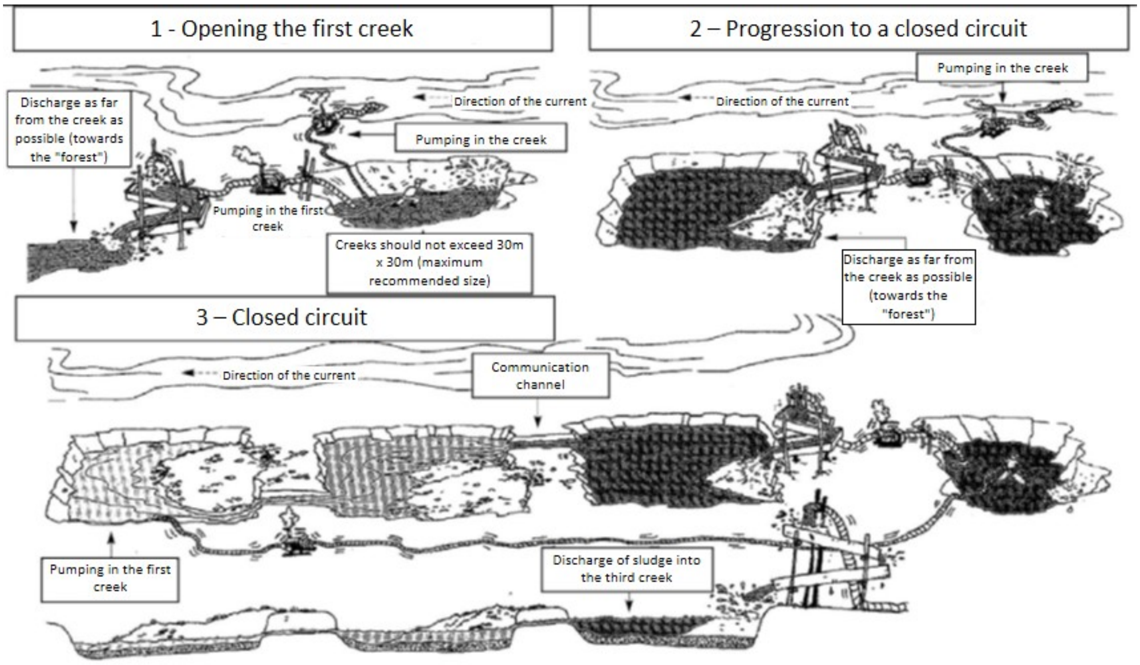

Figure 28: Schematic diagram of alluvial mining in French Guiana (DEAL Guiana, in Minefi, BRGM, Mine & Société [77])

Gravimetric ore processing has been the only gold recovery process to date. This technique was associated with the use of mercury until the end of 2005.

Due to the poor gold recovery performance in the oxidised zones of the deposits by simple centrifugal gravimetry, there is still a lot of gold in some of the tailings areas, with grades ranging from 2 to 20 g/t. Therefore, new operators will probably take back these old "tailings", to recover the gold by more modern and efficient processes such as cyanidation. With this aim of improving recovery efficiency, a cyanidation plant was approved in 2019 in Guiana [77].

All of these processes require large amounts of water, and the tailings are stored in "parks" bounded by dams, with the clear water being recovered and reused for treatment.

The tailings have a submillimetre composition of sands, silts and clays. Depending on the site, the tailings are deposited by spigoting or by cycloning.

At the outlets of the tailings parks, secondary settling or water storage structures can be composed of one or more successive ponds; the most downstream pond storing the clear water allows it to be reused for treatment (BRGM [16]).

In French Guiana, the dams or dykes of these parks, settling ponds and tailings storage ponds are generally formed by embankments (BRGM [16]). As a result, the central method can be considered to be the most commonly used. As the materials available on site are limited, the dams are often made of saprolite, a loose rock resulting from the in situ chemical alteration of sound rock, laterite, a hardened reddish ferralitic soil forming a shield, and alluvium. Because of their characteristics, saprolites are generally considered to have a waterproof effect, whereas alluvial gravels and laterites are used for drainage works.

A 2012 BRGM report [15] notes a lack of long-term design and undersizing of the tailings parks, leading mining operators to regularly raise dams in a way that is "not always properly managed or done according to industry standards".

To date, there are approximately ten mine tailings dams in French Guiana spread over four operating sites (oral source from the French Guiana Department of Environment, Energy and Local Government). No major failure has been recorded to date.

7 Collection of knowledge on the assessment of the flow-type phenomenon

This chapter firstly addresses the notion of hazard and the ground movements that can affect mining dams. The study then focuses on the flow phenomenon, addressing the failure conditions of dams and the propagation mechanisms of mobilised effluents. Finally, the statistical approaches and models, based on the literature, are discussed to estimate or help to estimate the intensity (speed, height) and potential extension of a flow.

7.1 Brief reminder of the concept of hazard and of land movements that may affect a mine tailings dam

Hazard is a term commonly used in risk prevention. It corresponds to the **likelihood** of a phenomenon taking place on a site, during a given period, reaching a **qualifiable** or **quantifiable intensity**. The characterisation of a hazard is classically based on the intersection of the foreseeable intensity of the phenomenon with its probability of occurrence.

In terms of risk prevention, a reference period is understood to be of the order of several decades, or even hundreds of years, to establish an order of magnitude. It is therefore important to include the inevitable degradation of structures over time in the analysis.

The ***intensity*** of the phenomenon corresponds to the extent of the damage, after-effects or pollution likely to result from the feared phenomenon. This includes the concept of the magnitude of the feared events and their potential effects on people and property.

The concept of ***likelihood of occurrence*** reflects the sensitivity of a site, a sector or a structure to the occurrence of a phenomenon. Whatever the nature of the feared mining events, the complexity of the mechanisms, the heterogeneous nature of the natural environment, the partial nature of the information available and the fact that any disturbance, after-effects or pollution are not repetitive, explain why it is generally impossible to reason with a quantitative probabilistic approach. A qualitative classification is therefore used which characterises the ***susceptibility*** of the site to be affected by a particular type of phenomenon. This is the concept that will be used from here on.

As the vast majority of tailings dams are made up of loose materials, the slope movement phenomena that can occur in them are landslides, surface movements and flows.

The flow type hazard is the focus of this report and will be further developed in the following chapters. We will confine ourselves here to a brief reminder of the other types of movement, on the basis of the mining hazard assessment guide drawn up by Ineris [49].

Landslides result from the movement of a land mass along a rupture zone defined by a continuous surface (which may be circular, flat or sometimes complex in shape).

The volumes involved depend on the depth of the rupture zone. Therefore, the term ***deep landslide*** is used when the surface of the rupture is a few tens of metres deep, and ***shallow landslide*** when this surface is a few metres deep.

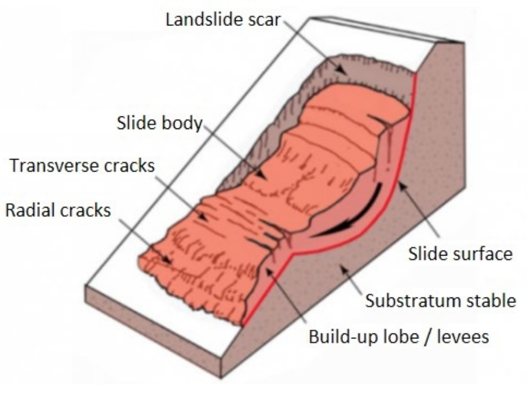

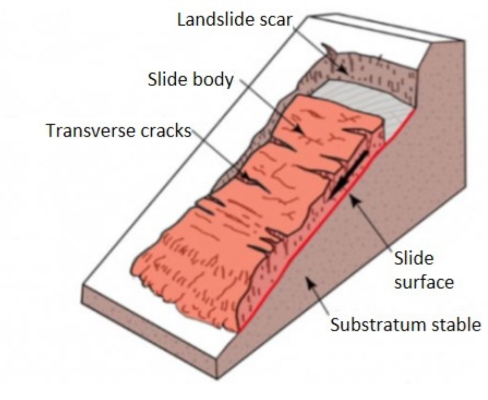

Figure 29: Circular (right) and planar (left) deep landslide patterns (www.protection-dangers-naturels.ch)

The consequences of a deep landslide can be significant, as it can spread out downslope in a cone shape and cause damage to any buildings and structures. It can also affect any buildings and infrastructures located at the top of the slope, near the starting zone (also called the "landslide scar") of the landslide. Therefore, deep landslides can only affect dams of significant height (several tens of metres).

The consequences of a shallow landslide, on the other hand, are much more limited, and only affect the slope itself or its near upstream and downstream edges. This phenomenon is much more frequent due to the large number of cases of mine slopes of limited height.

The term ***surface movement*** is used to describe phenomena which are not associated with the existence of a well-defined rupture surface: this may be soil or material creep due to changes in their mechanical behaviour in the presence of water, or gullying of a slope by water.

Table 7: Slope movements of loose materials: typologies and intensity classification taken from the Ineris guide to mining hazards [49]

Intensity classification	Description	Parameter and intensity threshold value
Very limited	Creep, gullying	A few m^3 in volume
Limited	Surficial landslides, large-scale gullying	Volume from 10 to $100m^3$
Moderate	Deep landslide	Volume from 100 to $5000m^3$
	Flow capable of damaging some buildings and endangering traffic	Flow height < 50cm
High	Major deep landslide	Volume > $5000m^3$
	Devastating flow for people and property	Flow height > 50cm

7.2 Definition of a flow-type phenomenon

Flows are movements where the slope material is unstructured and re-mobilised due to a high water content. It is then transformed into a viscous fluid (often called "mud" or "mudflow") which flows at a high speed (generally between 1m/s and 7m/s). This flow often has a front, usually steep, composed of blocks of material and various debris.

In the field of natural hazards in the mountains, the term "***debris flow***" is often used. This term covers flows that closely mix water and materials of all sizes, with an overall density of around 2 (i.e. between the density of a soil and that of a rock), which makes them capable of transporting blocks almost floating. Specialists generally distinguish debris flows from mudflows by:

- their higher speed;
- their mode of movement, which can be attributed to the flow of a fluid. Some flows may in fact consist of movements still resembling solid physics, with sliding and fracturing of a more or less compact mass;
- or their proportion of solid (maximum 30% for debris flows, at least 50% for flows).

These parameters are interdependent.

It is also unanimously accepted that the debris flow involves the existence of a pre-existing channel which the mobilised materials follow.

As the flow is a disturbance likely to affect the safety of people and property in its path, it is not easy to identify a characteristic quantity that would allow its consequences to be distinguished. In the Ineris guide to mining hazards [49], the height of the viscous fluid flow was therefore used, as the kinetics of the phenomenon are high and non-discriminatory. The value of 50cm was used to distinguish between intensity classifications (high above this value, moderate below).

7.3 Main failure conditions of a mine tailings dam

These elements are largely taken from the report "Document pédagogique pour l'établissement de prescriptions sur les bassins de rétention industriels" established by Ineris for the MEDDE in 2014 ([47]). The scope of the report is all industrial containment ponds, but the types of failure are essentially identical.

7.3.1 Failure of the structure's supporting soil

Before the works, the soil is in a state of equilibrium which will be disturbed by the construction of the structure. In fact, the structure will modify the state of stress of the supporting soil by adding a load. This modification can lead to a disequilibrium, generally during the construction phase or during operation (pond filling or embankment raising).

The main failures that can occur are shear failures but also deformations that can make the structure unfit for use.

Shear failures can occur in two ways:

- overall sliding of the embankment: the entire embankment slides on a slope, for example;
- punching: the load added by the embankment is too high compared to the bearing capacity of the soil in place.

Slope instability of the supporting soils

On a slope of precarious stability, the installation of a dam can cause a landslide (or even reactivate old failure surfaces). This phenomenon is frequent on clay slopes covered with colluvium (soil altered over several metres which may be the result of alteration in situ or of former landslides); these soils are often the seat of water circulation. The removal of the natural ground, which can sometimes happen quite slowly, sometimes accelerating during rainy periods, causes cracks in the fill, then its dislocation.

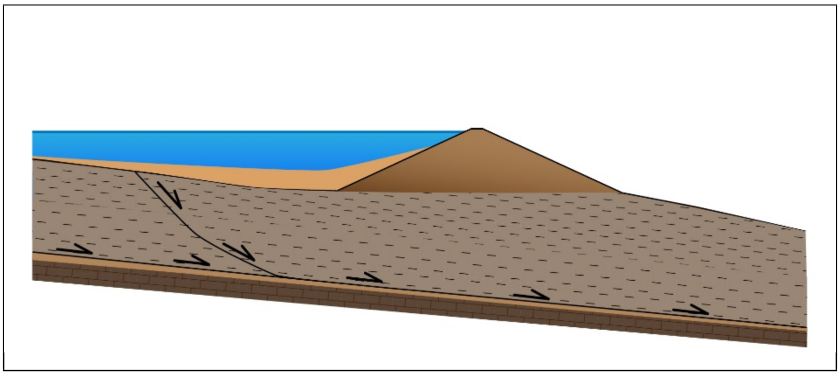

Figure 30 - Dam failure due to natural slope failure

Insufficient bearing capacity of the underlying soil

When the soil on which the embankment rests does not have sufficient mechanical strength, the placement of the embankment can cause either punching of the soil in place or a quasi-circular failure (Figure Figure 31 and Figure Figure 32). These soils, which are generally clayey, are mainly found in the valley bottoms. Such failures are mainly observed during the construction phase of the embankment or during the filling of the pond. After this critical construction phase, significant settlements can occur over time. In the vicinity of the foot of the embankment, horizontal "creep" of the natural soil can cause damage to existing buildings.

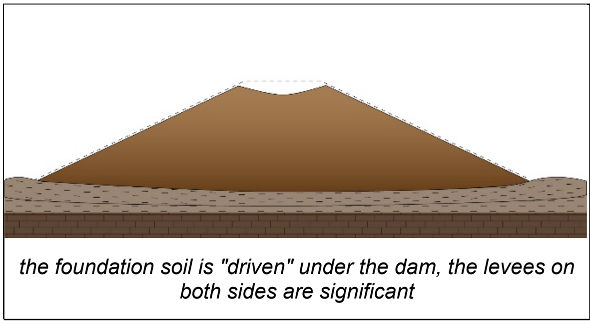

Figure 31 - Punching failure

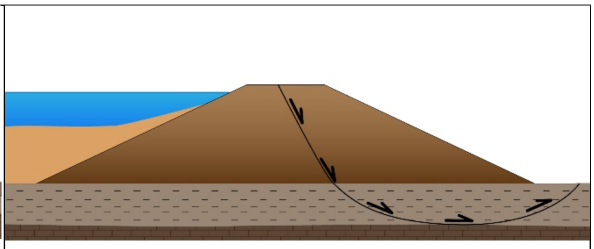

Figure 32 - Rotational shear failure

7.3.2 Failure of the body of the dam

Failures within the body of the dam can range from regressive surface sliding (Figure 33 - the body of the dam gradually decreases) to base sliding (Figure 34). Prior to the ultimate states of mass failure, significant deformations occur: bulging at the toe of the slope, cracking, etc.

The main origins of these failures are:

- for surface failures: the shear strength of the material is too low for the chosen slope, poor compaction of the soil when it is placed, leading to a low shear strength, erosion, poorly drained runoff, high sensitivity to shrinkage of the surface material;
- for failures in the mass: shear strength too low for the chosen slope, interstitial pressures due to flows not taken into account in the design, interstitial pressures due to the implementation (for example: compaction of a too wet material).

Contrary to the previous case of failure of the supporting soil, disturbances in the dam bodies can manifest themselves well after their construction. In addition, a long-term chemical action of certain effluents on the materials cannot be ruled out. Other examples include seismic stresses if the material is inadequately compacted, and failure of the inner lining if it is rapidly drained.

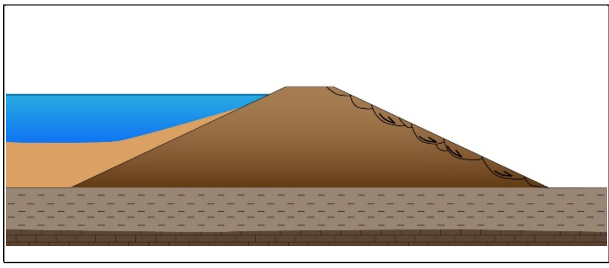

Figure 33 - Regressive surface failures

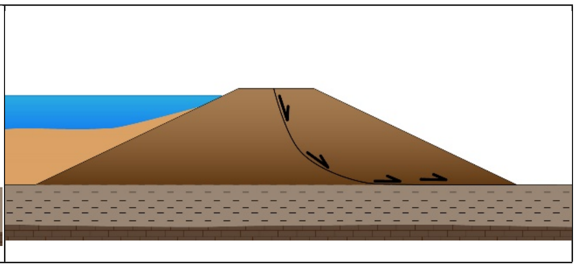

Figure 34 - Dam mass failure

7.3.3 Ruptures created in the mine tailings deposit

Ruptures may initiate in the mine tailings deposit rather than in the body of the dam that contains the tailings. In the example in Figure 36, the embankment, consisting of a succession of small elevations each of which is stable on its own, may have insufficient overall stability, with a failure surface developing mainly in the tailings. This is caused by the combination of a given slope of the embankment with too low a shear strength of the tailings (or a loading of the water contained in the tailings which causes a decrease in the frictional resistance).

In addition, deformations in the tailings can directly affect the dam. In the example in Figure 35, the high compressibility of the tailings will cause differential settlement and cause the dam materials to crack, which can take place over a long period of time (several years or more). If the tailings are made of low permeability materials, the installation of successive levels causes the consolidation of the underlying materials with the appearance of significant water overpressures which can lead to the failure of the tailings + dam assembly. Finally, the tailings can also undergo liquefaction, under the effect of an earthquake for example.

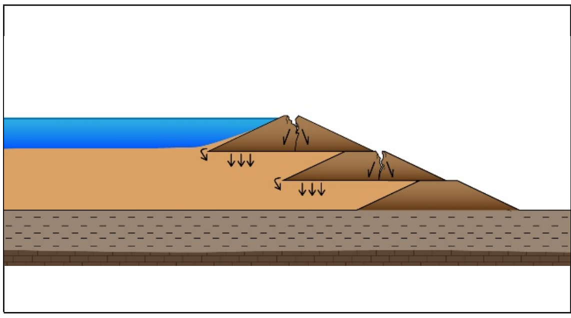

Figure 35 - Deformation, differential settlement

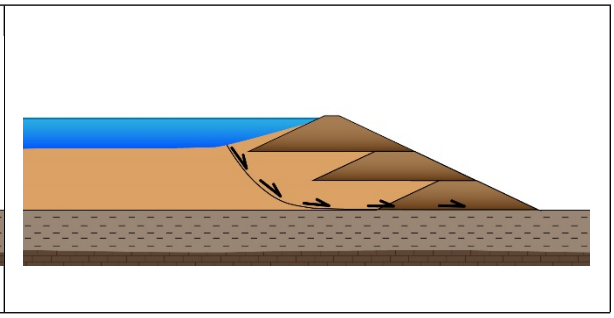

Figure 36 - Failure of the dam-tailings assembly

Liquefaction mechanism

The liquefaction mechanism consists of the total loss of mechanical strength of a material - in this case tailings with a given water content - undergoing rapid static or dynamic loading (earthquake, vibration). This loading leads to a rapid increase in pore pressure (voids between grains) and a decrease in normal stress at grain contacts, or even loss of contact between them. The material undergoes a complete and sudden loss of shear strength, becomes liquid and thus subject to flow and mobilisation (Lucia et al. [66]). This liquefaction results in a sudden additional shear force on the dam (ICOLD, [42]).

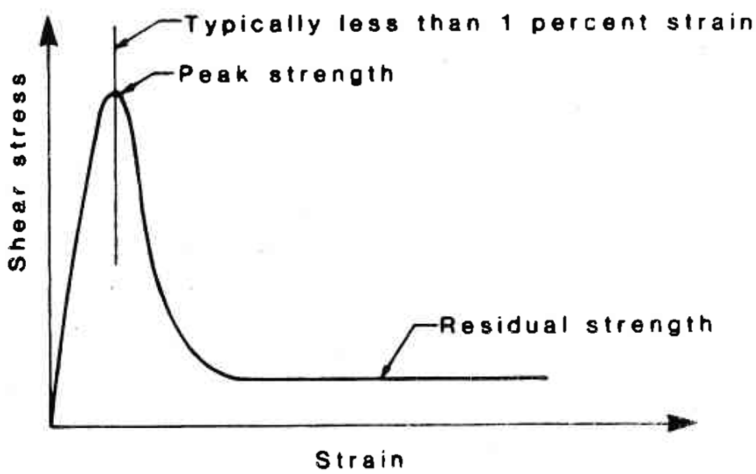

Figure 37: Typical stress-strain curve for loose sand (Lucia et al. [66])

The tailings likely to liquefy are materials with low plasticity, therefore without cohesion, and, with an equivalent void index, more silty than sandy. The presence of plastic materials (clays) increases resistance to liquefaction (Hallman and Dorey, 1995, [37]).

In this regard, Tsushida, 1970, [132], established a typical size range within which the material is potentially liquefiable or even probably liquefiable (Figure 38).

In configurations where the tailings are made up of fine sands, the estimation of the relative density[12] of the material can be an important input to judge the relevance of liquefaction. This assessment can be undertaken at relatively limited cost by conducting laboratory tests on intact samples. In view of the difficulty, for these sandy materials, of preserving the in situ conditions during their transfer to the

---

[12] $DR = \frac{emax - e}{emax - emin}$, e being the index of the voids of the soil in place, emax this index in the most compact state, emin this same index in the loosest state

laboratory, it is useful to carry out shallow dynamic or static penetrometer tests: there are a number of correlations in the literature between peak strength and this relative density (Villaviciencio et al, [103], for waste rock in Chile).

All other things being equal, deposition time increases the resistance to liquefaction, due to the progressive compaction of the material. For example, Troncoso, 1990 [131], cited by Kossoff et al, 2014 [61], indicates that this resistance can increase by 250% in thirty years of deposition.

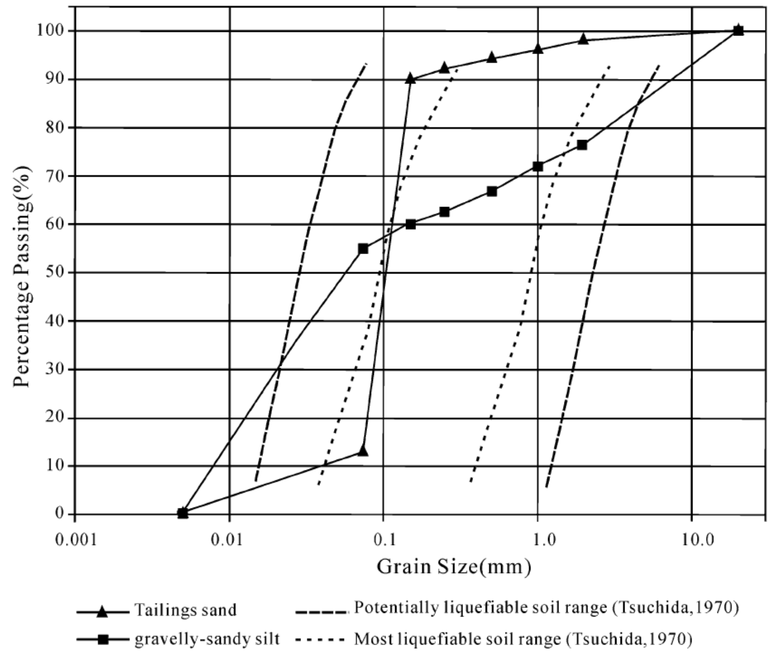

Figure 38: Grain size range of potentially (dashed) or probably (dotted) liquefiable soils from Tsuchida, [132] and grain size range of tailings and starter dyke material from a gold mine in China (Xu and Wang, [108])

Table 8: Estimation of compaction status, behaviour and liquefaction potential of sandy tailings with respect to their relative density (RD) - Espinace et al. [116], in Villavicencio et al. [103]

Table 2. Estimation of the state of compaction and associated mechanical behaviour for sand tailings. Source: Espinace et al., 2013.

qd_{N1}	$(N_1)_{60}$	DR%	State of compaction	Mechanical behaviour	Liquefaction potential
< 20	< 8	< 20	Very low	Contractant	Very high
20 – 48	8 – 15	20 – 45	Low	Contractant	High
48 –57	15 – 20	45 – 50	Compacted	Contractant	Equilibrium
57 – 81	20 – 30	50 – 65	Compacted to dense	Limit	Low
81 –193	30 – 50	65 – 85	Dense	Dilatant	Very Low
>193		85 – 100	Very dense	Dilatant	Null

$(N_1)_{60}$: SPT blow count normalized to an overburden pressure of approximately 100 kPa and a hammer energy ratio or hammer efficiency of 60%

7.3.4 Failures related to the erosive action of water

Some failures involving the water contained in the materials (subsoil, mine tailings, mine waste rock, embankments) have been mentioned above. These include interstitial pressures that develop in the subgrade or foundation soil, or even in the backfill or tailings depending on the material and the weather conditions during construction.

Water flows can also lead to erosion of the embankment material on the surface or even to a breach in the structure. These failures can occur even long after the structure has been commissioned, or due to its operation.

External erosion by gullying

This phenomenon is a result of poorly channelled or unchannelled rainwater runoff or leaking pipes and affects both faces[13] of the dam.

External erosion by scouring

This phenomenon, resulting from wave action[14], only affects the upstream face if it is not waterproofed or protected.

Photograph 6: Scouring of the face created by wave action in a water body (Ineris)

External erosion by overflow

The passage of supernatant or effluent over the crest of the mine tailings dam can have several origins.

It can be linked to a combination of operational and meteorological phenomena, which can be considered, for example, as follows:

- the water level in the tailings pond is already high due to overexploitation or insufficient drainage;
- adverse weather conditions, heavy rainfall raises the level in the pond which collects rainwater from part of the site;
- wind action can play a role if it blows in the direction of the largest side of the pond and generates waves that break on the face, submerge it, degrade it and then create a flow by dragging the crest and eroding the downstream face.

Depending on the importance of each of these phenomena and their conjunction, the outcome can be a simple overflow or the beginning of the ruin of the structure.

[13]External faces of the dam. A distinction is made between the upstream face (on the side of the retained materials and effluents) and the downstream face

[14]Wave action caused either by the movement of a boat or by the wind and which causes the banks to degrade by mechanical action and frequent variation of the water level.

The other aspect is mechanical and generated by the differential settlement of the dam. The heterogeneous foundation soil consolidates locally with a greater amplitude, leading to a low point in the structure which can become a point of overflow. This phenomenon, which is slower, is easy to see and can be treated rapidly by reloading.

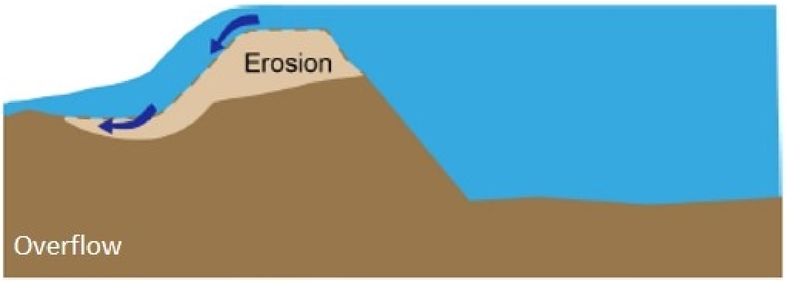

Figure 39: Diagram of overflow erosion (from www.ddrm-reunion.re)

Internal erosion

Internal erosion is mainly related to localised flow within the embankment and/or tailings mass, resulting in the detachment and mobilisation of fine particles from these materials. This can be exacerbated by the presence of pipes in or under the deposit or embankment, root channels and the action of burrowing animals. The particles being dragged can cause deterioration of the dam, with the contents spreading downstream. The phenomenon is all the more brutal as it is not anticipated: it is the so-called "erosion channel" phenomenon.

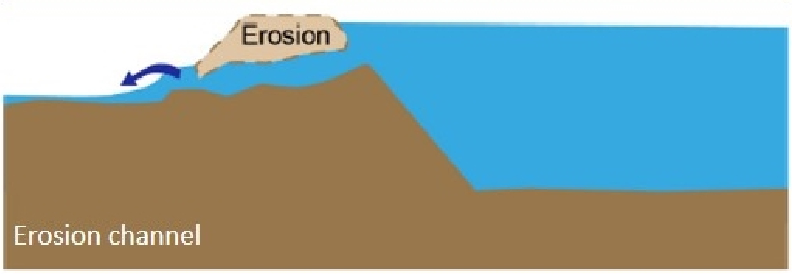

Figure 40: Diagram of internal "erosion channel" type erosion (from www.ddrm-reunion.re)

Photograph 7: Breach created by internal erosion within a levee (Irstea photo, in http://wikhydro.developpement-durable.gouv.fr)

Leaks can appear a few weeks after the first water flow, but sometimes much later. For embankments made of low permeability soils, the progression of the saturation line is very slow and the risks of the erosion channel phenomenon, essentially linked to the value of the hydraulic gradient, occur when the flow inside the embankment has reached the steady state.

7.4 Propagation mechanisms

This chapter includes elements from the Ineris report "Technical support for the development and updating of waste management regulations. Transposition of Directive 2006/21/EC on the management of waste from the extractive industries" of 19 October 2009 [44], to which elements from the documents consulted are added.

7.4.1 Immediate post-breakdown conditions

Observations of tailings dam failures generally show that there is a succession of two events (Martin et al. [73]): immediately after the failure, a wave containing water associated with the tailings and the dam material spreads very rapidly and even violently downstream, eroding and carrying away the materials it meets in its path. In a second phase, part of the tailings deposit not mobilised in the first phase is displaced by the loss of containment and the local steepening of slopes created by the initial event.

The interconnections between the voids in the non-mobilised tailings are limited and only allow for slow dissipation of the interstitial pressure. In contrast, voids in a moving body of material continually change location and geometry as the solid grains move, allowing pore pressure to dissipate in seconds or less (Spence [95]).

7.4.2 Behavioural conditions of the tailings-water mixture

The flow patterns of the tailings-fill (if any) - water mixture are governed by fluid mechanics.

It is accepted that the so-called shallow media approximation (or Saint Venant approximation, see Thual [130] and Appendix 4) can be established from the flow equations (conservation of mass and momentum) for a non-compressible free-surface fluid, which is suitable for flows where the depth (or height) is small compared to other dimensions.

However, it is difficult to characterise the behaviour of this mixture which, depending on its water content at initiation and then its flow velocity once mobilised, can take on any state between a solid-liquid two-phase state and a viscoplastic homogeneous flow, as shown in Figure 41.

However, it can be argued that a minimum or "threshold" shear stress must be applied to set the tailings-water fluid in motion. This fluid is therefore not "Newtonian"[15]; considering it as such is not an apt description of this fluid's behaviour.

The flows of such fluids are therefore approximated by threshold viscoplastic behaviour laws. The Herschel-Bulkley model thus relates the shear stress τ to the strain rate γ˙ according to the model:

$$\tau = \tau_{seuil} + k\dot{\gamma}^n$$

where τthreshold is the minimum or "threshold" shear stress, k and n are two parameters

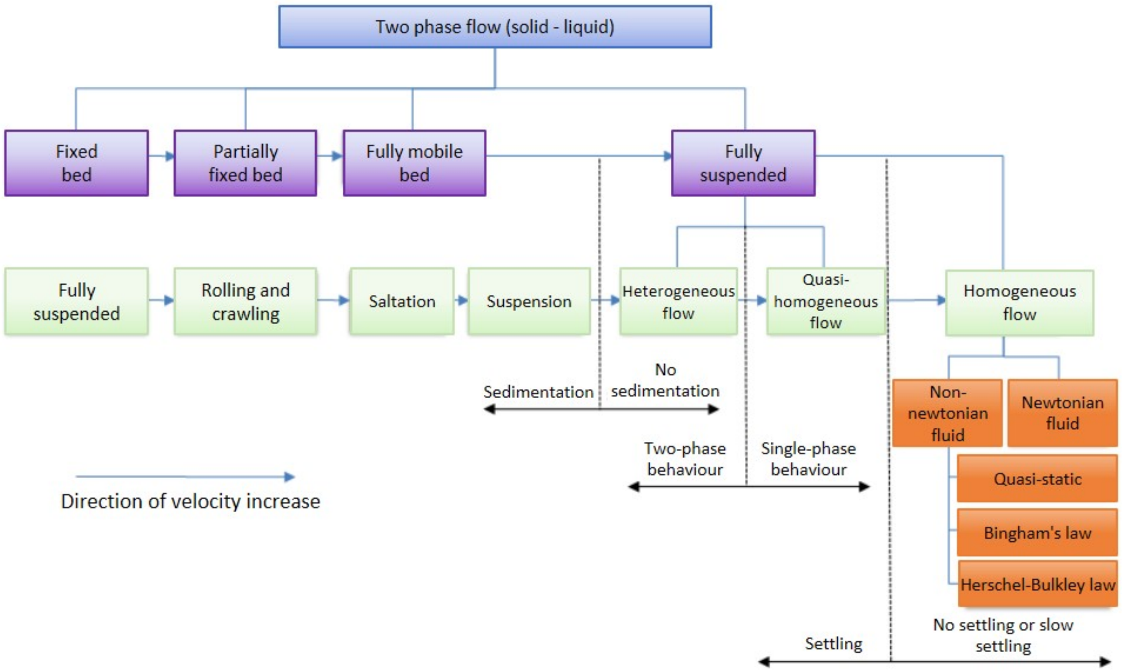

Figure 41: Classification of liquefied tailings, according to ICOLD, 1995 [115]

To describe the behaviour of this type of fluid, the Bingham model is frequently used, corresponding to the special case of the previous equation where the power n is equal to 1, i.e. the fluid has a Newtonian behaviour once it reaches the shear threshold.

The behaviour of a Bingham fluid is therefore characterised by two constants, the shear threshold and the plastic viscosity, which do not depend on the stress level or the shear strain rate (Blight et al. [13], Pastor et al. [82]). The Bingham fluid deforms elastically until the shear stress reaches this threshold, the corresponding deformations remain negligible. Once this threshold is reached, the deformation increases with the shear stress. If the external forces decrease, the velocity will also decrease until the stress falls below the threshold, at which point plastic flow stops. These fluids lead to the appearance of zones where the velocity is constant and the strain rate is zero (Pastor et al. [82]).

Some authors consider that, as soon as the tailings have a clay fraction greater than 10%, due to the interactions between particles, this shear threshold appears, and a viscoplastic model such as that of Bingham or Herschel-Bulkley can be considered preferentially (Quecedo et al. [85]).

These behaviour laws can only be calibrated by comparing the predictive models with observations made for typical configurations.

[15]A fluid whose viscosity does not depend on the mechanical stresses applied to it. It is, however, subject to the temperature

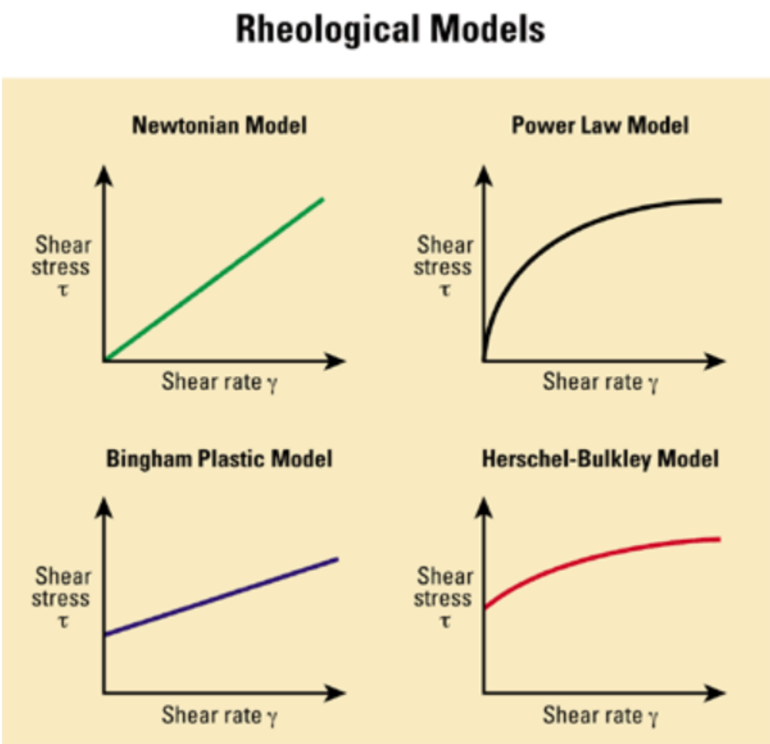

(source : http://www.glossary.oilfield.slb.com/)

Figure 42: Different rheological models (http://hmf.enseeiht.fr)

7.4.3 Flow state: laminar or turbulent?

Most of the scientific developments in fluid dynamics concern the failure of hydraulic dams, retaining water, where the flood wave generated is a turbulent flow.

It is not clear a priori whether the flow of the tailings-water fluid will be laminar[16] or turbulent following the failure of a mine dam. This is important because turbulent flow is likely to move at a much higher velocity than laminar flow, and velocity is one of the obvious variables to assess hazard.

The flow state of a fluid is characterised by its dimensionless Reynolds number, calculated from the density, velocity of a fluid and its viscosity, by the formula:

$$Re = \gamma VL/\mu$$

where:

- γ is the density of the fluid in kg/m^3;
- V is the characteristic velocity of the fluid in m/s;
- L is a characteristic dimension in m (e.g. the width of the flow channel);
- μ is the dynamic viscosity of the fluid in Pa.s.

For a Newtonian fluid, the transition between laminar and turbulent flow is established around Re = 2000 (Blight et al. [13], Jeyapalan et al. [56]).

For a Bingham fluid, it can be determined whether a flow will be laminar or turbulent using Hanks and Pratt (1967, [117]) or the Takahashi criteria (2007, [129]). The critical Reynolds number for the transition

[16]A flow is said to be laminar when it is regular (does not show too many spatial or temporal variations in velocity), often stationary. A flow is said to be turbulent when it is marked by sudden and random variations in velocity at each point.

from turbulent to laminar is expressed in terms of the Hedström number[17] (in Jeyapalan et al., [56], Figure 43)

Jeyapalan et al. [56] differentiate in this way between phosphate tailings which have a turbulent behaviour, unlike other tailings for which the flow would be laminar. This distinction is criticised by Vick [101] who believes that it is not easy to predict the nature of the flow state solely on the basis of the type of tailings.

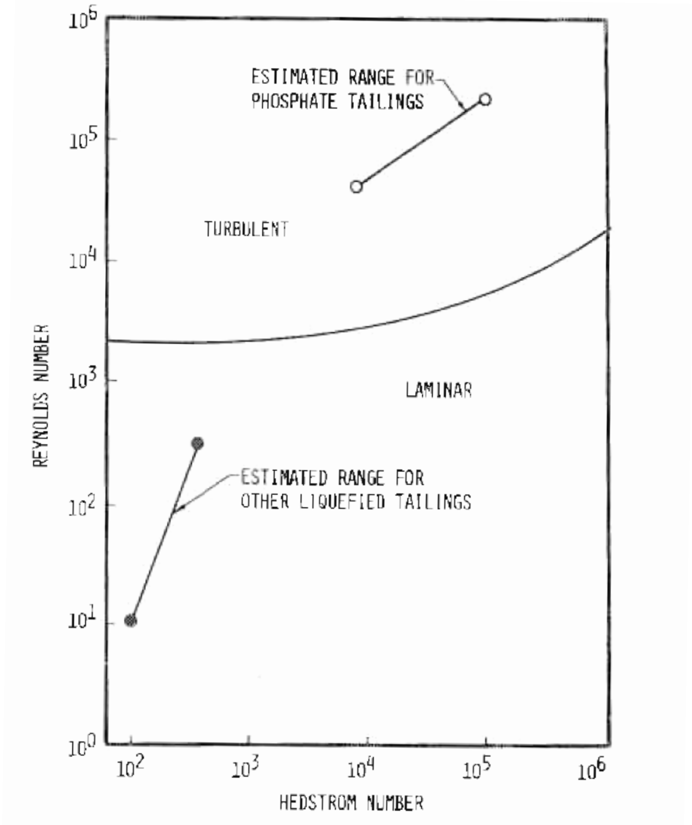

Figure 43: Positioning of laminar and turbulent flows according to critical Reynolds number and Hedstrom number. Positioning of phosphate and other tailings according to Jeyapalan et al. [56]

Table 9: low parameters of liquefied mine tailings from Jeyapalan et al., 1983, [56], and Jin and Fread, 1997,([121], in Pastor et al. [82])

Source	Parameter	Minimum	Maximum
[56]	Volumic mass	1400kg/m³	1800kg/m³
[121]	Volumic mass	1570kg/m³	1764kg/m³
[56]	Shear threshold	1kPa	7kPa
[121]	Shear threshold	38Pa	4.794kPa
[56]	Plastic viscosity	0.1kPa/s	5kPa/s
[121]	Plastic viscosity	2.1Pa/s	958Pa/s
[56]	Flow height	5m	15m
[56]	Flow speed	1.5m/s	6m/s
[56]	Reynolds number	10	300
[56]	Hedström number	100	350

It appears therefore that both flow states must be taken into consideration and that there are no criteria, to our knowledge, that would allow us to judge a priori whether the tailings-water fluid is turbulent or

[17] A dimensionless number used in rheology to treat the flow of non-Newtonian fluids, known as Bingham fluids. It is used to characterise the type of flow (laminar or turbulent) for these fluids. This number is a function of the shear stress, the dynamic viscosity and the density of the fluid.

laminar. The water content of the material stored behind the dam should be one of the most influential parameters in the nature of the flow, as well as the abrupt or gradual nature of the failure.

7.4.4 Classification of debris flows according to solid phase characteristics and flow height

Pirulli, in 2017 [83], provides a presentation of the different debris flows summarised below.

This author cites Takahashi (2007, [129]) who defines two main types of debris flows: one is the quasi-static debris flow, where the Coulomb-type shear stress between solid particles dominates, and the other is the dynamic debris flow.

Quasi-static casting assumes that the concentration of solids (C) is sufficiently high to ensure that the particles are always in contact, even if their position changes continuously. Bagnold (1966) estimated that this condition is met when C is greater than 0.51 for beach sand, but this value depends on the size of the particles. In this case of high solids concentration, non-contact stresses become negligible.

Dynamic debris flows can be divided into three subclasses:

- when grain collision forces dominate, the debris flow becomes a stony-type flow;
- when turbulent forces dominate, the flow becomes a turbulent-slurry type flow;
- and, when fluid viscosity forces dominate, the flow is in the viscous flow subclass.

Changing from one type of dynamic flow to another depends on:

- the concentration of solids;
- the "relative height" of the flow, h / d (where h is the flow height and d is the particle size);
- the dimensionless Bagnold number[18] (which is essentially the ratio of the characteristic shear stresses due to grain collisions and liquid viscosity) and the Reynolds number. When the Bagnold number is large and the relative depth is small, there is a stony debris flow. When the Bagnold and Reynolds numbers are small, there is a viscous flow. When the relative depth and Reynolds number are high, there is a turbulent, muddy debris flow.

During the flow there is still contact between particles and a so-called residual shear strength, depending on the type of material, its initial density, and the flow rate.

The interconnections between the voids in the non-mobilised tailings are limited and only allow for slow dissipation of the interstitial pressure. In contrast, voids in a moving body of material continually change location and geometry as the solid grains move, allowing the interstitial pressure to dissipate in seconds or less (Spence, 1992, [95]).

[18]Number used to characterise the flow of sand grains. It is used to determine the conditions under which the flow changes from a threshold fluid to a granular fluid where the energy is dissipated by impact between the grains and no longer by friction. It represents the ratio between the kinetic energy dissipated and the energy dissipated by impact between the grains of sand. When the Bagnold number is higher than 450, the flow has a granular state and when it is lower than 40, the state is viscous. The Bagnold number can be expressed as follows:

$$Ba = \frac{3 \cdot C \cdot \rho_f \cdot v^2}{4 \cdot d_p \cdot \rho_p \cdot g}$$

where C is a constant, ρ_f is the density of the fluid, v is its velocity, d_p is the diameter of the solid particles, ρ_p is their density and g is the acceleration of gravity

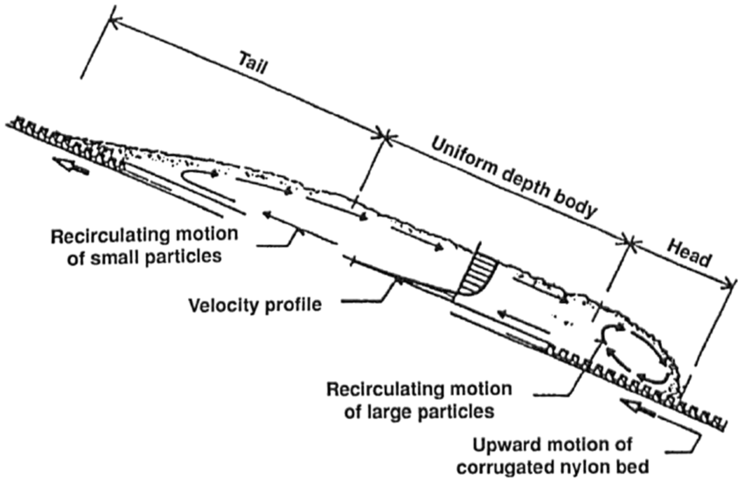

Figure 44: Diagram of a granular fluid flow (Davies, 1988, in Spence, [95])

7.5 Estimation of intensity and geographical extension parameters: the different approaches

7.5.1 General considerations

The intensity of a flow, i.e. by extension its potential for danger and destruction, depends on its height at a given point downstream of the breached dam.

This intensity is also dependent on the velocity of the flow, also at a given point; this parameter is complex to analyse, depending on the numerous intrinsic and extrinsic parameters which govern the flow conditions and states, as mentioned in the previous chapter.

Due to this complexity in assessing velocity, and in order to take a safety perspective, the Ineris guide to mining hazards [49] only uses the height parameter to assess intensity (Table 7). When this height is greater than 50cm, whatever the speed of the flow, the intensity is said to be high.

The geographical extension of a flow is important to estimate in order to map the areas that may be impacted by the flow, and in particular the areas of expected high intensity where risk management and planning measures need to be taken, both during the operation of the dam and in the post-mining phase.

The following chapters describe the main geometric input parameters, which are the basis for the assessment of these intensity criteria, and the assessment tools that have been found in the literature, without aiming to be exhaustive, but by specifying the interests and limitations of the methods used.

7.5.2 Geometric input parameters

The volume mobilised

Without taking into account the type of failure occurring within the tailings dam, the proportion of mobilised volume in relation to the total volume of the tailings deposit is an input parameter that should be assessed and is discussed by many authors. According to the statistical model of Rico et al. [87], based on feedback from failures, this volume can be estimated to be about one third of the total volume, and this approach is used quite commonly, for example in Canada. Martin et al, 2015 [73] compared this statistical assessment with an approach based on the volume of free water within the deposit, where the mobilised volume is considered to contain, by mass, 65% solid.

We note that, for an equal volume of tailings, this mobilised value of approximately one third of the total volume is exceeded as soon as the volume of free water exceeds 10% of the tailings volume. In addition, we saw in the previous chapter that the volume of water stored has a considerable influence on the flow condition and state.

Table 10: Evaluation in millions of cubic metres of the volume mobilised after rupture, according to the approach of Rico et al. [87], and that related to the volume of free water of Martin et al. [73]. The dry density of the tailings is taken to be constant and equal to 14kN/m³, the density of the solid grains being taken to be equal to 26.5kN/m³

Volume of Free Water	Volume of Stored Tailings(1)	Total Impounded Volume	Outflow Volume(1) (Rico et al. 2007)	Outflow Volume(1) (65% Solids)
1	214	215	80 (37%)	5 (2%)
5	214	219	82 (37%)	23 (10%)
10	214	224	84 (37%)	45 (20%)
19	214	233	87 (37%)	87 (37%)
40	214	254	95 (37%)	181 (71%)

1. Volume of stored tailings and outflow volume include interstitial water.

The height of the breach in the dam

The height of the breach is a parameter that is sometimes used to estimate the mobilisable volume of mine tailings located in a set-back area, and to draw up charts. The evaluation of this breach height assumes that the prospective failure mechanism is well understood, wherever the structure definitely has a stable foundation, in order not to consider the total height of the dam.

It should be noted here that the width of the breach within a dam is a parameter rarely explicitly considered in the literature.

7.5.3 Statistical models and empirical formulae related to feedback

Flow distance - Rico et al.

Rico et al. [87] have established interesting correlations based on feedback from twenty-nine cases of failure (Table 11).

An approach to the quality of the correlation, presented in Annex 2, was established by Ineris in a report entitled "Technical support for the development and updating of regulations related to waste management. Transposition of Directive 2006/21/EC on the management of waste from extractive industries" of 19 October 2009 [44].

On this basis, the graph in Figure 45 makes it possible to assess, for a given site with its specific characteristics, the potential flow distance D (in km in what follows), by linear regression and according to an envelope curve, as a function of the "dam factor" (product of its height H, in m, and the mobilisable volume V_{mob}, in millions of m³).

Table 11: List of the 29 cases of retention dyke failure used by Rico et al. [87].

Historical tailings dam failures used in the correlation analysis

Ref. no.	Name of the dam	Date of failure (year)	Type of dam	Dam height (m)	Impoundment volume ($\times 10^6$ m^3)	Run-out distance (km)	Dam factor ($H \times V_F$)	Released volume ($\times 10^6$ m^3)
1	Arcturus (Zimbawe)	1978	RING	25	1.7–2.0 Mt	0.3	0.5	0.0211
2	Bafokeng (South Africa)	1974	RING	20	13	45	60	3
3	Baia Mare (Romania)	2000	UPS	7	0.8	0.18	0.7	0.1
4	Bellavista (Chile)	1965	RING	20	0.45	0.8	1.4	0.07
5	Buffalo Creek (USA)	1972	UPS	14–18	0.5	64.4	7–9	0.5
6	Cerro Negro No.3 (Chile)	1965	UPS	20	0.5	5	1.7	0.085
7	Cerro Negro No.4 (Chile)	1985	MXSQ	40	2	8	20	0.5
8	Churchrock (USA)	1979	WR	11	0.37	96.5–112.6	4.07	0.37
9	Cities Service (USA)	1971	WR	15	12.34	120	135	9
10	El Cobre Old Dam (Chile)	1965	UPS	35	4.25	12	66.5	1.9
11	Galena Mine (USA)	1974	UPS	9		0.61	0.034	0.0038
12	Gypsum Tailings Dam (USA)	1966	UPS	11	7 Mt	0.3	0.88–1.43	2×10^5t
13	Hokkaido (Japan)	1968	UPS	12	0.3	0.15	1.08	0.09
14	Itabirito (Brazil)	1986	Gravity	30		12	3	0.1
15	La Patagua New Dam (Chile)	1965	RING	15		5	0.525	0.035
16	Los Frailes (Spain)	1998	RING	27	15–20	41	53.51	4.6
17	Los Maquis (Chile)	1965	UPS	15	0.043	5	0.315	0.021
18	Merriespruit (South Africa)	1994	RING	31	7.04	2	18.6	2.5 Mt
19	Mochikoshi No.1 (Japan)	1978	UPS	28	0.48	8	2.24	0.08
20	Mochikoshi No.2 (Japan)	1978	UPS	19		0.15	0.057	0.003
21	Ollinghouse (USA)	1985	WR	5	0.12	1.5	0.125	0.025
22	Omai (Guyana)	1995	WR	44	5.25	80	184.8	4.2
23	Phelps-Dodge (USA)	1980	UPS	66	2.5	8	132	2
24	Sgurigrad (Bulgaria)	1966	UPS	45	1.52	6	9.9	0.22
25	Stancil (USA)	1989	UPS	9	0.074	0.1	0.342	0.038
26	Stava (Italy)	1985	RING	29.5	0.3	4.2	5.605	0.19
27	Tapo Canyon (USA)	1994	UPS	24		0.18		
28	Unidentified (USA)	1973	UPS	43	0.5	25	7.31	0.17
29	Veta del Agua N°1 (Chile)	1985	MXSQ	24	0.7	5	6.72	0.28

RING: ring dyke; WR: water retention; UPS: dams subsequently raised upstream; MXSQ: dam comprising different raising typology (upstream, centreline and downstream); H: dam height; V_F: volume of tailings released.

The analysis of this model by Ineris ([44], Appendix 2) showed that estimates could be made from these models but that the quality of the estimate was, a priori, low.

The results obtained by this statistical model do not concern either the height or the speed of the flood wave.

Nevertheless, the attractiveness of synthetic expressions remains undeniable from the point of view of the simplicity of use of the expressions and the accessibility of the input data. Expressions aimed at estimating the distance travelled by the flow permit an initial sorting among the retention dams, in relation to the stakes located in the estimated perimeter of influence.

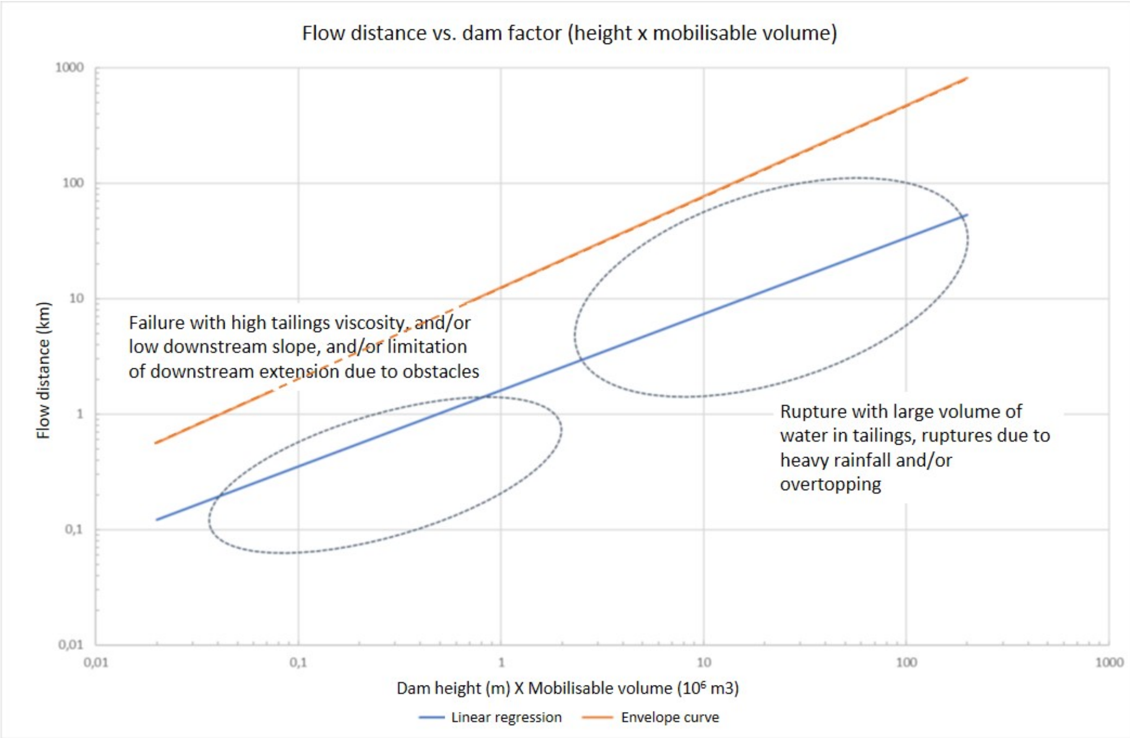

Figure 45: Chart relating flow distance and dam factor, constructed after Rico et al. [87]. The linear regression is shown in blue and the envelope curve in orange. The failure cases studied by Rico et al. are roughly grouped in two families added on this chart

Table 12: Relationships proposed by Rico et al. [87] from linear regressions, and evaluation of the quality of the estimate (Ineris, [44])

N°	Expression obtained from the linear regression Correlation coefficient r and determination coefficient r²	Number of cases used Pearson coefficient at 95% confidence level	Quality of the estimate
1a	$D = 0.05\ H^{1.41}$ $r = 0.4$ $r^2 = 0.16$	N= 29 C_p=0.367	The correlation coefficient is borderline significant. The proposed linear model does not explain the spread of values.
2a	$D = 14.45\ V_{mob}{}^{0.76}$ $r = 0.75$ $r^2 = 0.56$	N= 26 C_p=0.388	The correlation coefficient is significant. The expected quality of the estimates from equation 2a is low.
3a	$D = 1.61\ (HV_{mob})^{0.66}$ $r = 0.75$ $r^2 = 0.57$	N= 27 C_p=0.381	The correlation coefficient is significant. The expected quality of the estimates from equation 3a is low.
4a	$V_{mob} = 0.354\ V^{1.01}$ $r = 0.93$ $r^2 = 0.86$	N= 21 C_p=0.433	The correlation coefficient is significant. The expected quality of the estimates from equation 4a is average

Table 13: Expressions of the envelope curves put forward by Rico et al. [87], and evaluation of the quality of the estimate (Ineris, [44])

N°	Expression of the envelope curve	Quality of the estimate
1b	$D = 0.01\ H^{3.23}$	Average
2b	$D = 112.61\ {V_{mob}}^{0.81}$	Average
3b	$D = 12.46\ (HV_{mob})^{0.79}$	Average
4b	$V_{mob} = V$	Good

Estimation of peak flow at dam failure and distance from the dam

Costa [23] has drawn up charts, based on feedback from American dam failures (hydraulic, natural), which show the flow rate of materials as a function of the height of the dam, the volume of the impoundment and the product of the 2 (Figure 46). However, only one mining case, Buffalo Creek 1972, seems to be listed among the 31 cases studied.

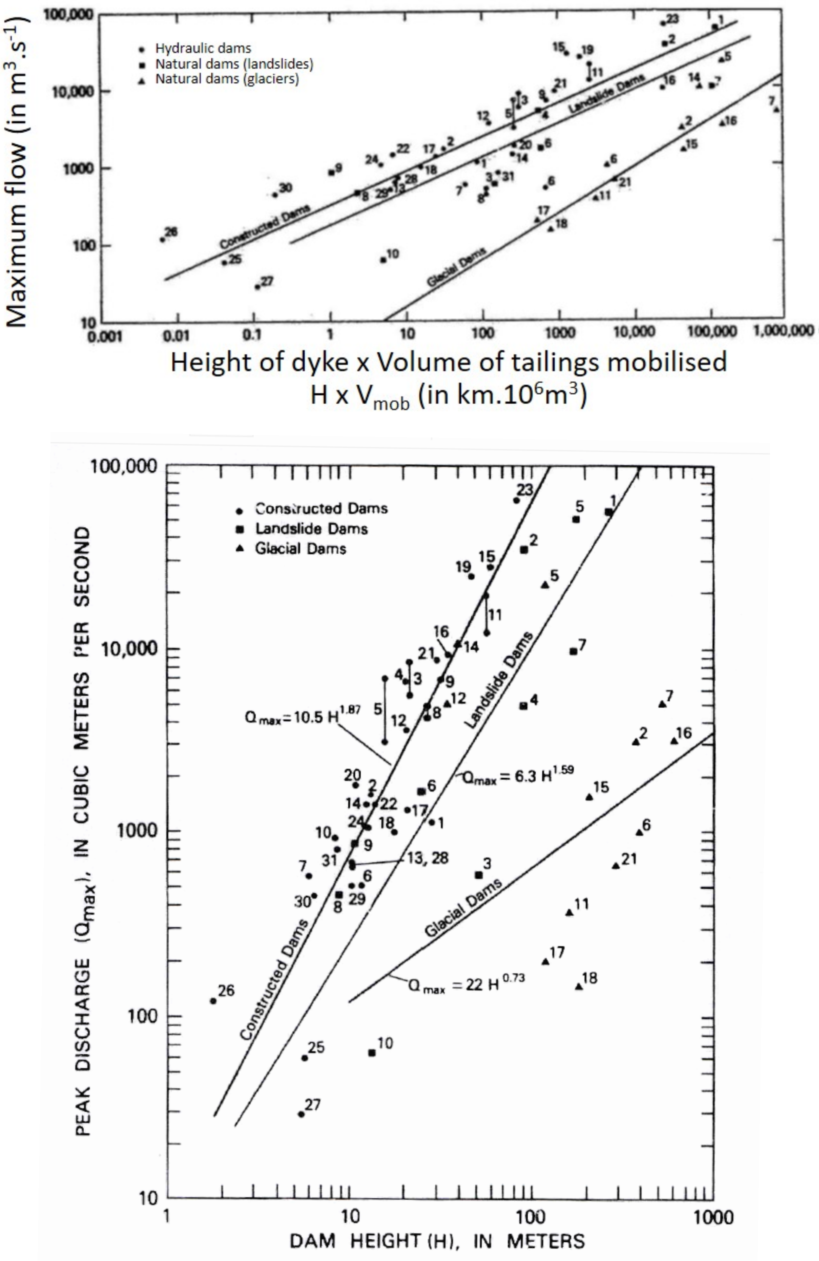

Figure 46: Graphs in logarithmic scales where the different pairs of values (HxVmob , H; Q) are plotted according to the type of dams, as well as the linear regressions obtained (Costa [23])

Based on the feedback of accident cases collected by the Yellow River Institute of Hydraulic Research of China, 1983 ([133], in Liu et al. [64]), and considering the simplified Saint-Venant equations, the maximum flow at the time of failure (in m3/s) was evaluated by Singh, 1996 ([126], in Liu et al. [64]), according to the following empirical formula:

$$Q_M = \frac{8}{27}\sqrt{g}(B/b)^{1/4}bH^{3/2}$$

where g is the acceleration of gravity, B is the length of the dam (in m), H is the height of the water near the breach at the time of failure (in m), and b is the average width of the breach (in m). This width b is itself assessed according to the following empirical formula:

$$b = K\left(W^{\frac{1}{2}}B^{\frac{1}{2}}H\right)^{1/2}$$

where W is the volume of water in the vicinity of the breach at the time of failure (in m^3), and K is a coefficient related to the nature of the dam and its strength, taken to be 0.65 for clay and 1.3 for silt.

Based on unsteady flow theory, the peak flow rate at a downstream distance L (in m) from the breach is empirically estimated by Li, 2006 ([122], in Liu et al. [64]) according to the formula:

$$Q_{LM} = \frac{W}{\frac{W}{Q_M} + \frac{L}{vk}}$$

where v is the maximum flow velocity, and k is an empirical coefficient related to the topography (0.8-0.9 in lowland areas, 1 in hilly areas, 1.1 to 1.5 in mountainous areas).

Martin et al. [73] compare peak flow values assessed according to the empirical formulas of several authors (based either on the "dam factor" or on multiple linear regressions) considering a 60m high dam with a mobilised volume of tailings and water of 23 million m^3, and then this same retention volume for a 120m high dam. The results are shown in Table 14 The values obtained for a height of 60m are fairly clustered, those for 120m are much more dispersed, which is explained in particular by the fact that the authors worked mainly on feedback from the failure of structures of lesser height.

Table 14: Comparison of peak flow values estimated, according to the formulas of different authors, for the failure of a 60m high dam, then a 120m high dam, the volume mobilised (tailings + water) being fixed at 23Mm3 (Martin et al, [73])

Table 2: Peak Outflow Estimates for a 60 m High Dam (values shown in m^3/s)

Methodology	Macdonald(1,2)	Froehlich(3)	Pierce(4,5)	Rico, Costa(6)
Dam Factor (V_w x H_w)	6,682	-	6,025	6,724
Multiple Regression	-	14,378	10,266	-
Envelope Equation	21,828	-	-	-

1. Macodnald & Langridge-Monopolis (1984) dam factor equation (Source: Wahl 2004): $Q_P = 1.154(V_{OUT} * H_w)^{0.412}$

2. Macodnald & Langridge-Monopolis (1984) envelope equation (Source: Wahl 2004): $Q_P = 3.85(V_{OUT} * H_w)^{0.411}$

3. Froehlich (1995a) multiple regression equation: $Q_P = 0.607(V_{OUT}^{0.295} * H_w^{1.24})$

4. Pierce et al. (2010) dam factor equation: $Q_P = 0.0176(V_{OUT} * H_w)^{0.606}$

5. Pierce et al.(2010) multiple regression equation: $Q_P = 0.038(V_{OUT}^{0.475} * H_w^{1.09})$

6. Rico et al. (2007) and Costa (1985) dam factor equation for constructed dams: $Q_{max} = 325[(V_{OUT}*10^{-6}) * H_w]^{0.42}$

Table 3: Peak Outflow Estimates for a 120 m High Dam (values shown in m^3/s)

Methodology	Macdonald(1,2)	Froehlich(3)	Pierce(4,5)	Rico, Costa(6)
Dam Factor (V_w x H_w)	8,890	-	9,170	8,996
Multiple Regression	-	33,960	21,853	-
Envelope Equation	29,022	-	-	-

7.5.4 Deformable solid mechanics models. Model by Lucia et al.

Lucia et al. [66] have established, on the basis of the feedback of 25 cases of failure, abacuses that make it possible to determine the final slope and the length of the spill for downstream slopes lower than or equal to 4°. The final height of the flow can therefore be determined at any point.

The details of this approach, taken from the Ineris report of 2009 [44], are presented in Appendix 3.

The schematic section of the model is shown in Figure 47. It assumes the existence of a levee of height H_B at the downstream end of the flow, and a straight slope formed by the tailings. Only three forces are considered and presented in Figure 49:

- the weight of the mobilised tailings;
- the frictional force at the interface between the natural terrain and the tailings;
- the thrust force exerted by the tailings upstream of the initial vertical axis of the dyke.

Inputs include the mobilised volume and the limit shear stress of the S_u tailings. This quantity, similar to the threshold stress of rheological laws such as the Bingham model, is difficult to estimate. However, Lucia et al. put forward values, calculated from real cases, which are provided in Table 15.

They can be presented in the form of a distance travelled chart such as the one shown in Figure 50 taken from [44]. In this case, the input data are in particular a slope of natural ground of 2%, and a total volume of stored tailings (related, in 2D, to a surface) of 1000m². The shear stress on the x-axis and four ratios of mobilised volume to total volume (four curves) have been set.

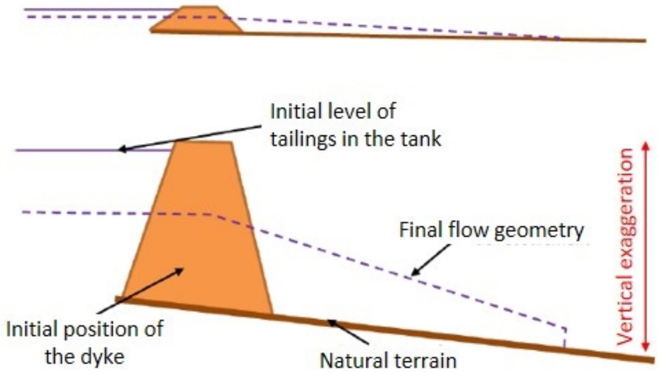

Figure 47: Schematic cross-section showing the initial and final states envisaged by Lucia et al. [66] (Ineris [44])

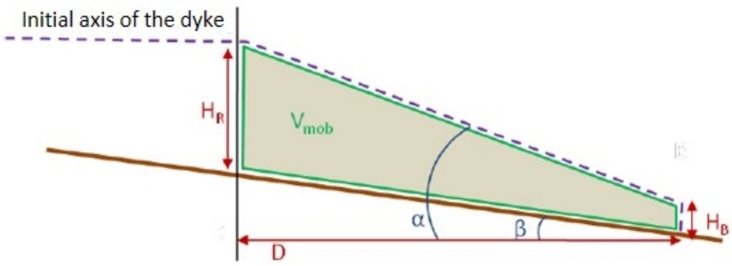

Figure 48: Typical cross-section of the final state of the flow and notations of geometric quantities (Ineris [44])

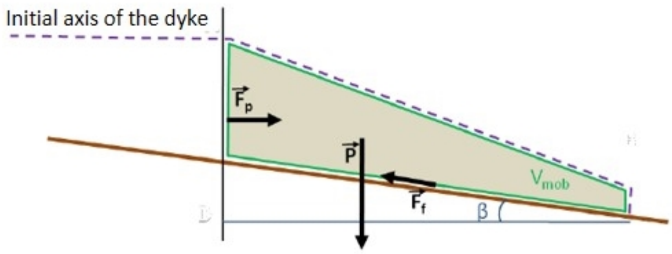

Figure 49: Balance of 2D forces on the mass of tailings mobilised in the final state of the flow, according to the assumptions of Lucia et al. [66] (Ineris [44])

Table 15: Feedback from 14 cases and estimation of final slope and shear stress of tailings after flow (S_u), from Lucia et al. [66].

N°	Type of residue	α (°)	S_u (kPa)
1	Copper processing tailings	1.5	2.4
2	Platinum processing tailings	1.3	0.7
3	Gypsum waste	1	1
4	Gold processing tailings	4 to 5	10,1
5	Coal waste	12	18
6	Coal waste	12	15.8
7	Coal waste	12	21.6
8	Tailings from porcelain manufacture	7	6.7
9	Tailings from porcelain manufacture	7	16.3
10	Tailings from carbide processing	1.5	2.5
11	Clay-fine sand	2.5	12
12	Fine sand	4	1
13	Fine sand	4	1.2
14	Fine sand	4	1.7

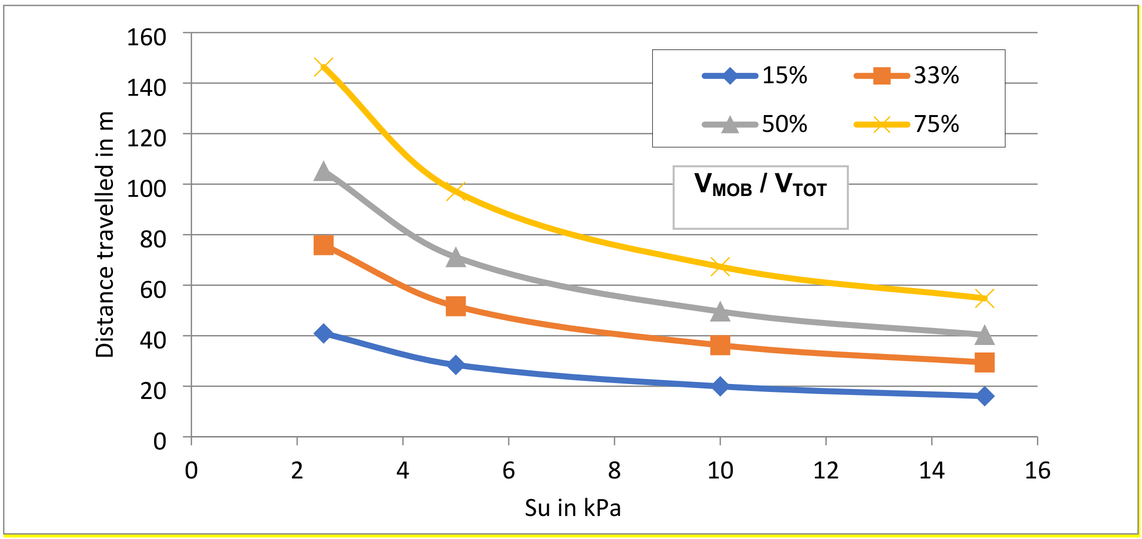

Figure 50: Example of a chart, according to Lucia et al. [66]'s model, providing the distance travelled as a function of the shear stress S_u, the ratio of the mobilised volume to the total volume. In the present case, the volume of stored tailings, reported in 2D, is 1000m2 (Ineris [44])

Limits of use

Observations of tailings flows in the field have allowed Lucia et al. to conclude that an equilibrium is difficult to envisage for natural slopes of more than 9°. Therefore the authors suggest using their model only for natural slopes of less than 4°.

This model is relatively easy to use by integrating the equations in a spreadsheet, and allows the flow distance and indirectly the residual height of the flow to be estimated at any point between the dyke and the terminal levee. The theoretical foundations of this model are satisfactory, even if certain hypotheses could be reviewed and improved, in particular the intrinsic mechanical behaviour of the tailings (see Appendix 3).

On the other hand, this type of model is not interested in the flow state and does not allow access to the velocity variable. Distances can be largely underestimated when the water content / proportion of free water in the tailings is high, as we have seen this parameter largely influences the ratio between the mobilised volume and the total volume. In other words, it is more prudent to consider low ratios, such as those observed by Rico et al. [88], when using these charts. These can be used to make an initial selection of dams where the flow-type hazard is relevant, by assessing the issues within the defined perimeter of influence.

7.5.5 Fluid mechanics models

Fluid mechanics models can easily become complex, due to the numerous parameters governing the behaviour of the tailings/water mixture, its flow condition and its interface with the ground during its course. There do not seem to be any simple models that can satisfactorily calculate the fluid flooding wave generated by the failure of a dam. We suggest the following models which can make it possible to give orders of magnitude of the sought-after values.

Ritter's Newtonian solutions and their use

This model is detailed in Appendix 4, which is based on work carried out by Ineris in 2009 [44]. It considers the flow of a Newtonian fluid in a frictionless channel

The exact solutions, quoted in Chanson [20], of the fluid velocity U and the height h as a function of time t and distance x are as follows:

$$h = \frac{H}{9}\left(2 - \frac{x}{t\sqrt{gH}}\right)^2$$

$$U = \frac{2\sqrt{gH}}{3}(1 + \frac{x}{t\sqrt{gD}})$$

$$avec\ -1 \leq \frac{x}{t\sqrt{gD}} \leq 2$$

with g being the gravity and H the initial height of the dyke.

When t leans towards infinity:

- the velocity U tends towards its minimum $2\sqrt{gH}/3$ in the definition interval. A calculation based on this limit value shows that all dykes with a height of more than 5.7cm are likely to generate a flood wave with a velocity greater than $0.5 m.s^{-1}$, which is the velocity threshold used in the hazard criterion recommended by the administration (Decree of 17 April 2010, [8]);
- the height h tends towards $4H/9$ in the definition interval. A calculation based on this limit value shows that all dykes with a height of more than 1.6m are likely to generate a flood wave of more than 0.7m in height, the threshold of the 2010 decree. This result stems from two assumptions in the model: on the one hand, the reservoir upstream of the dam is considered infinite and therefore the volume likely to flow is infinite, and on the other hand, the fluid is Newtonian and therefore stability is obtained when the fluid surface is horizontal.

These results reflect the fact that the assumptions of a Newtonian fluid in a frictionless flow are particularly safe.

By making the strong assumption that the fluid flows in a Newtonian manner but stabilises in an equilibrium position as soon as a slope criterion is reached (value lower than this criterion), it is possible, for a given configuration, to evaluate the flow time to reach this slope, and the distance covered for a desired fluid height. The following graphs give an example, for a dam height of 10m and the search for an equilibrium slope of 1° (recall that Lucia et al. estimated slope values in the context of feedback from 14 cases, Table 15).

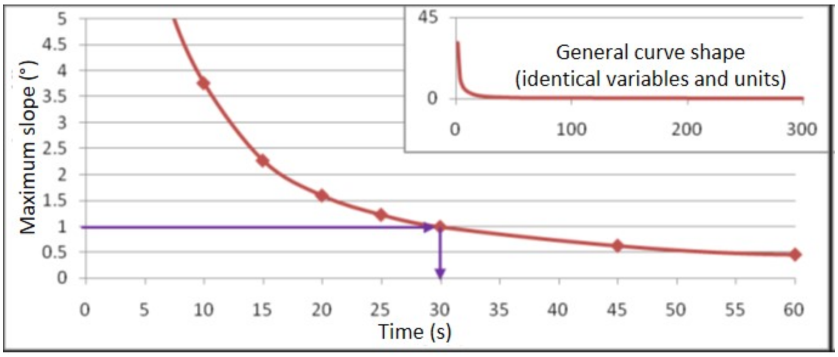

Figure 51: Maximum slope of the flow as a function of time after the failure of a 10m high dam. In purple, search for the flow time to reach a slope of 1° for the Newtonian fluid (Ineris [44])

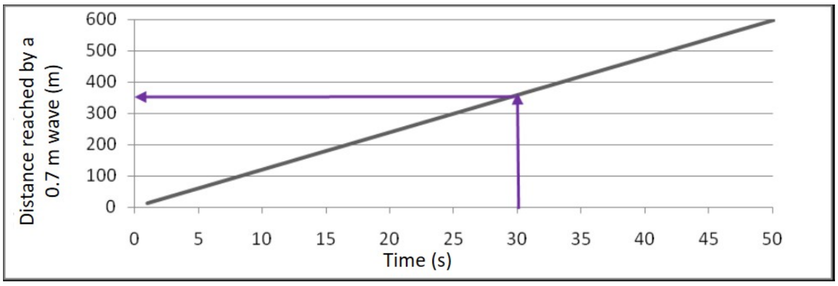

Figure 52: Application of the time taken to assess the distance travelled by a fluid of height 0.7m (Ineris [44])

The same approach can also be used for a non-zero downstream slope. The equations are reproduced in Appendix 4. For example, using the example of a 10m high dyke, with a natural slope of 2% and an equilibrium slope of 2.5%, the flow time is 75 seconds and the distance over which the wave is greater than 0.7m is estimated at 1860m.

These solutions are convenient and easy to use, but they overestimate the speed and height. In the case of no or low slope (recall that Lucia et al. [66] consider that equilibrium cannot be achieved if the natural slope exceeds 9°), these equations can nevertheless provide a safe a priori estimate of the area where the height of the tailings-water fluid is likely to be greater than a value deemed to be 'potentially dangerous', i.e. 0.5m or 0.7m.

Jeyapalan et al. model

Jeyapalan et al., 1983 [56], working on the laminar behaviour of a Bingham fluid, proposed charts (Figure 53) for the tip velocity and tip displacement as a function of time, for different values of two dimensional strength parameters related to the viscosity (parameter R) and the strength of the fluid (parameter S) which can be calculated by knowing the height of the dam, the density, the plastic viscosity and the shear threshold of the fluid[19].

The distance travelled x_f and the time taken by the flow to stop t_f, which are dimensionless parameters[20], are also provided by graphs as a function of R and S, taking into account the slope downstream of the failure zone. Figure 54 shows these charts for a zero downstream slope.

Laboratory experiments were carried out by Jeyapalan et al. [57] to confirm these analytical calculations. The application of these calculations to the observation of gypsum flows in Texas, 1966, and the Aberfan disaster in Wales, 1965, was undertaken by the same authors. It shows a fairly good correlation, with

---

[19] $R = \frac{2\eta_p\sqrt{\frac{g}{H_0}}}{\gamma H_0}$, $S = \frac{\tau_y}{\gamma H_0}$, where H_0 is the initial height of the dam, g is the acceleration of gravity, γ, η_p, τ_y are the density, plastic viscosity, fluid shear threshold, etc.

[20] To calculate the distance, the parameter x_f should be multiplied by the dam height H_0, to calculate the stopping time, the parameter t_f should be multiplied by $\sqrt{\frac{H_0}{g}}$

rather safe analytical calculations, the difficulty being the evaluation of the plastic viscosity and the shear threshold of the fluid. The calculations are even safer in the case of downstream slope, probably underestimating the effects of friction of a thin sludge layer on a rough soil.

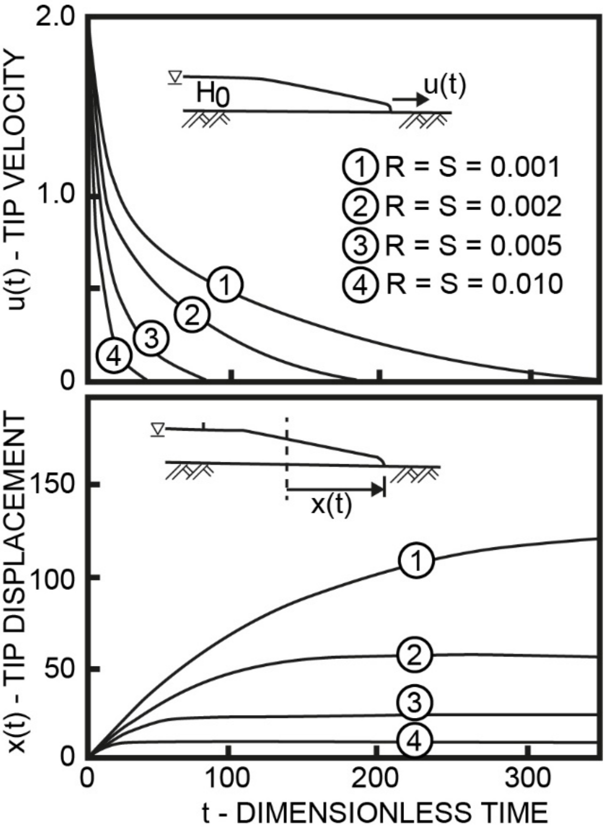

Figure 53: Abacus showing the velocity and displacement at the head of the flow, according to identical values of the dimensionless parameters R and S (after Jeyapalan et al. [56])

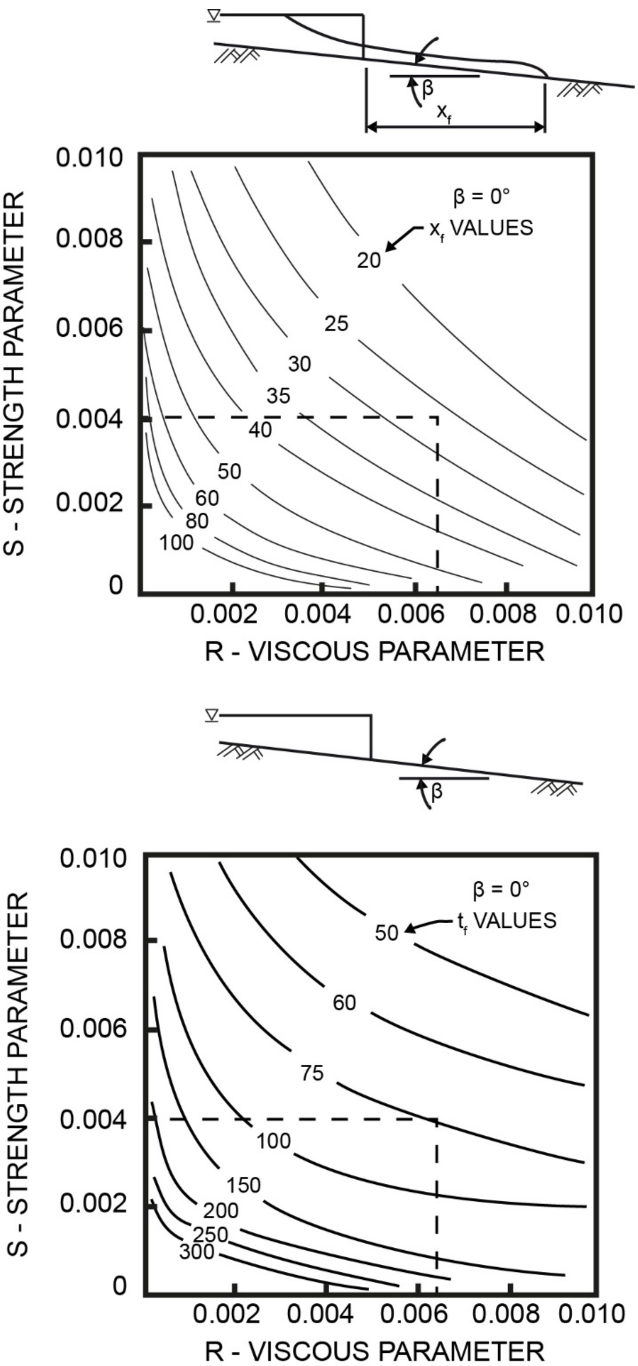

Figure 54: Graphs expressing the distance travelled x_f and the stopping time of the flow t_f, as a function of the dimensionless parameters R and S, for a zero downstream slope (after Jeyapalan et al. [56])

However, the method is criticised by Vick, 1983 [101], who points out the lack of consideration of the water content in the flowing material, its composition, and the nature of the initial failure, and calls for further investigations to support the analysis.

Chanson's model

Chanson [20] put forward implicit analytical solutions for turbulent and laminar flows. He considered a turbulent flow of a perfect fluid of the type of Ritter's solution presented above with a different treatment for the front zone as illustrated in Figure 55. Different assumptions are made at the wavefront depending on whether the flow is assumed to be laminar or turbulent. These assumptions are included in the friction term (see Appendix 4).

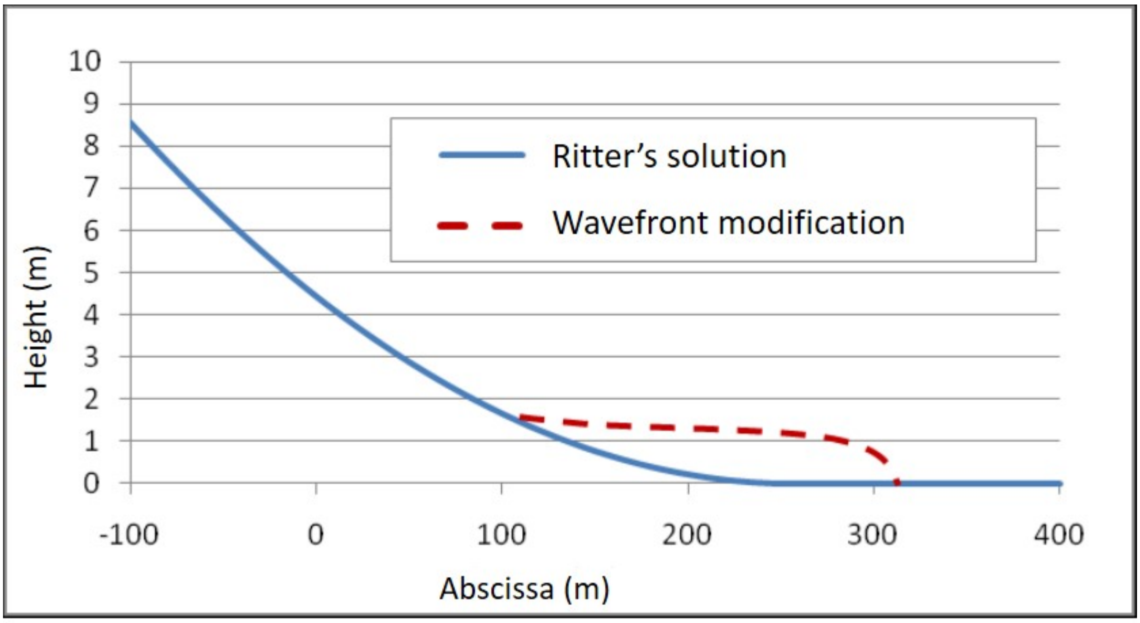

Figure 55: Principle of wavefront modification (Ineris [44])

Other models

Without aiming to be exhaustive (many 2D and 3D models exist based on the Navier-Stokes and Saint-Venant flow equations), we can note the work of Hungr, 1995 [40] which establishes the correlation between the DAN (Dynamic ANalysis) model and the field concerning the failure of mining dams.

Pastor et al, 2002 [82], refer to Hungr's frictional fluid model, where pore pressure plays an important role in the shear stress at the base of the fluid, and where an apparent friction angle is introduced:

$$(1 - r_u) \tan \emptyset'$$

r_u constant depending on the pore pressure, ϕ' effective friction angle.

By applying this and Hutchinson's [118] model to the case of the 1966 gypsum deposit rupture in Texas (East Texas), the correlation between the model and what is observed is correct except for the distance, which is less in the model. The 1966 Aberfan rupture is also well approximated by this 1D model.

7.6 Summary

Of the phenomena affecting tailings dams, the flow phenomenon is the most destructive, but also the least understood in terms of the propagation of mobilised sludge. The causes of failure described above are varying, and it can affect the whole dam and tailings from the outset and be relatively sudden (recent case of Brumadinho in Brazil) or be the consequence of erosion, natural or accidental water inflow, or mechanical instabilities initiated in the body or foundation of the dam, with very variable speeds between the first problems and the final failure.

The mobilisation of mine tailings by liquefaction, provided that their grain size is sensitive to this phenomenon, should be considered. It is caused by saturation of the materials (particularly linked to a large influx of water and insufficient or defective drainage of the effluents) and/or dynamic stresses.

While the criteria of susceptibility to triggering can be relatively easily understood, the criteria of intensity - height and speed of the sludge - and geographical extension of a flow are difficult to assess. Empirical, statistical and mechanical approaches - the latter depending on the expected flow mode - from the literature and certainly not exhaustive, have been outlined above, as an aid to analysis on a given site. The limit of use and the warning of under- or over-estimation of the intensity or extension of the phenomenon are discussed for each of the types of analysis.

Four key parameters are used to establish more detailed calculations and analyses of intensity and extent: volume of tailings, volume of free water, height of the dam and slope and morphology of the downstream area. Even if these parameters may appear trivial at first glance, it is their combined assessment and their respective weight, in relation to the type of rupture, that will allow a better appreciation of the mode of propagation and thus guide targeted models. Acquiring knowledge of these four parameters is discussed in Chapter 8.2.2.

8 How to assess the flow-type phenomenon

8.1 Limited feedback in the context of post-mining

It is worth recalling here the specificity of the tailings dam compared to other types of dam.

After operation, a structure containing potentially toxic solids and fluids must be returned to the natural environment, and the attenuation of its toxicity may continue for several decades or even hundreds of years. This means that the retention function of the structure must be considered in the long term. Therefore, potential conditions for failure, some of which may lead to flows in particular cases, must be assessed and evaluated over this long period.

In many cases, the structures have required the use of in situ materials, including mine waste rock, mine tailings and local borrow soils (fill), with variable geo-mechanical behaviour, often poor, and often dependent on their water content. During operation, the often progressive construction, depending on the evolution of the tailings disposal volume, has allowed the mine operator to adapt to the behaviour of his structure, thus allowing some flexibility in the dam project. However, this flexibility during operation can lead to a lack of quality control and monitoring of the dam which is problematic after the active life of the dam (ICOLD, [42]).

However, in general, it can be considered that the characteristics of materials improve with time, particularly through compaction and reduction in water content, and that they are, apart from major disturbances or failures in the environment of the structure, less sensitive to variations in external factors. However, there are counter-examples where the water content of the structures remains significant due to poor sealing or drainage conditions.

In any case, there is a lack of experience with the behaviour of these structures. Most tailings dams, at least the largest ones in terms of retention volume and height, were built during the twentieth century, and even, for many of them, during the last decades. We therefore have little feedback on the long-term performance of these structures once the mine has been closed or abandoned. This was emphasised by ICOLD in 2006 [119]:

> *"Experience regarding the long term behavior of tailings storage facilities (TSFs) is limited. Most are still in the phase of after care. Our knowledge is constantly increasing, but the closed and remediated tailings dams today are less than one or two decades old i.e. most experience of the long term stability of tailings dams after closure is still limited. In this case the long term is defined as 1000 years, or more."*

In France, including French Guiana, there are about sixty tailings structures. This number is relatively low compared to other Asian or American countries, but it is not insignificant.

8.2 Guiding elements to assess the flow-type phenomenon

8.2.1 Susceptibility and relevant factors

For a flow to occur within a tailings dam, various factors need to be considered.

Susceptibility factors can be divided into four categories:

- factors related to the potential for mobilisation, or even liquefaction, of the material making up the dam and/or the stored tailings;
- factors related to the natural potential for water accumulation in the vicinity of the dam;
- factors related to the potential for failure of the structure;
- Finally, factors related to the potential for degraded conditions in the vicinity of the dam, linked to external factors that may be responsible for triggering the phenomenon.

The following paragraphs present the most important factors by category, indicating their degree of importance, if necessary the more precise sub-criteria to be looked for, the ease or otherwise of acquiring data in the context of a post-operational structure, the possibility of acquiring details on these criteria through additional investigations, and, if necessary, the changing nature of the factor over time. A final summary table (Table 16) including all the criteria is then presented.

8.2.1.1 Mobilisation potential

Nature of the tailings deposit/dam materials

We have seen that the nature of the materials which make up the tailings repository and the dam is a major criterion in terms of their susceptibility to mobilisation in the form of flows. Materials dominated by fine sands and silts are the most sensitive to this type of phenomenon, which is why research into the grain or sediment composition of the tailings is important, even fundamental. If the material is gravelly or stony, or on the contrary very clayey, the mobilisation mode is no longer the same and consideration of the flow phenomenon is no longer relevant. The liquefaction capacity of a material is more or less in the same category of silts and very fine sands, so the Tsushida charts ([132], which can be seen in Figure 38) are interesting to use.

We have also seen that the estimation of relative density, in the case of fine sands, can be an important input to judge the relevance of the liquefaction phenomenon (see Table 8).

If the dam material holding the tailings is made of the same types of material, the susceptibility is further increased.

In the analysis of post-mining tailings dams, except in the case of recent structures, data on the composition of the tailings constituting the repository or the materials used to construct the dam are often not available. However, samples of materials can be taken by test pits or excavations with a mechanical shovel for grain or sediment characterisation. For excavations, care should be taken to preserve the covering and sealing devices if they exist, and to take precautions if there are potentially polluted materials. Relative density can be assessed by laboratory tests on intact samples, or by dynamic or static penetrometer testing.

Dam construction method

The method of construction of the tailings dam is also an important criterion, and is not independent of the previous one. We have seen that the dams built according to the upstream method were the most sensitive to failure, due to the use of tailings for their construction and elevation, their support on poorly consolidated materials and the absence or low proportion of materials with a more spread out and compacted grain size during the earthwork. *In contrast,* tailings dams constructed using downstream or central, or conventional methods, may have less or no sensitivity to failure resulting in tailings flow, all other things being equal.

This data on construction is relatively easy to acquire for the most recent structures, but it is more difficult to assess for the oldest structures. Characterisation of the dam materials by test pits or excavations can determine whether it is made up of mine tailings, mine waste rock or local borrow material (fill), and to assess its grain size.

Nature and state of consolidation of the subsoil

This criterion should be taken into account, although it is less sensitive than the previous ones. Indeed, it can be considered that failures linked to problems with the foundation of a dam occur preferably during the design and operation phase.

However, it is necessary to consider, for foundation materials of low characteristics (silts, sands, clays), whether variations in other factors (rise or variation in the water table, or seismicity, for example) are likely to remobilise these soils.

The nature of the bedrock should also be considered in the case of hillside dams. Due to the existence of a slope, these soils can be mobilised by sliding, creep or erosion phenomena.

This data on the bedrock is relatively difficult to assess, particularly for the oldest structures. Consultation of local geological data and observation of nearby outcrops can, however, help to assess the nature and constitution of the bedrock.

8.2.1.2 Water storage potential

Topographical position

The topographical position of the dam is a first important criterion for assessing the potential for water accumulation. A dam at the bottom of a valley is thus more sensitive than a dam located on the top of a hill or on a plateau. This criterion is very easy to obtain.

Surface area and slope

The surface area and slope of the catchment area upstream of the dam are also important criteria. The surface area of the catchment area makes it possible to assess the volume of water likely to accumulate behind the dam, according to the leakage rate of the structure and the rainfall to be considered (storm, ten-year rainfall, one hundred-year rainfall, etc.). It is important to evaluate the runoff and contribution coefficients of the areas constituting the pond, taking into account the land use (meadows, forests, surfaces sealed by human activity, etc.). Many guides exist and the calculations are relatively simple; for complex cases, consultancy firms are specialised in these fields.

The slope of the catchment area influences the time it takes for the rainwater to reach the dam (this is called the concentration time). The steeper the catchment, the shorter this time, and therefore the higher the water velocity, which can remobilise susceptible materials (see previous chapter). The calculation of the concentration time is more complex and requires specialised consultancies.

It should be noted that these two criteria evolve over time according to changes in land use: the sealing of land upstream of dams, according to the increase in human occupation and/or infrastructures, generates greater volumes and speeds of water.

Presence and position of a water table

Dams rest on a bedrock and are surrounded by formations (alluvium in the valley, colluvium on the slope) where there may be a water table and close to the foundations and base of the mining structure. Fluctuations in the water table can lead to the base of the tailings being temporarily, or even permanently, saturated.

Some recent dams that are no longer in operation are monitored with piezometry readings within the tailings repository, and sometimes within the bedrock to monitor the water table. However, over time, when not maintained or serviced, these structures can become clogged, or deteriorate, and fail or no longer perform their function.

The oldest tailings dams are, for the most part, not monitored at all. At best, for the largest dams, documents relating to piezometric monitoring during the operational phase can be found in the archives.

In the absence of data, the use of this criterion requires the construction of deep piezometers near the dam and outside the repository. The cost of such shallow structures is moderate, but provisions to prevent clogging should be taken if the evolution of the water table is to be monitored over the medium and long term.

This criterion is subject to change over time, depending on climate change, which can lead to a drop or rise in the water table depending on the region, and on human activities that can modify the drainage and fluctuation conditions of the water table.

Presence of water management and sealing devices

Tailings dams, especially the more recent ones, may have been built with devices to drain water downstream of the dam (peripheral ditches, overflow devices, drainage devices within and/or around the tailings storage and the dam). In contrast, such devices are rarely found for older dams.

In addition, some tailings ponds have undergone work to prevent water from seeping into the repository. A cover, generally made of waterproof materials (clay), was put in place in these cases. Similarly, it is rare to find such devices for the oldest tailings deposits.

It is relatively easy to assess whether such surface devices exist, but it is difficult to assess the existence of underground structures under the tailings and dam body. Work to confirm or disprove their presence is necessary in some cases (geophysical methods and/or boreholes).

8.2.1.3 Potential for failure

Age of the dam

The age of the tailings dam is not in itself a criterion that can systematically increase the potential for failure. Very old dams in good condition may be part of an environment that has returned to a natural equilibrium after the mining period, all other things being equal. Other old dams, on the other hand, may be obsolete because their constituent parts have deteriorated over time. A recent dam can contribute to disturbance of the surrounding environment, and the slightest failure of one of its constituent devices can lead to failure.

Age is therefore a criterion of information, generally easy to acquire when consulting archival documents, which implies many parameters that can play in favour or against a failure.

Condition of the dam

The condition of the tailings dam, a set of factual data based on the analysis of archival documents and the observation or even the precise auscultation of the structure, can be focused on.

The condition of the dam relates to the body of the structure itself, as well as to the associated water management works.

On the body of the structure, in the first place, the amount of vegetation can constitute a degradation factor. The roots of tree species can penetrate deeply into the material and break it down, in the event of strong winds, by mechanical mobilisation, or when the plants die, the root system no longer performing its retention function. Shrubby species have more superficial roots and have the advantage of limiting water infiltration into the structure.

Burrowing animals can damage the surface of the structure by creating cavities. These cavities are places where water can accumulate and spread in the body of the structure and cause internal erosion mechanisms.

In addition, works (reprofiling, material intake) or human developments (roads, infrastructures, overloading) can weaken the structure or constitute zones where water can accumulate or infiltrate.

The condition of associated water management structures is an important point in assessing the condition of the dam. Local mobilisation, loss of continuity and watertightness of these structures over time can favour the infiltration of water passing through the dam or constitute accumulation points for water that is no longer drained.

The existence of a tailings cover and its condition are also important. Deterioration of the cover can lead to point source water infiltration into the tailings.

It is relatively easy to assess by observation the state of the body of the structure (vegetation, presence of cavities or material intakes), the state of the lateral ditches, spillways or other surface structures, covering devices, but it is difficult to assess the state of the underground structures under the tailings mass and the body of the dam. It should also be noted that older dams often lack information on the location of these underground structures, although their outlets can be observed downstream of the structure. Camera inspections in the pipes are usually required to determine the condition of these deep structures. For old structures, preliminary location work is necessary in some cases (geophysical methods and/or surveys).

It goes without saying that this condition evolves over time, particularly due to the progressive deterioration of the structures and devices.

Management of the dam

This criterion is a linked to the previous one. A tailings dam with a high risk potential which is subject to regular, even simple, management (observations at a defined frequency, regular inspection of underground structures, localised clearing or reinforcement work) is, all other things being equal, less prone to failure or breakage than a structure which is not managed by an entity which has responsibility for it. However, it may be difficult to maintain this level of oversight over time.

8.2.1.4 Factors of degraded conditions in the dam environment

Climate-related factors

A one-off episode of heavy rainfall (storm), or a period of heavy rainfall, are climatic factors likely to cause the failure or rupture of the structure. For example, in France, Mediterranean episodes (Cevennes being the most notable) where the equivalent of several months of rainfall falls in a few days or even a few hours (more than 200mm in 24 hours). The rainy season and the cyclonic period in tropical environments can also generate very heavy rainfall over a 24-hour period, which is the cause of many failures when you look at the bibliography of accidents.

As we have seen, most recent hydraulic structures are designed to cope with rainfall for recurrence intervals of 10, 20, 30 years, and more rarely 100 years. But this is not the case for most tailings dams, including the oldest ones.

Furthermore, the forecasts, in connection with global warming, consider an increase in extreme precipitation for certain areas of the globe: this is the case in mainland France for the period 2071-2100, with a high degree of variability depending on the area (Jouzel, 2014, [59]).

In the same report, an increase in heat waves and drought episodes is also reported for the end of the 21st century in mainland France. The alternation of these dry spells and consecutive heavy rainfall fosters the infiltration of water into the cavities and crevices generated in the tailings due to their very low water content, the failure of the Malvési pond mentioned in this report being an illustration of this.

This climate data in the vicinity of a facility under study can be acquired fairly easily from a national or regional meteorological service. Climate forecasts for this century can also be obtained, with varying resolution and confidence levels depending on the country and the predictive models. In France, the Drias portal (http://www.drias-climat.fr/) provides regionalized simulations with a resolution of up to 12km.

Earthquakes

One of the known factors for triggering the liquefaction mechanism of sandy-silty tailings (see chapter 7.3.3) and then failure or rupture of the dam is the consequence of an earthquake near the structure.

Information on the threshold for liquefaction, in terms of the value of acceleration generated by the earthquake, appears to be patchy, and is also dependent on the ratio between the shear stress generated by the earthquake and the cyclic shear strength of the material (Javelaud, Serratrice, 2018, [55]).

The most widely used seismic zonings in the world refer to the value of the peak ground acceleration (PGA). The French seismic regulatory zoning implemented since 2011, considering a reference recurrence interval of 475 years, qualifies the seismic hazard as moderate in areas where this acceleration is greater than $1.1 m/s^2$, medium when this value exceeds $1.6 m/s^2$ and high when above the value of $3 m/s^2$.

Using these values, it can be considered that the influence of a potential earthquake on the susceptibility to failure should be addressed for acceleration values above $1.1 m/s^2$ (or 0.1g, where g is the acceleration of gravity) and should be the subject of a detailed study in areas of acceleration above $3 m/s^2$ (or 0.3g). Of course, the liquefaction capability of the tailings, discussed above, should be considered first. It is also necessary to consider whether the ground on which the dam is to be built is not also conducive to liquefaction.

It goes without saying that these studies should be used to establish a stability analysis of the body of the dam, which may be made of another material. On this subject, reference can be made to the MEDDE report on seismic risk and the safety of hydraulic structures drawn up in 2014 [134].

Presence of voids

Tailings dams may have been built in the vicinity of underground voids, whether mining or otherwise, whose instability could result in mobilisation of the dam and/or tailings. These include underground mine workings (panels and chambers), mining infrastructure (mine shafts, drifts and galleries, boreholes or shafts for hydrocarbon or salt mining), but also voids of natural origin (karst, gypsum dissolution zones) or human origin (former underground quarries, galleries or cavities of historical origin or linked to former infrastructure).

The most exhaustive inventory possible of these cavities in the vicinity of the dam and tailings pond should be made, using archival documents and plans and evidence in the field. Soundings may be taken to assess the condition of shallow cavities. The objective is to determine whether a failure of these cavities could lead to mobilisation of the dam and tailings.

Table 16: Susceptibility factors - Summary table

Potential	Susceptibility factors	Weight of the factor	Ease of acquisition through documentation / observation	Additional possible investigation	To look out for	Changing factor in the long term
Mobilisation potential	Nature of the material	High	*	Sampling, boreholes, penetrometers, excavations, laboratory tests	Grain size analysis, size analysis by sedimentation Fraction sables/silts Grain size range Relative density (sand)	No
	Construction method	High	*	Soundings, excavations with mechanical shovels)	Nature of the material (tailings or compacted material) Upstream method or other	No
	Nature and state of consolidation of the subsoil	Moderate	**	Soundings Potential laboratory tests	Rocky or loose nature Classification of the soil Presence of possible embankments	No
Water storage potential	Topographical position	High	***	Not relevant	Valley bottom dam, hillside dam, other	No
	Surface area and slope	High	**	Usual hydrology calculations	Retention volume, time of concentration, according to a given recurrence interval (100 years)	Yes
	Presence and position of a water table	High	*/ **	Piezometer	Depth and fluctuation of water table. High position in residue?	Yes
	Presence or absence of drainage/waterproofing devices	High	*/ ***	If necessary, geophysics and surveys for the presence or absence of underground structures	Presence or absence of these devices	No
Potential for failure	Age of the dam	Limited	***	Not relevant	See "Condition of the dam"	Yes
	Condition of the dam	High	*** (dam body), */ ** (water management structures)	Survey/auscultation/camera survey of the condition of underground drainage systems If necessary, geophysics and surveys to locate underground structures	Body: condition, presence of cavities (burrowing animals), taking of materials, penalising vegetation Condition, continuity, watertightness, maintenance of the slope (absence of low points), absence of obstacles	Yes
	Management of the dam	Moderate	***	Not relevant	Is there a site manager? Sustainability of the latter over time? What maintenance and monitoring arrangements are in place and how often?	Yes
Potential factors of degraded conditions in the dam environment	Climate-related factors	High	**	Site-specific climate projections	Current balances and 50-100 year forecasts: Monthly, daily rainfall, or even shorter time steps depending on site specificity Number of dry days, correlation between dry periods / periods of high rainfall	Yes
	Earthquakes	Variable depending on region (seismic zoning)	***	Not relevant except for very specific case	Acceleration from ground to rock. Signal analysis / Associated shear stress for specific complex cases	No
	Presence of voids	High	**	Soundings to recognise voids	Distance, depth, volume and condition of cavity Is the dam/tailings pond within the area of influence of a potential rupture of the void(s)?	Yes (evolution of the cavities)

8.2.2 Geographic (mapping) intensity and extension factors

Here we present the main factors involved in the assessment of the intensity and the cartographic extension. As these two objectives of intensity and propagation distance assessment are closely intertwined in the case of the flow phenomenon, they have been deliberately grouped together.

In the same way as for the susceptibility factors, the ease or otherwise of acquiring data in the context of a post-exploitation structure, the possibility of acquiring details on these criteria by complementary investigations and, if necessary, the changing nature of the factor over time are addressed. A final summary table (Table 17) including all the criteria is then presented.

8.2.2.1 Volume of tailings

The volume of tailings stored behind the dam that can be released is, as we have noted, a prominent factor in the intensity. The proportion of the mobilisable volume to the total tailings volume is difficult to assess, ranging from one third to 100% depending on the proportion of free water. The total tailings volume is therefore an important data to acquire.

For the oldest dams, this information is rarely available in the archives. For the more recent structures, this data is easier to find.

Examination of documents such as old topographic records and aerial photographs can help to estimate the extent and surface geometry of the tailings pond. This can be fairly easily corroborated by field observation where the break in slope, the difference in outcrops, the difference in vegetation are all clues to the delineation between the natural terrain and the tailings.

If there is no evidence of this in the archive documents, the height of the tailings on the path is less easy to acquire. It can be estimated if the natural slope prior to deposition is considered to be relatively even, but this is more difficult if the natural slope is uneven. Boreholes can then be drilled, spread over the tailings area, down to the bedrock. For large areas, geophysical profiles can also be used if the expected contrast between the tailings and the bedrock is significant (e.g. tailings / solid rock).

8.2.2.2 Volume of free water in the tailings

The volume of free water (i.e. not physically and chemically bound to the soil/tailings particles) within the tailings, and in particular in the vicinity of the dam, is also a prominent factor. This is in line with the considerations of water accumulation potential mentioned in the predisposition factors, but it is a factor of intensity and extension in the sense that an increase in the head of free water behind the dam can lead to higher flow velocities and distances.

This factor, which evolves over time, is difficult to assess without specific investigations. The investigations to assess the volume of water in the dam and the position and fluctuation of the water table in the tailings, discussed in Chapter 8.2.1.2, are identical. It is recommended that degraded situations (100 year rainfall for the calculation of the retention volume, highest possible water level in the tailings) be considered when assessing this free water volume.

It should be noted that this factor is subject to change with respect to the climate forecasts discussed in Chapter 8.2.1.4.

8.2.2.3 Height of the dam

We have seen that many organisations and authors consider the product of mobilisable volume and dam height (often referred to as the dam factor) as a relevant intensity parameter.

It can be noted that the height of the dam has a significant influence on the mobilisable volume and on the potential free water level behind the structure, which is why this factor is also very important.

Therefore, all other things being equal, a low height structure retaining tailings spread over a large area will lead to a lower intensity than a high height structure retaining tailings of small extension upstream.

This data has the advantage of being easy to acquire through field observation, except in the case of inaccessible or overgrown structures.

It should be noted that the length of the dam was not taken into account, a factor rarely used in the literature. The assessment of the width of the breach in case of failure is indeed very difficult, as almost the entire structure (case of Brumadinho, Brazil) or part of it can be mobilised instantaneously or by successive failures over a short time.

8.2.2.4 Slope and morphology of the downstream area

Downstream of the tailings dam, the slope and morphology of the terrain play an undeniable role in both the intensity (height, speed) and the extension of the flow. Topographic information provides an overall idea of the topography, but the scale is too small to appreciate local variations in slope, obstacles, vegetation, infrastructures and buildings. Therefore, detailed field observation is essential to identify these elements.

If you want 3D flow models, when the susceptibility to failure justifies it, accurate Digital Terrain Models (DTMs) can be made. Many tools are now available to obtain detailed topography and ortho-referenced photography: traditional surveyor's surveys, terrestrial laser scanning or airborne Lidar (the latter two requiring little vegetation in the area studied), etc.

This factor changes over time, insofar as plant species can develop and vary, and human occupation (buildings, infrastructures) can also be modified.

Table 17: Intensity factors - Summary table

Intensity factors	Weight of the factor	Ease of acquisition through documentation / observation	Additional possible investigation	To look out for	Changing factor in the long term
Volume of tailings	High	*	Soundings, geophysical profiles if there is a strong contrast between tailings and bedrock *Link to 'nature of material' and 'mode of construction' criteria in*	Height of tailings at several points, mesh to be adapted according to the surface of the tailings and the expected topographic variability of the terrain under the tailings	No
Volume of free water	High	*	Usual hydrology calculations Piezometers (at least one near the dam) Site-specific climate projections *Link to "catchment area and slope", "presence and position of water table" and "climatic factors" criteria in*	Retention volume, time of concentration, according to a given recurrence interval (100 years) Depth and fluctuation of the water table in the tailings. PHE value in tailings Current balances and 50-100 year forecasts: Monthly, daily rainfall, or even shorter time steps depending on site specificity	Yes
Height of the dam	High	***	Not relevant, except for works allowing access in particular areas (steep location, vegetation)	Height, (width, length)	No
Slope and morphology of the downstream area	High	*	Survey, terrestrial laser scan, airborne lidar, DTM	Total slope, slope per section, morphology, width, natural or man-made obstacles, nature of vegetation cover	Yes

8.2.3 Elements for estimating the intensity and geographical extent

Here we group together the elements from the bibliography compiled to estimate the intensity of the phenomenon and its geographical extension. The previous chapters have shown how difficult it is to evaluate these parameters, so we insist on the fact that the models used only give a first idea of the estimate of the spread of the flow.

These estimates will have to be compared with the presence or absence of issues downstream of the dam (dwellings, infrastructures, buildings, tourist areas and paths, etc.).

Table 18: Estimation of the intensity and distance travelled - Summary of the models mentioned in the report

Estimated parameter	Model	Chapter and annex	Articles	Comments
Height of the flow	Lucia et al. Deformable solid mechanics	7.5.4 Appendix 3	[66]	Indirect estimation of height as a function of distance travelled. Simple use (Excel spreadsheet). Not valid for downstream slopes greater than 9°. Use with caution above 5°. Underestimation of distance ➔**overestimation of height**
	Ritter Newtonian fluid mechanics	7.5.5 Annex 4		Practical and easy to use solutions (Excel spreadsheet integration) Not valid for downstream slopes greater than 9°. Use with caution above 5°. **Overestimation of height**
Flow speed	Ritter Newtonian fluid mechanics	7.5.5 Annex 4		Practical and easy to use solutions (Excel spreadsheet integration) Not valid for downstream slopes greater than 9°. Use with caution above 5°. **Overestimation of speed**
	Jeyapalan et al. Bingham type fluid mechanics	7.5.5 Annex 4	[56]	Input data not easy to acquire (plastic viscosity, shear threshold). The downstream slope can be integrated. Overestimation of the distance ➔**Possible underestimation of the height**
Distance covered by flow	Rico et al. Statistics	7.5.3 Appendix 2	[87]	Practical and easy to use solutions (abacuses). Need to assess the mobilisable volume of tailings (Table 10 Chapter 7.5.2) Low correlation coefficients in simple regression Envelope curve **overestimates distance**
	Jeyapalan et al. Bingham type fluid mechanics	7.5.5 Annex 4	[56]	Input data not easy to acquire (plastic viscosity, shear threshold). The downstream slope can be integrated. **Overestimation of distance**

Empirical flow estimates are also discussed in the body of the report. As this parameter is not directly related to an intensity, it is not discussed in this table.

It should be noted that in the case of a steep downstream slope most of these models are no longer valid, and specific studies become indispensable.

8.2.4 Proposed hazard assessment

Table 19 recommends "flow" hazard levels according to susceptibility and intensity classes, following the spirit and adopted nomenclature of the Ineris mining hazard guide [49]. Due to the potentially damaging nature of this phenomenon, no low level hazard and limited class intensity is retained. The analysis of susceptibility factors such as the nature of the materials and the mode of construction of the dam can lead to considering this phenomenon to be irrelevant, as shown in the table.

Of course, the irrelevance of this hazard does not exclude the assessment and evaluation of other ground movement phenomena related to these structures.

No weight is given here to the factors leading to a particular susceptibility or intensity class. The analysis of the factors in chapters 8.2.1 and 8.2.2 should enable the expert in charge of a site-specific study to evaluate the classes.

Table 19: Proposed flow hazard levels

Intensity ➡ *Susceptibility* ⬇	Moderate	High	Comments on relevance/susceptibility
Not relevant	None		Factors such as the nature of the material and the method of construction of the dam may be irrelevant (gravelly material or blocks, method of construction)
Barely noticeable	Average	High	The analysis of the factors in Chapter 8.2.1 should make it possible to assess a susceptibility class
Noticeable to Very Noticeable	High	High	
Comments on intensity	The analysis of the factors in Chapter 8.2.2 should make it possible to assess an intensity class in accordance with the mining hazard guide, given the potentially damaging nature of the "flow" hazard, a limited intensity is not taken into account		

9 Conclusions

Post-mining tailings dams can generate damaging flow-type hazards, the relevance, susceptibility and intensity of which have been outlined in this report, based on literature and industry experience.

The difficulty lies in the fact that most of the structures are relatively recent, and their performance over time is relatively unknown. The evolution of climate conditions is a factor that can increase the conditions of rupture and the intensity of the phenomenon.

In addition, the areas near dams may be subject to progressive anthropisation or, contrariwise, progressive vegetation leading to the loss of knowledge of their existence.

However, the susceptibility factors for failure are relatively easy to understand in a site-specific study, although they may require further investigation; these factors have been grouped in this report into four families relating to the potential for tailings mobilisation, the potential for water accumulation, the potential for dam failure and the potential for degraded conditions in the environment.

The main source of difficulty is the assessment of the intensity of the phenomenon, i.e. the height or even the velocity of the sludge after failure. It is not easy to determine, as it combines multiple factors related to the tailings (water content, rheology of the material, etc.), to the conditions of their storage (height of the dam) and to the morphology of the terrain downstream. This document has attempted to indicate relatively simple models that allow an initial estimate of the intensity in order to be able to assess, on a specific site, whether issues may be impacted.

The tools presented here are not, by any means, an end in themselves: if a site is assessed as having a high hazard with exposed issues, specific investigations and more advanced models must be carried out.

In view of the multitude of sometimes imposing structures that are no longer in use, or for which the operator is no longer present, the question arises of the inventory of structures where such risks may arise in the coming years or decades. This risk is generally under control in mainland France where potentially dangerous structures have been identified, even if they require a certain amount of vigilance and appropriate management (surveillance, maintenance), but this does not seem to be the case in certain other European countries and in the world.

This question of prioritising sensitive sites with regard to dangerous and/or high environmental impact ruptures, allowing targeted analyses to be carried out, must be at the heart of the concerns of countries where mining is prevalent, but it must also be asked of countries where mining is declining and where accidents could occur in the future.

The management of these evolving structures over time is also an important concern. In situations where the mining operator no longer manages the structure and it becomes the responsibility of the administration, the community or private owners, depending on the local situation, uniform and shared monitoring and maintenance procedures must be established so that the structures are not forgotten and do not constitute a source of delayed danger.

10 References

10.1 Documents consulted

[1]. Agurto-Detzel H., et al., 2016. The tailings dam failure of 5 November 2015 in SE Brazil and its preceding seismic sequence. Geophysical Research Letters 43(10) : 4929-4936

[2]. Aires U. R. V., et al, 2018. Changes in land use and land cover as a result of the failure of a mining tailings dam in Mariana, MG, Brazil. Land Use Policy 70 (2018) : 63-70

[3]. https://www.aria.developpement-durable.gouv.fr/accident/39857/ (rupture du barrage de Stava, Italie)

[4]. https://www.aria.developpement-durable.gouv.fr/accident/47369/ (rupture du barrage de Fundao, Brésil)

[5]. https://www.aria.developpement-durable.gouv.fr/accident/46323/ (rupture du barrage des Montmins, Echassières, France)

[6]. https://www.aria.developpement-durable.gouv.fr/accident/26764/ (rupture de la digue Malvési, Narbonne, France)

[7]. Atkinson G. M., 2016. Analysis of ground motions from Nov. 5, 2015 earthquake sequence neaur Fundao dam, Brazil

[8]. Arrêté du 19 avril 2010 relatif à la gestion des déchets des industries extractives

[9]. Azam S, Li Q., 2010. Tailings dam failures : a review of the last one hundred years

[10]. Banu, D. M., Mihai, S., 2016. The probabilistic modeling of safety factor for mining tailing ponds. 16th International Multidisciplinary Scientific Geoconference, Sgem 2016: Science and Technologies in Geology, Exploration and Mining, Vol Ii. Sofia, Stef92 Technology Ltd: 921-928

[11]. Beebe R. R., 2001. Process considerations before and after failure of the Omai tailings dam, August 19 to 24, 1995. Warrendale, Minerals, Metals & Materials Soc

[12]. Bjelkevic A., Knutsson S, 2006. Failures and incidents at Swedish tailings dams – experiences and comparisons

[13]. Blight G. E., et al., 1983. The behavior of mine tailings during hydraulic deposition. Journal of the South African Institute of Mining and Metallurgy

[14]. BRGM, 1980. Fiches signalétiques de digues à stériles concernant quelques exploitations minières françaises. 80 SGN 433 GEG

[15]. BRGM, 2012. Caractérisation des déchets miniers de quatre mines d'or de Guyane. RP-61027-FR

[16]. BRGM, 2012. Digues de barranques et de lagunes d'exploitations minières en Guyane : guide de bonnes pratiques. RP-61065-FR

[17]. Castro-Bolinaga C. F., Zavaleta E. R. Diplas P., 2014. A coupled modelling effort to study the fate of contaminated sediments downstream of the Comes Hill deposit, Virginia, USA. Sediment Dynamics from the Summit to the Sea. IAHS Publ. 367, 2014

[18]. Center for Science in Public Participation (CSP2), 2019. World mine tailings failures – from 1915. About the database. Fichier Excel associé "World-MineTailings-Failures-as-of-March-12019", https://worldminetailingsfailures.org/

[19]. Chambers D. M., Higman B., 2011. Long term risks of tailings dam failure

[20]. Chanson H, 2005. Analytical solutions of laminar and turbulent dam break wave

[21]. Code de l'environnement, articles R541-7 et R541-8

[22]. Commission Européenne, Ministère de l'Ecologie, de l'Energie, du Développement durable et de la Mer, 2009. Document de référence sur les meilleures techniques disponibles. Gestion des résidus et stériles des activités minières.

[23]. Costa, J. E., 1985. Floods for dam failures. United States Department of the Interior Geological Survey.

[24]. Davies, M. R, 2001. Impounded mine tailings: What are the failures telling us?" Cim Bulletin 94(1052): 53-59

[25]. Davies, M. P., T. E. Martin, et al, 2000. Upstream constructed tailings dams - A review of the basics. Leiden, A Balkema Publishers.

[26]. Décision n° 2000/532/CE du 03/05/00 remplaçant la décision 94/3/CE établissant une liste de déchets en application de l'article 1er, point a), de la directive 75/442/CEE du Conseil relative aux déchets et la décision 94/904/CE du Conseil établissant une liste de déchets dangereux en application de l'article 1er, paragraphe 4, de la directive 91/689/CEE du Conseil relative aux déchets dangereux

[27]. Décret 2010-369 du 13 avril 2010 modifiant la nomenclature des installations classées

[28]. Décret 2015-526 du 12 mai 2015 relatif aux règles applicables aux ouvrages construits ou aménagés en vue de prévenir les inondations et aux règles de sureté des ouvrages hydrauliques

[29]. Directive 2006/21/CE du 15 mars 2006 concernant la gestion des déchets de l'industrie extractive et modifiant la directive 2004/35/CE

[30]. Edraki, M., et al., 2014. Designing mine tailings for better environmental, social and economic outcomes: a review of alternative approaches. Journal of Cleaner Production 84 : 411-420

[31]. Eriksson, N., Adamek, P., 2000. The tailings pond failure at the Aznalcollar mine, Spain. Enviironmental Issues and Management of Waste in Energy and Mineral Production

[32]. European Commission, JRC Science for Policy Report, 2018. Best available techniques (BAT) reference document for the management of waste from extractive industries, in accordance with directive 2006/21/EC

[33]. Franca, M. J., et al., 2008. The failure of the Fonte Santa mine tailing dam (Northeast Portugal). London, Taylor & Francis Ltd

[34]. http://fundaoinvestigation.com/ (rupture barrage Fundao, Germani Mine, Brésil)

[35]. GEODERIS, 2012. Inventaire des dépôts issus des exploitations minières selon l'article 20 de la directive 2006/21/CE. Synthèse des résultats. Rapport N2012/009DE – 12NAT2120

[36]. Ginige, T., 2002. Mining waste : the Aznalcollar tailings pond failure. European Environmental Law Review

[37]. Hallman, D. S., Dorey, R., 1995. Mine tailings deposition practices, liquefaction potential and stability implications. Third International Conference on Recent Advances in Geotechnical Earthquake Engineering & Soil Dynamics

[38]. Hossain, M. S., Fourie, A., 2013. Stability of a strip foundation on a sand embankment over mine tailings. Geotechnique 63(8): 641-650

[39]. Huang., S., et al., 2014. Stability evaluation of fill dam in graphite mine tailings impoundment. Advanced materials Research Vols 1010-1012 (2014) pp 288-291

[40]. Hungr, O., 1995. A model for the runout analysis of rapid flow slides, debris flows, and avalanches. Canadian Geotechnical Journal

[41]. ICOLD, 1982. Manual on Tailings dams and Dumps. Manuel des barrages et dépôts de stériles. Bulletin 45

[42]. ICOLD, 1989. Tailings dams Safety. Guidelines. Barrages de stériles miniers. Recommandations. Bulletin 74

[43]. ICOLD, 2001. Tailngs Dams. Risk of Dangerous Occurrences. Lessons learnt from practical experiences. Bulletin 121

[44]. Ineris, 2009. Appui technique pour l'élaboration et l'actualisation de la réglementation liée à la gestion des déchets. Transposition de la Directive 2006/21/CE relative à la gestion des déchets des industries extractives. Ineris-DRS-09-103738-08175A

[45]. Ineris, 2012. Référentiels, normes et guides de bonnes pratiques concernant les ouvrages de rétention industriels de grande hauteur en matériau meuble. Ineris-DRS-10-110463-09795C

[46]. Ineris, 2013. Appui technique pour le suivi et le traitement géotechnique de la stabilité des retenues de Cotillon. Echassières (03). Ineris-DRS-13-138776-12132A

[47]. Ineris, 2014. Document pédagogique pour l'établissement de prescriptions sur les bassins de retention industriels. Version B. Ineris-DRS-13-133405-04385B

[48]. Ineris, Cerema, Geoderis, 2017. Guide de gestion du risque minier post-exploitation. INERIS-DRS-17-164640-01814A

[49]. Ineris, 2018. Guide d'évaluation des aléas miniers. Ineris 17-164640-01944A

[50]. Ineris, 2019. Eléments relatifs à la rupture du barrage minier du complexe de Corrego de Faijao, Brumadinho, Minas Gerais, Brésil. Ineris-DRS-19-178736-00915A

[51]. Ineris, 2020. Recherche documentaire sur les impacts écologiques liés aux ruptures de barrages miniers. Ineris - 200243 - 664453

[52]. International Commission on Large Dams, 1983. Deterioration of dams and reservoirs. Examples and their analyses

[53]. International Council on Metals and the Environment, 1998. Case studies on tailings management. ISBN 1-895720-29-X

[54]. Jamiolkowski, M., 2014. Soil mechanics and the observational method: challenges at the Zelazny Most copper tailings disposal facility. Geotechnique 64(8) : 590-619

[55]. Javelaud, E., Serratrice, J.-F., 2018. La liquéfaction des sols sous l'effet des séismes. Techniques de l'Ingénieur

[56]. Jeyapalan, J.K., Duncan, J.M., Seed, H.B., 1983. Analyses of flow failures of mine tailings dams

[57]. Jeyapalan, J.K., Duncan, J.M., Seed, H.B., 1983. Investigation of flow failures of mine tailings dams

[58]. Johnson, A.M., 1984. Debris flow

[59]. Jouzel, 2014. Le climat de la France au XXXIème siècle. Volume 4 Scénarios régionalisés : édition 2014 pour la métropole et les régions d'outre-mer

[60]. Ju, H. Y., et al., 2012. Analysis of Safety and Risk Factors about the Tailings Dam in the Metal Mines. Advances in Industrial and Civil Engineering, Pts 1-4. L. H. Wang and G. Xu. Durnten-Zurich, Trans Tech Publications Ltd. 594-597. 299

[61]. Kossoff D., et al, 2014. Mine tailings dams : characteristics, failure, environmental impacts, and remediation. Applied Geochemistry 51

[62]. Kourdey, A., 2002. Une approche mixte (numérique/équilibre limite) pour le calcul de stabilité des ouvrages en terre. Développement et application aux barrages et talus miniers. Mémoire de thèse de l'INPL

[63]. Li, Y., et al., 2013. The analysis of stability of mine's tailing dam based on the FLAC(3D). Advances in Civil and Industrial Engineering, Pts 1-4. L. Tian and H. Hou. Durnten-Zurich, Trans Tech Publications Ltd. 353-356. 650

[64]. Liu, R. et al, 2015. Accidental water pollution risk analysis of mine tailings in Guanting reservoir watershed, Zhangjiakou City, China. International Journal of Environmental Research and Public Health

[65]. Loupasakis, C. and G. Konstantopoulou (2010). "Safety assessment of abandoned tailings ponds: an example from Kirki mines, Greece." Bulletin of Engineering Geology and the Environment 69(1): 63-69

[66]. Lucia, P.C., Duncan, J.M., Seed, H.B, 1981. Summary of research on case histories of flow failures of mine tailings impoundments. Technology Transfer Workshop on Mine Waste Disposal Techniques, Information Circular 8857, U.S. Bureau of Mines pp. 46-53

[67]. Luino, F., De Graff, J. V., 2012. The Stava mudflow of 19 July 1985 (Northern Italy) : a disaster that effective regulation might have prevented. Natural Hazards and Earth System Sciences 12 : 1029-1044

[68]. Luminita, D. P., D. Stematiu, et al., 2014. STRUCTURAL SAFETY OF MINING TAILINGS REFLECTED IN NATIONAL AND EUROPEAN REGULATIONS. Geoconference on Science and Technologies in Geology, Exploration and Mining, Sgem 2014, Vol Iii. Sofia, Stef92 Technology Ltd: 559-566.

[69]. Lv, S. R., Lv, S. J., 2011. The discussion about the safety management of the mine tailings pond near the mine stope. Ismsse 2011. X. He, H. Mitri, N. Azizet al. Amsterdam, Elsevier Science Bv. 26. Na

[70]. Ma, S. Q., et al., 2012. Seepage-Stability Analysis of a Mine Tailings Dam in Yunnan Province Based on ANSYS. Vibration, Structural Engineering and Measurement Ii, Pts 1-3. C. Zhang and P. P. Lin. Durnten-Zurich, Trans Tech Publications Ltd. 226-228. 1406

[71]. Macias, J. L., et al., 2015. The 27 May 1937 catastrophic flow failure of gold tailings at Tlalpujahua, Michoacan, Mexico. Natural Hazards and Earth System Sciences 15(5) : 1069-1085

[72]. Mara, S., et al, 2011. NATECH events at the tailings dams – risk, hazard and vulnerability assessment. IMWA 2011

[73]. Martin, V. et al, 2015. Challenges with conducting tailings dam breach studies. Proceedings Tailings and Mine Waste

[74]. MEDDE, 2015. Référentiel technique digues maritimes et fluviales

[75]. Mei, G., 2011. Quantitative assessment method study based on weakness theory of dam failure risks in tailings dam. First International Symposium on Mine Safety Science and Engineering

[76]. Meriggi R., Del Fabbro M., Blasone E., Zilli E., 2008. Dynamic slope stability analysis of mine tailing deposits : the case of Raibl mine. AIP Conference Proceedings 1020

[77]. Ministère de l'Economie et des Finances, BRGM, Mine & Société, 2017. Exploration et exploitation minière en Guyane. Tome 8

[78]. Morgenstern N. R., Vick S. G., Viotti C. B., Watts B. D., 2016. Fundao talilings dam review panel. Report on the immediate causes of the failure of the Fundao dam

[79]. Nimbalkar, S., et al, 2018. A simplified approach to assess seismic stability of tailings dams. Journal of Rock Mechanics abd Geotechnical Engineering 10 (2018) : 1082-1090

[80]. Official Journal of the South African Coal Processing Society and the SA Flameproof Association. Tragedy at Merriespruit

[81]. Ozcan, N. T., et al., 2013. A study on geotechnical characterization and stability of downstream slope of a tailings dam to improve its storage capacity (Turkey). Environmental Earth Sciences 69(6): 1871-1890

[82]. Pastor, M., et al., 2002. Modelling tailings dams and mine waste dumps failures. Géotechnique 52, No. 8, 579-591

[83]. Pirulli, M., et al, 2017. The failure of the Stava valley tailings dams (Northern Italy) : numerical analysis of the flow dynamics and rheological properties. Geoenvironemental Disasters

[84]. Psarropoulos, P. N., Y. Tsompanakis, N., 2008. Stability of tailings dams under static and seismic loading." Canadian Geotechnical Journal 45(5): 663-675.

[85]. Quecedo, M., et al., 2004. Numerical modelling of the propagation of fast landslides using the finite element method. International Journal for Numerical Methods in Engineering 59(6) : 755-794.

[86]. Règlement (UE) n° 1357/2014 de la Commission du 18/12/14 remplaçant l'annexe III de la directive 2008/98/CE du Parlement européen et du Conseil relative aux déchets et abrogeant certaines directives

[87]. Rico, M., Benito, G., Diez-Herero, A., 2007. Floods from tailings dam failures. Journal of Hazardous Materials 154(1-3): 79-87

[88]. Rico, M., et al., 2007. Reported tailings dam failures. A review of the European incidents in the worldwide context. Journal of Hazardous Materials 152(2) : 846-852

[89]. Robertson, P. K., De Melo, L., Williams, D. J., Ward Wilson, G., 2019. Report of the Expert Panel on the Technical Causes of the Failure of Feijão Dam I

[90]. Roche, C., K. Thygesen, Baker, E., 2017. Mine Tailings Storage: Safety Is No Accident. A UNEP Rapid Response Assessment. Nairobi and Arendal, United Nations Environment Programme and GRID-Arendal: 70.

[91]. Rudolph, T., Coldewey, W. G., 2009. Implications of earthquakes on the stability of tailings dams. Ostrava, Vsb-Tech Univ Ostrava

[92]. Santamarina J. C., Torres-Cruz L. A., Bachus R. C., 2019. Why coal ash and talings dam disasters occur. Science 364 (6440) : 526-528

[93]. Shakesby, R. A., Whitlow J. R., 1991. "Failure of a mine waste dump in Zimbabwe : causes and consequences. Environmental Geology and Water Sciences 18(2) : 143-153

[94]. Song, L., et al., 2012. On the Seepage Stability of a Tailing Dam in Wushan Copper Mine. Advances in Industrial and Civil Engineering, Pts 1-4. L. H. Wang and G. Xu. Durnten-Zurich, Trans Tech Publications Ltd. 594-597. 207

[95]. Spence, K.J., 1992. Investigation of flowsides from the failure of mining tailings dams. University of Sheffield

[96]. Sun, E. et al., 2012. Tailings dam flood overtopping failure evolution pattern. International Conference on Modern Hydraulic Engineering

[97]. Swidzinski, W., et al., 2016. Stability analysis of Zelazny most tailings dam loaded by mining-induced earthquakes. Dordrecht, Springer

[98]. United Nations Environment Program, 2017. Mine tailings storage : safety is no accident. A rapid response assessment.

[99]. http://www.vale.com/EN/aboutvale/news/Pages/Clarifications-regarding-Dam-I-of-the-Corrego-do-Feijao-Mine.aspx

[100]. Vick, S. G., 1983, 1990. Planning, design and analysis of tailings dams. ISBN 0-921095-12-0

[101]. Vick, S.G, 1983. Analyses of flow failures of mine tailings dams / Investigation of flow failures of tailings dams. Discussio

[102]. Vick, S.G., 1996. Failing of the Omai tailings dam. Geotechnical News

[103]. Villavicencio, G., et al., 2016. Liquefaction potential of sand tailings dams evaluated using a probabilistic interpretation of estimated in- situ relative density. Revista De La Construccion 15(2): 9-18

[104]. www.wise-uranium.org. Chronology of major tailings dam failures

[105]. https://worldminetailingsfailures.org/. World mine tailings failures – from 1915

[106]. https://worldminetailingsfailures.org/corrego-do-feijao-tailings-failure-1-25-2019/ (page spécifique rupture du barrage de Brumadinho)

[107]. Xin, Z., et al, 2011. Study on the risk assessment of the tailings dam break. First international Symposium of Mine Safety Science and Engineering

[108]. Xu, B., Wang, Y., 2015. Stability analysis of the Lingshan gold mine tailings dam under conditions of a raised dam height. Bulletin of Engineering Geology and the Environment 74 (1): 151-161.

[109]. Yin, G. Z., G. Z. Li, et al., 2011. Stability analysis of a copper tailings dam via laboratory model tests: A Chinese case study. Minerals Engineering 24(2): 122-130

10.2 Documents quoted but not consulted

[110]. Blight, J. E., 1969. Shear stability of dumps and dams of gold mining waste. The Civil Engineering in South Africa, v. 11, p. 49-55

[111]. Breitenbach, A.J., 2010. Overview : tailings disposal and dam construction practices in the 21st century. International Conference on Talings & Mine Waste, vol 10, pp 49-57

[112]. Bryant S., Duncan J. M., Seed H. B., 1983. Application of tailing flow analyses to field conditions. US Department of Interior, Bureau of mines, Open-File Report 53-84

[113]. Caldwell J.-A., Smith A., 1985. Material considerations in the design of downstream embankments for tailing impoundments. Mining Science and Technology, Vol. 3, pp 35-49

[114]. CANMET, 1977. Pit slope manual, chapter 9 : waste embankments. Canada Centre for Mineral and Energy Technology Report 77-01, Canadian Government Publishing Centre, Ottawa

[115]. Commission Internationale des Grands Barrages, 1995. Dépôts de stériles. Transport, mise en place et décantation.

[116]. Espinace, R., Villavicencio, G., Lemus, L., 2013. The PANDA technology applied to design and operation of tailings dams. Tailings 2013 : First International Seminar on Tailings Management, Santiago

[117]. Hanks, R. W., Pratt, D.R., 1967. On the flow of Bingham plastic slurries in pipes and between parallel plates. Journal of Society of Petroleum Engineers 7 : 342-346

[118]. Hutchinson, J. N., 1986. A sliding-consolidation model for flow slides. Can. Geotech. J. 23, 115-126

[119]. ICOLD, 2006. Improving Tailings Dam Safety, Critical Aspects of Management, Design, Operation and Closure, Bulletin 139, International Commission on Large Dams-United Nations Environmental Programme, Draft December 11, 2006

[120]. Iverson, R.M., LaHusen, R.G., 1993. Friction in debris flows : inferences from large-scale flume experiments. Proceedings Conference on Hydraulic Engineering, 1604-1609, San Francisco : ASCE

[121]. Jin, M., Fread, D.L., 1997. One-dimensional routing of mud/debris flows using NWS FLDWAW model. Debris-flow hazards mitigation : Mechanics, prediction and assessment, pp. 687-696. New York : American Society of Civil Engineers

[122]. Li, W., 2006. Hydraulics Reckoner, 2nd ed. China Water and Power Press, Beijing

[123]. Pells, S., Fell, R., 2003. Damage and cracking of embankment dams by earthquake and the implications for internal erosion and piping. Proceedings of the 21st internal congress on large dams, Montreal. ICOLD, Paris Q83-R17, pp 62-29

[124]. Rickenmann, D., et al, 2003. Erosion by debris flows in field and laboratory experiments. In Debris-flow hazards mitigations : mechanics, prediction, and assessment, ed. D. Rickenmann and c. Chen, 883-894

[125]. Sarsby, R.W., 2000. Environmental Geotechnics. Thomas Telford, London

[126]. Singh, V.P., 1996. Dam breach modeling technology. Springer Science & Business Media : Dordrecht, The Netherlands

[127]. Swaisgood, JR., 2003. Embankment dam deformations caused by earthquakes. Proceedings of the 2003 Pacific conference on earthquake engineering

[128]. Takahashi, T., et al, 1992. Routing debris flows with particle segregation. Journal of Hydraulic Engineering 118 (11) : 1490-1507

[129]. Takahashi, T., 2007. Debris flows : Mechanics, predictions and countermeasures. Rotterdam : Monograph, Balkema

[130]. Thual, O., 2003. Dérivations des équations de Saint Venant. Cours Institut National Polytechnique de Toulouse.

[131]. Troncoso, J.H., 1990. Faliure risks of abandoned tailings dams. Proc. Int. Sump. On Safety and Rehabilitation of Tailings Dams, Int. Commission on Large Dams, Paris, pp 82-89

[132]. Tsushida, H., 1970. Prediction and counter measure against the liquefaction in sand deposits. Seminar Abstract In : Port Harbour Research Institute, pp 3.1-3.33

[133]. Xu, Y.Y., Qiao, Y.A., 1983. Several problems on dam breach numerical calculation, Yellow River (in Chinese)

[134]. MEDDE, 2014. Risque sismique et sécurité des ouvrages hydrauliques

ANNEXES

- Annex 1: table of the main failures, drawn up by Ineris based on data from http://www.wise-uranium.org/mdaf.html, supplemented by elements from the documents compiled (classified by continent and then by decreasing year)
- Annex 2: statistical models (extract from the Ineris report, 2009, [44])
- Appendix 3: Estimation of slope and distance travelled. Model of Lucia et al. [66] in the framework of deformable solid mechanics (extract from the Ineris report, 2009, [44])
- Annex 4: models developed in the context of fluid mechanics (extract from the Ineris report, 2009, [44])

Annex 1: table of the main failures, drawn up by Ineris based on data from http://www.wise-uranium.org/mdaf.html, supplemented by elements from the documents compiled (classified by continent and then by decreasing year)

Name	Continent	Country, Region	Year	Substance	Characteristics of the dam	Deposit properties	Downstream properties	Fault properties	Main causes mentioned	Consequences	Comments	Sources consulted	Details online
Kokoya	AFR	Liberia	2017	Gold				11,500 m3 of tailings mobilised	Geomembrane failure / overflow after heavy rainfall	Contaminated water resource and river		Wise-uranium.org	
Nchanga	AFR	Zambia	2006	Copper				Rupture of a pipeline leading from the plant to settling		Very acid tailings contaminating the river. Water consumption prohibited for residents downstream		Wise-uranium.org	
Merriespruit	AFR	South Africa	1994	Gold	Circular retention, downstream method, height 31 m	7 Mm3		Breach 150 m wide, 600,000 m3 of tailings and 90,000 m3 of water mobilised, distance travelled 2 km, 400 m wide	Overflow following a storm, insufficient freeboard, slope instability and liquefaction	17 dead	Inactive deposit	SA Mining World, Davies 2001, Rico et al 2007, Wise-uranium.org	
Arcturus	AFR	Zimbabwe	1978	Gold	Circular retention, height 25 m, slopes 38 to 42°.	Rise of the deposit 1.6 m/year		55 m wide breach, 21,000 m3/30,000 tonnes mobilised, distance travelled 300 m, average slope 2°.	Intense rainfall exceeding the capacity of the vertical drainage, inadequate basal drainage requiring pipes to be driven into the dykes beforehand. Base relief bringing water to the central part of the reservoir (highest part), steep slope of the side dykes, saturation of these dykes	1 fatality		Shakesby, 1991, Rico et al, 2007	
Bakofeng	AFR	South Africa	1974	Platinum	Circular retention, upstream method, height 20 m	13 Mm3	1° slope	3Mm3 mobilised, distance travelled 600 m Final slope 1.3°	Erosion due to concentrated percolation	12 dead, river affected and transport over 45 km		Lucia et al 1981, Wise-uranium.org, Rico et al 2007	
Mufulira	AFR	Zambia	1970	Copper	Upstream method			Around 1 Mt mobilised	Liquefaction of tailings	89 miner dead		Wise-uranium.org	
San José de Los Manzanos	AME	Mexico	2020	Lead, zinc				6000 m3 mobilised		Road, river affected, 8000 m2 of land impacted		Wise-uranium.org	
Corrego de Faijao, Brumadinho	AME	Brazil	2019	Iron	Height 87 m, raised ten times, crest length 720 m, upstream method, built 1976	11.7 million m3 stored over 249,500 m2		Failure of the upper part of the dam, bulging of the lower part and loss of structure of the whole construction	Too steep a slope of the structure, presence of tailings of a weak character near the crest, building of the upper dams on top of fine tailings of weaker character, lack of significant internal drainage which resulted in a constantly high water level in the dam, high iron content in the tailings, making them potentially very brittle in an undrained condition, high and intense regional precipitation prior to failure	249 dead, 21 missing		Wise-uranium.org, Robertson et al 2019	http://www.vale.com/EN/aboutvale/news/Pages/Clarifications-regarding-Dam-I-of-the-Corrego-do-Feijao-Mine.aspx https://worldminetailingsfailures.org/corrego-do-feijao-tailings-failure-1-25-2019/
Machadinho d'Oeste	AME	Brazil	2019	Lead					Heavy rainfall	Seven damaged bridges, 100 families isolated	Inactive dam	Wise-uranium.org	
Nossa Senhora do Livramento	AME	Brazil	2019	Gold						Distance travelled 1 to 2 km, power line affected		Wise-uranium.org	
Cobriza	AME	Peru	2019	Copper				67,188 m3 of tailings mobilised		41,574 m2 covered, river affected		Wise-uranium.org	
Barcarena	AME	Brazil	2018	Bauxite					Overflow due to heavy rainfall	Contaminated water resource		Wise-uranium.org	
Cieneguita	AME	Mexico	2018	Gold, silver				249,000 m3 of tailings and 190,000 m3 of dam material mobilised, 29 km travelled		3 dead, 4 missing		Wise-uranium.org	
Huancapati	AME	Peru	2018					80,000 m3 of tailings mobilised	Heavy rainfall	Contaminated rivers		Wise-uranium.org	
New Wales plant, Mulberry	AME	USA, Florida	2016	Phosphate				14 m funnel in the phosphogypsum where 840,000 m3 of water rushed in		Affects the Florida aquifer, a major water resource		Wise-uranium.org	
Fundao, Germano mine, Bento Rodrigues	AME	Brazil	2015	Iron	Length 500 m, height 90m			32 Mm3 mobilised	Rise, saturation and liquefaction of tailings-contaminated sands near the left abutment of the dam, failure and mobilisation of these. Low magnitude earthquakes may have contributed to the cause (effects induced by these earthquakes: preliminary deterioration/cracking of dam more likely than liquefaction of tailings)	158 houses destroyed, 19 dead Rivers contaminated over 663 km total. 15 km2 of rivers contaminated		Wise-uranium.org, Agurto-Detzel et al 2016, Morgenstern et al. 2016, Roche et al. 2017	http://fundaoinvestigation.com/ https://www.aria.developpement-durable.gouv.fr/accident/47369/
Herculano	AME	Brazil	2014	Iron						2 dead, 1 missing		Wise-uranium.org	
Mount Polley	AME	Canada, British Columbia	2014	Copper, gold				7.3 Mm3 tailings, 17 Mm3 water mobilised	Rupture of foundation	Lakes affected		Wise-uranium.org	http://www.wise-uranium.org/mdafmp.html
Buenavista del Cobre	AME	Mexico	2014	Copper				40,000 m3 of copper sulphate mobilised		River contaminated over 420 km, directly affecting 800,000 people		Wise-uranium.org	
Dan River Steam Station	AME	USA, North Carolina	2014	Coal		Coal ash		74,000 t of ash and 100,000 m3 of water mobilised	Rupture of an old drainage pipe	River contaminated		Wise-uranium.org	
Obed Mountain	AME	Canada, Alberta	2013	Coal				670,000 m3 of water and 90,000 t of sediment mobilised		Contaminated rivers		Wise-uranium.org	
Gullbridge	AME	Canada	2012	Copper				50 m breach				Wise-uranium.org	
Huancavelica	AME	Peru	2010					21,420 m3 mobilised		Rivers contaminated over 110 km		Wise-uranium.org	
Barracena	AME	Brazil	2009	Bauxite					Overflow of drainage systems after heavy rain			Wise-uranium.org	
Kingston fossil plant	AME	USA, Tennessee	2008	Coal		Coal ash		4.1 Mm3 mobilised	Rupture of the retaining wall	1.6 km2 covered (thickness 1.80 m). 12 houses damaged		Wise-uranium.org	
Mirai	AME	Brazil	2007	Bauxite				2 Mm3 mobilised	Heavy rainfall	4000 residents left homeless. Reduced water supply for some towns		Wise-uranium.org	
Bangs Lake	AME	USA, Mississippi	2005	Phosphate				64,350 m3 mobilised	Too rapid an increase in retention capacity, high rainfall			Wise-uranium.org	
Pinchi Lake	AME	Canada, British Columbia	2004	Mercury	Height 12 m, length 100 m			6000 to 8000 m3 of red sludge mobilised	Restoration work	Lake affected			
Riverview	AME	USA, Florida	2004	Phosphate	Height 30 m	570,000 m3		227,000 m3 of acid water mobilised	Hurricane Frances	River and bay contaminated		Wise-uranium.org	

Name	Continent	Country, Region	Year	Substance	Characteristics of the dam	Deposit propertie	Downstream properti	Fault properties	Main causes mentioned	Consequences	Comments	Sources consulted	Details online
Cerro Negro	AME	Chile	2003	Copper				50,000 tonnes mobilised, 20 km travelled	Failure of the dam	River contaminated		Wise-uranium.org	
Sebastiao das Aguas Claras	AME	Brazil	2001	Iron						6 km covered by tailings, 2 dead, 3 missing		Wise-uranium.org	http://www.wise-uranium.org/mdafsa.html
Inez	AME	USA, Kentucky	2000	Coal				950,000 m3 of coal tailings sludge dumped, 120 km travelled	Rupture of underground mine workings under the deposit	Contaminated rivers		Wise-uranium.org	http://www.wise-uranium.org/mdafin.html
Pinto Valley	AME	USA, Arizona	1997	Copper				230,000 m3 mobilised		16 hectares covered		Wise-uranium.org	
Mulberry Phosphate	AME	USA, Florida	1997	Phosphate		Phosphogypsum stockpile		Phosphogypsum stockpile 200,000 m3 of process water mobilised		River biotope eliminated		Wise-uranium.org	
El Porco	AME	Bolivia	1996	Zinc, lead, silver				400,000 tonnes mobilised	Breach following heavy rain	300 km of river contaminated		Wise-uranium.org, Kossoff et al 2014	
Amatista	AME	Peru	1996		Upstream method			Over 300,000 m3 of tailings mobilised, distance travelled 600 m	Liquefaction due to earthquake	River affected		Wise-uranium.org	
Omai	AME	Guyana	1995	Gold	Upstream method, height 45 m			4.2 Mm3 mobilised of which 2.9 reached the river, 4.5 m3/s	Rupture of an old filling pipe at the base of the dam, cavities created and water intrusion. Rise in the water table and sudden mobilisation of a sand filter and then the rest of the dam	River pollution over 80 km		Wise-uranium.org, Vick, 1996, Beebe, 2001	http://www.wise-uranium.org/mdgr.html
Tapo Canyon	AME	USA	1994		Upstream method, height 24 m			60 m breach, distance travelled 180 m	Magnitude 6.7 earthquake			Rico et al 2007, Rudolph et al 2009	
Fort Meade	AME	USA, Florida	1994	Phosphate				76,000 m3 of water		River affected		Wise-uranium.org	
Hopewell Mine	AME	USA, Florida	1994	Phosphate				1.9 Mm3 of water mobilised		River affected		Wise-uranium.org	
IMC-Agrico	AME	USA, Florida	1994	Phosphate					Sinkholes in phosphogypsum			Wise-uranium.org	
Payne Creek Mine	AME	USA, Florida	1994	Phosphate				6.8 Mm3 of water mobilised		500,000 m3 affecting a river		Wise-uranium.org	
Marsa	AME	Peru	1993	Gold	Upstream method				Overflow	6 victims		Davies 2001, Wise-uranium.org	
Gibsonton	AME	USA, Florida	1993	Phosphate								Wise-uranium.org	
Fording Greenhills	AME	Canada, British Columbia	1992					200,000 m3 mobilised, distance travelled 700 m	Snowmelt, sandy-gravelly layers at the foot with low permeability, which have drained poorly and liquefied			Pastor et al 2002	
Sullivan	AME	Canada, British Columbia	1991	Lead, zinc	Height 21m, upstream method, slopes 2.5H/1V to 3H/1V			Height 12 m, length 300 m, 75,000 m3 of material mobilised. Displacement of the foot from 15 to 45 m. Distance travelled 100 m	Liquefaction of the foundation. Dynamic overloads related to the building site			Davies 2000, Wise-uranium.org	
Stancil	AME	USA	1989	Sand and gravel	Upstream method, height 9 m	74,000 m3		38,000 m3 mobilised, distance travelled 100 m	Saturation of the reservoir after heavy rainfall			Rico et al 2007, Wise-uranium.org	
Riverview	AME	USA, Florida	1988	Phosphate					Acid spill			Wise-uranium.org	
Tennessee Consolidated n°1	AME	USA, Tennessee	1988	Coal				250,000 m3 mobilised	Drainage pipe rupture and internal erosion			Wise-uranium.org	
Montcoal n°7	AME	USA, Virginia	1987	Coal				87,000 m3, Distance travelled 80 km	Ruptured drainpipe			Wise-uranium.org	
Itabirito	AME	Brazil	1986		Gravity method, height 30 m			100,000 m3 mobilised, distance travelled 12 km	Rupture of dam wall?			Rico et al 2007, Wise-uranium.org	
Cerro Negro n°4	AME	Chile	1985	Copper	Multi-method, height 40 m	2 Mm3		500,000 m3, Distance travelled 8 km	Liquefaction due to earthquake			Rico et al 2007, Wise-uranium.org	
Veta del Agua n°1	AME	Chile	1985	Copper	Multi-method, height 24 m	700,000 m3		280,000 m3 mobilised, distance travelled 5 km				Rico et al 2007, Wise-uranium.org	
Olinghouse	AME	USA, Nevada	1985	Gold				25,000 m3 mobilised, distance travelled 1.5 km	Dam saturation failure			Wise-uranium.org	
Ages	AME	USA, Kentucky	1981	Coal				96,000 m3 of "coal slurry", distance travelled 1.3 km	Heavy rain	1 dead, 33 houses destroyed or damaged		Wise-uranium.org	
Phelps-Dodge	AME	USA, New Mexico	1980	Copper	Upstream method, height 66 m	2.5 Mm3		2 Mm3 mobilised, 8 km travelled	Rapid dam building, high pore pressure, breach created			Rico et al 2007, Wise-uranium.org	
No name	AME	Canada, British Columbia	1979					40,000 m3 of water	Erosion channel phenomenon			Wise-uranium.org	
Church Rock	AME	USA, New Mexico	1979	Uranium				400,000 m3 of tailings mobilised	Differential settlement of the foundation	Radioactive water, river contaminated over 110 km		Wise-uranium.org, Kossoff et al 2014	
Homestake	AME	USA, New Mexico	1977	Uranium				30,000 m3 mobilised	Tailings pipeline rupture			Wise-uranium.org	

Name	Continent	Country, Region	Year	Substance	Characteristics of dam	Deposit propertie	Downstream properti	Fault properties	Main causes mentioned	Consequences	Comments	Sources consulted	Details online
Silverton	AME	USA, Colorado	1975					116,000 tonnes mobilised		River affected and pollution over 160 km		Wise-uranium.org	
Mike Horse	AME	USA, Montana	1975	Lead, zinc				150,000 m3 mobilised	Heavy rain			Wise-uranium.org	
Galena Mine	AME	USA	1974		Upstream method, height 9 m			3800 m3 mobilised, 610 m travelled				Rico et al 2007	
Deneen Mica	AME	USA, North Carolina	1974	Mica				38,000 m3 mobilised	Heavy rain	River affected		Wise-uranium.org	
No name	AME	USA	1973	Copper	Upstream method, height 43 m	500,000 m3		170,000 m3 mobilised, distance travelled 25 km		Tailings transported over 25 km		Wise-uranium.org	
Buffalo Creek	AME	USA, Virginia	1972	Coal	Three dams, upstream method, height 14-18 m	Massive amount of water 500,000 m3 retained		Gradual failure of three dams. 500,000 m3 mobilised Turbulent flow. Flow of 1.4 m3/s. Distance travelled 64 km	Spill	125 dead, 500 houses destroyed		Wahler et al [in Costa 1988], Jeyapalan et al 1983, Rico et al 2007, Wise-uranium.org	
Chungar	AME	Peru	1971						Magnitude 4.8 earthquake, landslide and torrent of mud	Sludge sweeping over stone floors and entering the mine shafts. Only 25 miners survived		Rudolph et al 2009	
Fort Meade	AME	USA, Florida	1971	Phosphate	Height 4 m			8 Mt mobilised	Cause unknown	River polluted up to 120 km from the site		Lucia, Wise-uranium.org	
Fort Meade	AME	USA, Florida	1967	Phosphate				250,000 m3, 1.8 Mm3 of water		River pollution		Wise-uranium.org	
East Texas	AME	Texas	1966	Gypsum	Height 11 m	7 Mt, non-plastic silt, D50 of 0.07 mm, average moisture content 30%	No slope	Approx. 100,000 m3/200,000 tonnes mobilised, 300 m distance travelled in 60-120 s, speed 2.5 - 5 m/s. Final slope 1°	Instability and leakage of drains, Infiltration			Kleiner 1976, Lucia et al 1981, Jeyapalan et al 1983, Rico et al 2007	
Bellavista	AME	Chile	1965	Copper	Circular retention, height 20 m	450,000 m3		70,000 m3, distance travelled 800 m	Earthquake			Wise-uranium.org, Rico et al 2007	
Cerro Negro n°3	AME	Chile	1965	Copper	Upstream method, height 20 m	500,000 m3		85,000 m3, distance travelled 5 km	Earthquake			Wise-uranium.org, Rico et al 2007	
El Cobre New Dam	AME	Chile	1965	Copper				350,000 m3, distance travelled 12 km	Earthquake, liquefaction			Wise-uranium.org	
El Cobre Old Dam	AME	Chile	1965	Copper	Upstream method, height 35 m	4.25 Mm3		1.9 Mm3, distance travelled 12 km	7.1 magnitude earthquake, liquefaction	Over 300 dead		Wise-uranium.org, Rico et al 2007, Rudolph et al 2009	
La Patagua New Dam	AME	Chile	1965	Copper	Circular retention, height 15 m			35,000 m3, distance travelled 5 km	Earthquake, liquefaction			Wise-uranium.org, Rico et al 2007	
Los Maquis	AME	Chile	1965	Copper	Upstream method, height 15 m	43,000 m3		21,000 m3, distance travelled 5 km	Earthquake, liquefaction			Wise-uranium.org, Rico et al 2007	
Almivirca	AME	Peru	1962						Heavy rain, earthquake, liquefaction			Wise-uranium.org	
Dos Estrellas, Tlalpujahua	AME	Mexico	1937	Gold	Wooden wall. Upstream method	Clayey (7-10%clay) and sandy (7-38%fine sand) silts		Estimated 2.5 M m3 mobilised (material and water), estimated velocity 20-25 m/s, estimated maximum flow 8000 m3/s. Distance greater than 11 km	Exceptional rainfall, saturated tailings, and dam failure	300 dead		Davies, 2001, Macias et al, 2015	
Barahona	AME	Chile	1928	Copper	Height [61,65] m		9° slope	Opening 500 m wide, 2.8 Mm3 mobilised	Liquefaction due to magnitude 8.3 earthquake?	54 dead		Lucia et al 1981, Rudolph et al 2009	
San Ildfonso, Potosi	AME	Bolivia	1626	Silver, mercury						Around 4000 dead		Kossoff et al, 2014	
Tieli	ASI	China	2020	Molybdenum				2.53 million m3 mobilised	Settling tower failure, release of water and tailings through a drainage tunnel	River affected after 3 km. Pollution spread reaches 208 km (4/04/2020). Threat to drinking water resources of 68,000 people		Wise-uranium.org	
Hpakant	ASI	Myanmar	2020	Jade				Ruptured waste in a lake causing a mud wave	Significant rainfall	126 dead (staff)		Wise-uranium.org	
Muri	ASI	India	2019	Bauxite						Railway line affected, number of victims unknown		Wise-uranium.org	
Hpakant	ASI	Myanmar	2019	Jade						3 workers killed, 54 missing		Wise-uranium.org	
Tonglvshan	ASI	China	2017	Copper, gold, silver, iron				200 m breach/crevasse, 200,000 m3 of tailings mobilised		2 dead, 1 missing		Wise-uranium.org	
Mishor Rotem	ASI	Israel	2017	Phosphate				Phosphogypsum dam failure, 100,000 m3 of acid water mobilised		Dry river contaminated over 20 km		Wise-uranium.org	
Dahegou Village	ASI	China	2016	Bauxite				2 Mm3 of red sludge mobilised		Village submerged, 300 residents evacuated		Wise-uranium.org	
Antamok	ASI	Philippines	2016	Gold				50,000 m3 of tailings mobilised	Presence of underground tunnels or mine structures into which tailings have spilled	Rivers affected	Inactive mine	Wise-uranium.org	
Hpakant	ASI	Myanmar	2015	Jade						At least 113 dead		Wise-uranium.org	

Name	Continent	Country, Region	Year	Substance	Characteristics of dam	Deposit properties	Downstream properties	Fault properties	Main causes mentioned	Consequences	Comments	Sources consulted	Details online
Zangezur	ASI	Armenia	2013	Copper, Molybdenum					Damaged pipeline	River contaminated		Wise-uranium.org	
Padcal Mine	ASI	Philippines	2012	Copper, gold				20.6 Mt mobilised	Heavy rainfall	Contaminated rivers		Wise-uranium.org	
Mianyang City	ASI	China	2011	Manganese					Landslide due to heavy rainfall	Residential houses damaged, 272 people evacuated, river contaminated, 200,000 people without water supply		Wise-uranium.org	
Huayuan County	ASI	China	2009	Manganese	Capacity 50,000 m3					3 dead		Wise-uranium.org	
Taoshi, Xiangfen County	ASI	China	2008	Iron				190,000 m3 mobilised, 2.5 km travelled, 36 hectares submerged	Heavy rainfall	277 dead, many houses and infrastructures buried	Illegal mine	Wise-uranium.org, Mei 2011, Ju et al 2012	
Western Group	ASI	China	2007					540,000 m3 mobilised	Failure of the dam	13 dead		Ju et al 2012	
Miliang, Zhenan	ASI	China	2006	Gold	Upstream method				Failure during the sixth raising of the dam	17 dead, 40 houses buried, 130 people evacuated, river contaminated over 5 km		Wise-uranium.org, Yin et al 2011	
San Marcelino	ASI	Philippines	2002		Two dams				Overflow and failure of the spillway following heavy rainfall	Rivers contaminated Villages evacuated	Abandoned dams	Wise-uranium.org	http://www.wise-uranium.org/mdafsm.html
Dachang, Nandan	ASI	China	2000	Tin	Upstream method				Failure of the dam	29 dead, 100 missing Over 100 houses destroyed		Wise-uranium.org, Yin et al 2011, Ju et al 2012	
Placer	ASI	Philippines	1999	Gold				700,000 tonnes of cyanide tailings	Damaged concrete nozzle, tailings carryover	17 houses buried		Wise-uranium.org	
Marcopper	ASI	Philippines	1996	Copper	Pit			1.6 Mm3 mobilised	Mobilisation of waste rock in old drainage tunnels	18 km of river affected by tailings		Wise-uranium.org	
Surigao del Norte	ASI	Philippines	1995	Gold	Upstream method			50,000 m3 mobilised	Magnitude 6.2 earthquake damaging the internal structure of the dam. Rupture of foundation	12 dead, coastal pollution		Wise-uranium.org, Davies, 2001, Rudolph et al 2009	
Longjiaoshan	ASI	China	1994	Iron	Upstream method				Storm	28 dead		Yin et al 2011, Ju et al 2012	
Xinye	ASI	China	1994	Copper					Overflow failure	26 dead		Ju et al 2012	
YongFu	ASI	China	1994	Tin					Digging in the sand below the dam	13 dead		Ju et al 2012	
Padcal n°2	ASI	Philippines	1992	Copper				80 Mt mobilised	Rupture of foundation			Wise-uranium.org	
Jinduicheng	ASI	China	1988	Molybdenum	Upstream method			700,000 m3 mobilised	Obstruction of spillways, overflow	Around 20 victims		Davies 2001, Wise-uranium.org	
Huangmeishan	ASI	China	1986	Iron	Upstream method			840,000 m3 tailings and water mobilised	Infiltration/slope instability	19 victims		Davies 2001, Ju et al 2012, Wise-uranium.org	
Dongpo	ASI	China	1985						Overflow failure	46 dead		Ju et al 2012	
Niujiaolong	ASI	China	1985	Copper	Upstream method				Overflow failure	49 dead		Yin et al, 2011	
Sipalay	ASI	Philippines	1982	Copper				28 Mt mobilised	Instability of the clay foundation			Wise-uranium.org	
Mochikoshi n°1 and 2	ASI	Japan	1978	Gold	Upstream method, three small dams, heights 28 m and 19 m		20° slope	Failure of 2 of the 3 dams. 83,000 m3 mobilised, 8 km travelled Final slope 1.5°	Slope instability, earthquake?	1 fatality, river and bay polluted up to 30 km from the site		Lucia et al 1981, Rico et al 2007, Wise-uranium.org	
Hokkaido	ASI	Japan	1968		Upstream method, height 12 m	300,000 m3		90,000 m3, distance travelled 150 m	Earthquake, liquefaction			Wise-uranium.org, Rico et al 2007	
Huogudu	ASI	China	1962	Tin	Upstream method			3.3 Mm3 tailings and 380,000 m3 of water mobilised		171 dead, 13,970 people affected		Yin et al 2011, Ju et al 2012	
Echassières	EUR	France, Allier	2015	Tungsten				Breach 30 m wide and 15 m high. Entire water body emptied		Waterways affected	Post-mine situation	ARIA database	https://www.aria.developpement-durable.gouv.fr/accident/46323/
Sotkamo	EUR	Finland	2012	Nickel				Gypsum pond leak through funnel-shaped hole		River contaminated		Wise-uranium.org	
Kolontar	EUR	Hungary	2010	Bauxite				700,000 m3 of red sludge mobilised	Shear failure due to increased interstitial pressure	Several cities affected, 10 persons killed		Wise-uranium.org	http://www.wise-uranium.org/mdafko.html https://www.aria.developpement-durable.gouv.fr/fiche_detaillee/39047/
Karamken	EUR	Russia	2009	Gold				Over 1 Mm3 of water, 155,000 m3 of tailings and 55,000 m3 of dam material mobilised	Heavy rain	At least one fatality, 11 houses swept away		Wise-uranium.org	http://www.sric.org/enr/docs/2009-09-07_KaramkenDamBreak.pdf
Fonte Santa	EUR	Portugal	2006		Height 25 m, volume 4500 m3, built in "as-dug " material	D50 = 0.0186 mm, 12.5 Mm3 tailings	Very narrow valley over 350 m	80-90%of dam washed away. 230,000 m3 of water mobilised, 1600 m3 of sludge. Maximum water height 5.5 m near the dam. Bank erosion up to 380 m from the dam. Overall impact distance 2500 m	Exceptional rainfall, obstruction of the spillway, overflow and creation of a breach. Material intake at the foot of the dam for local construction needs		Mining complex abandoned over 30 years before the failure	Franca et al 2008	
Malvési	EUR	France, Aude	2004	Uranium		Settling and evaporation tank of a treatment plant		30,000 m3 of liquid mobilised	Significant rainfall	High concentration of nitrates in a nearby canal for several weeks		Wise-uranium.org	http://www.wise-uranium.org/mdafma.html https://www.aria.developpement-durable.gouv.fr/accident/26764/

Name	Continent	Country, Region	Year	Substance	Characteristics of the dam	Deposit properties	Downstream properties	Fault properties	Main causes mentioned	Consequences	Comments	Sources consulted	Details online
Partizansk	EUR	Russia	2004	Coal	Enclosure dam	20 M m3 of Coal ash		50 m opening in dam, 160,000 m3 of ash mobilised		River contaminated		Wise-uranium.org	http://www.sric.org/mining/docs/Partizansk%20Coal%20Ash%20Dam%20Break%20and%20Spill.pdf
Aurul	EUR	Romania	2000	Gold					Overflow due to heavy rainfall	River 5.2 km away affected, then confluence		Davies 2001	
Baia Mare	EUR	Romania	2000	Gold	Upstream method, height 7 m	800,000 m3		100,000 m3 mobilised, 180 m travelled	Rupture at the summit following heavy rainfall	Contaminated river and drinking water (2 million Hungarians affected)		Wise-uranium.org, Rico et al 2007	https://www.aria.developpement-durable.gouv.fr/fiche_detaillee/17265/ http://www.wise-uranium.org/mdafbm.html
Borsa	EUR	Romania	2000					22,000 tonnes of heavy metal-rich tailings mobilised	Heavy rainfall	Contaminated rivers		Wise-uranium.org	
Aitik	EUR	Sweden	2000	Copper					Insufficient permeability of the drain	2.5 M m3 discharged into the settling pond, subsequently, to maintain the stability of the dyke, 1.5 M m3 discharged into the environment		Wise-uranium.org	http://www.wise-uranium.org/mdafai.html https://www.aria.developpement-durable.gouv.fr/accident/21970/
Aznalcollar	EUR	Spain	1998	Zinc, lead, copper, silver	Circular retention, downstream method, height 27 m	15 M m3 on the day of the accident		1.3 M m3 mobilised	Fracture in the marl bedrock created by interstitial overpressure	River and ground pollution. Cost of cleaning USD 25 million, closure of unmobilised tailings USD 37 million, purchase of fruit crop USD 10 million		Eriksson 2000, Rico et al 2007, Kossoff et al 2014	http://www.wise-uranium.org/mdaflf.html
Huelva	EUR	Spain	1998	Phosphate				50,000 m3 of acidic water disseminated	Storm			Wise-uranium.org	http://www.wise-uranium.org/ptail.html#HUELVA
Maritsa Istok 1	EUR	Bulgaria	1992	Ash				500,000 m3 mobilised	Flooding of the settling strand			Wise-uranium.org	
Stava	EUR	Italy	1985	Fluorine	Upstream method, height 25m and 34m, two superimposed dams, external slope 1.2 to 1.5H/1V	300,000 m3	Average slope 10°	185,000 m3 of liquefied tailings mobilised, of which 47.6% was solid particles. Speed reached 60 km/h. Downstream devastated over 4.2 km and 43.5 ha, sludge thickness 20 to 40 cm.	Settlement leading to pipe leakage and loading of the upper dam. Slope instability of the upper dam, overflow and failure of the lower dam. Significant rainfall recorded two days before the failure and throughout the previous winter (aggravating but not triggering factor)	269 victims, 62 buildings destroyed, 8 bridges destroyed	No stability testing in the previous 20 years	Davies 2001, Rico et al 2007, Pirulli et al 2017, Luino 2012, Wise-uranium.org	https://www.aria.developpement-durable.gouv.fr/accident/39857/ http://www.wise-uranium.org/mdafst.html
Balka Chuficheva	EUR	Russia	1981	Iron				3.5 M m3 mobilised, 1.3 km travelled				Wise-uranium.org	
Zlevoto	EUR	Yugoslavia	1976	Lead, zinc				300,000 m3 mobilised	Water table height and percolation in the dam	Nearby river affected		Wise-uranium.org	
Madjarevo	EUR	Bulgaria	1975	Lead, zinc, gold				250,000 m3 mobilised	Overload on settling/drainage structures due to a higher dam height than planned			Wise-uranium.org	
Brunita	EUR	Spain	1972	Zinc, lead				70,000 m3 mobilised	Heavy rain	1 fatality		Wise-uranium.org	
Bilbao	EUR	Spain	1969					115,000 m3	Heavy rain, liquefaction			Wise-uranium.org	
No name	EUR	United Kingdom	1967	Coal				4 hectares covered				Wise-uranium.org	
Mir, Sgorigrad	EUR	Bulgaria	1966	Lead, zinc, copper, silver	Upstream method, height 45 m	1.52 M m3		[220 000, 450 000] m3, distance travelled 6-8 km	Intense rainfall, rising water level and/or rupture of diversion channel	488 dead		Wise-uranium.org, Rico et al 2007	
Geising/Erzgebirge	EUR	German Democratic Republic	1966	Tin				70,000 m3	Collapse of the diversion tunnel below the dam	River polluted up to the Elbe and Hamburg		Wise-uranium.org	
Derbyshire	EUR	United Kingdom	1966	Coal				30,000 m3, Distance travelled 100 m	Rupture of foundation			Wise-uranium.org	
Aberfan	EUR	United Kingdom, Wales	1966	Coal	Height 37 m-67 m ?		12° slope	162,000 m3, 190,000 tonnes mobilised, distance travelled 600 m in 120 s, speed 4.5 - 9 m/s	Intense rainfall, liquefaction at base, surface erosion	144 dead		[32, Jeyapalan], Lucia, Wise-uranium.org, www.nuff.ox.ac.uk/politics/aberfan/home.htm, Pastor et al. 2002	https://www.nuff.ox.ac.uk/politics/aberfan/home.htm
Tymawr	EUR	United Kingdom	1965	Coal				Distance travelled 700 m	Overflow failure			Wise-uranium.org	
Tymawr	EUR	United Kingdom	1961	Coal				Distance travelled 800 m				Wise-uranium.org	
Aberfan	EUR	United Kingdom, Wales	1944	Coal	Height 46 m		12° slope	Distance travelled 610m, final thickness 4 m				Lucia	
Abercynon	EUR	United Kingdom, Wales	1939	Coal	Height 37 m		12° slope	180,000 tonnes mobilised, distance travelled 610m, final thickness 6 m				Lucia	
Cadia	OCE	Australia	2018	Gold, copper					Two 2.7 magnitude earthquakes one day earlier?			Wise-uranium.org	
Golden Cross	OCE	New Zealand	1995	Gold		3 M tons						Wise-uranium.org	
Olympic Dam	OCE	Australia	1994	Copper, uranium				Tailings leak for more than two years				Wise-uranium.org	

Annex 2: Statistics models (extract from the Ineris report, 2009, [44])

The first category of models presented is that using the tools of statistical description and prediction. In the case of the flood wave generated following the failure of a retention dyke, the random variables of the statistical problem are as much the known characteristics of the dyke as those sought from the flood wave. In this context, statistical models consist of relationships between the different random variables, obtained by analysing samples of values of these variables.

In theory, the samples should be obtained by repeating the same experiment (repeated breaches of a control dyke in a standard environment), where the random variables are changed and measured while the other characteristics remain constant. In practice, the samples are made up of historical accident cases and the theoretical requirement is to assume that all the retention dykes used to construct the sample are comparable and differ only in the random variables listed. This assumption is very strong since it implies determining a priori the most important variables in order to reference them. These predominant variables, as well as the variables involved in the dangerousness criterion, must also be available in the reviews. In general, it seems that:

- Geometric variables, the initial height of the dyke, the volume of stored tailings, the distance travelled by the flood wave or the slope of the natural terrain, are often available since they characterise configurations at rest and are easily measured;
- variables such as flow rate and velocity are difficult to access since they characterise the transient phenomenon which has not necessarily been observed or measured;
- variables characterising the physical properties of the tailings, such as water content or granulometry, should be fairly easily accessible if the structure were instrumented. Nevertheless, they are not included in the statistical models presented.

On the other hand, statistical models are more reliable and accurate the more observations are included in the sample. In practice, referenced cases of retention dyke failures are rare.

Nevertheless, leaving aside the expected low accuracy and the strong assumptions necessary for a robust theoretical foundation, statistical models have the clear advantage of being mostly simple to use. Indeed, the proposed relationships between the variables are classically of the affine, logarithmic or exponential type and therefore do not require very significant computing resources.

In this section, the statistical models of Rico et al. [88] and Costa [23] are presented and three practical relationships are explained from the two models.

Presentation of the model proposed by Rico et al.

Rico et al. analysed a sample of 29 tailings or water retention dyke failures, listed in Table 20, for which the following geometric parameters were listed:

- height of the dyke H *(in metre);*
- the total volume of tailings and/or water contained in the reservoir V *(in* $10^6 m^3$*);*
- the volume of tailings and/or water mobilised by the flow V_{mob} *(in* $10^6 m^3$*);*
- the distance travelled by the flood wave D *(in km).*

An interesting piece of information in the table is the design of the dykes, depending on whether they are ring dykes or dykes built using the upstream, central or downstream methods. This information was not used in the analysis by Rico et al. [88].

Table 20: List of the 29 cases of retention dyke failure used by Rico et al. [88]

Historical tailings dam failures used in the correlation analysis

Ref. no.	Name of the dam	Date of failure (year)	Type of dam	Dam height (m)	Impoundment volume ($\times 10^6$ m^3)	Run-out distance (km)	Dam factor ($H \times V_F$)	Released volume ($\times 10^6$ m^3)
1	Arcturus (Zimbawe)	1978	RING	25	1.7–2.0 Mt	0.3	0.5	0.0211
2	Bafokeng (South Africa)	1974	RING	20	13	45	60	3
3	Baia Mare (Romania)	2000	UPS	7	0.8	0.18	0.7	0.1
4	Bellavista (Chile)	1965	RING	20	0.45	0.8	1.4	0.07
5	Buffalo Creek (USA)	1972	UPS	14–18	0.5	64.4	7–9	0.5
6	Cerro Negro No.3 (Chile)	1965	UPS	20	0.5	5	1.7	0.085
7	Cerro Negro No.4 (Chile)	1985	MXSQ	40	2	8	20	0.5
8	Churchrock (USA)	1979	WR	11	0.37	96.5–112.6	4.07	0.37
9	Cities Service (USA)	1971	WR	15	12.34	120	135	9
10	El Cobre Old Dam (Chile)	1965	UPS	35	4.25	12	66.5	1.9
11	Galena Mine (USA)	1974	UPS	9		0.61	0.034	0.0038
12	Gypsum Tailings Dam (USA)	1966	UPS	11	7 Mt	0.3	0.88–1.43	2×10^5t
13	Hokkaido (Japan)	1968	UPS	12	0.3	0.15	1.08	0.09
14	Itabirito (Brazil)	1986	Gravity	30		12	3	0.1
15	La Patagua New Dam (Chile)	1965	RING	15		5	0.525	0.035
16	Los Frailes (Spain)	1998	RING	27	15–20	41	53.51	4.6
17	Los Maquis (Chile)	1965	UPS	15	0.043	5	0.315	0.021
18	Merriespruit (South Africa)	1994	RING	31	7.04	2	18.6	2.5 Mt
19	Mochikoshi No.1 (Japan)	1978	UPS	28	0.48	8	2.24	0.08
20	Mochikoshi No.2 (Japan)	1978	UPS	19		0.15	0.057	0.003
21	Ollinghouse (USA)	1985	WR	5	0.12	1.5	0.125	0.025
22	Omai (Guyana)	1995	WR	44	5.25	80	184.8	4.2
23	Phelps-Dodge (USA)	1980	UPS	66	2.5	8	132	2
24	Sgurigrad (Bulgaria)	1966	UPS	45	1.52	6	9.9	0.22
25	Stancil (USA)	1989	UPS	9	0.074	0.1	0.342	0.038
26	Stava (Italy)	1985	RING	29.5	0.3	4.2	5.605	0.19
27	Tapo Canyon (USA)	1994	UPS	24		0.18		
28	Unidentified (USA)	1973	UPS	43	0.5	25	7.31	0.17
29	Veta del Agua N°1 (Chile)	1985	MXSQ	24	0.7	5	6.72	0.28

RING: ring dyke; WR: water retention; UPS: dams subsequently raised upstream; MXSQ: dam comprising different raising typology (upstream, centreline and downstream); H: dam height; V_F: volume of tailings released.

Rico et al. [88] only looked for expressions linking variables in pairs. For each pair, the approach was to perform a linear regression between the neperian logarithms of the variables. This approach is explained in the following section.

Application of the approach to an example

In this section, the approach of Rico et al. [88] is explained for the couple distance travelled by the flood wave *D (in km)* / height of the dyke x volume of mobilised tailings HxV_{mob} *(in km.10⁶m³)*.

Obtaining the expressions

The different pairs of values *(HxV_{mob}; D)* have been plotted on the graph in Figure 56 in logarithmic scales.

The regression line is drawn as a solid line and the equation is:

$$\ln(D) = 0.66 \ln(HV_{mob}) + 0.476$$

The exponential function is then applied to the equation and the following relationship is determined between the variables:

$$D = 1.61\ (HV_{mob})^{0.66}$$

Rico et al. [88] also dotted the graph with a straight line that is the major component of the set of points (ignoring the points corresponding to hydraulic dams). By applying the exponential function in the same way, Rico et al. [88] put forward an envelope curve with equation:

$$D = 12.46\ (HV_{mob})^{0.79}$$

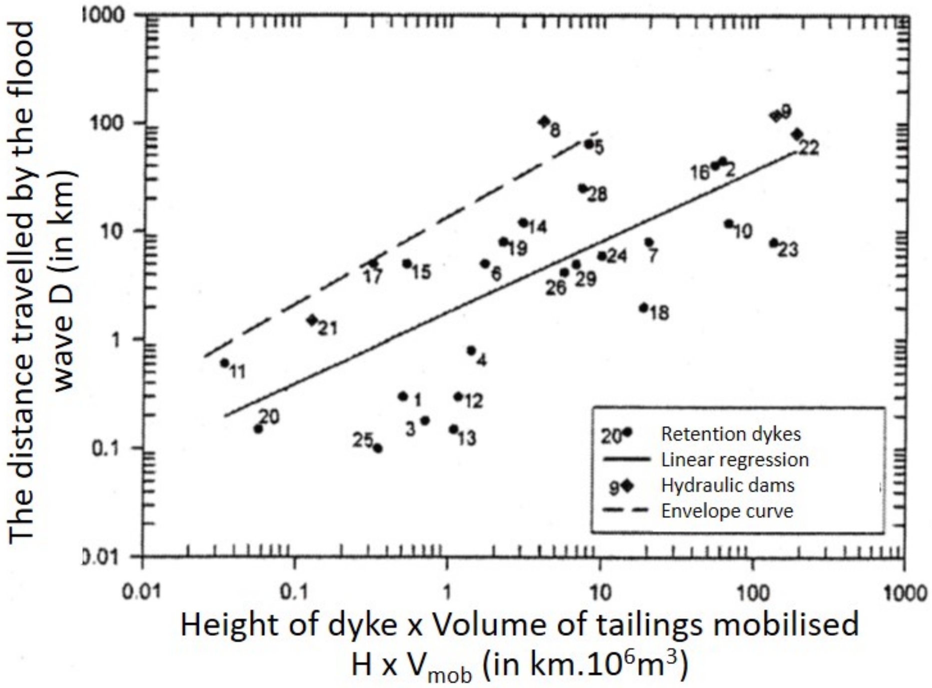

Figure 56: Logarithmic scale plot with the different pairs of values (HxV_{mob}; D) from Table 20, the linear regression line as a solid line and the envelope curve as a dashed line, (Rico et al. [88])

Quality of the estimation

The quality of the estimate from the two expressions is not discussed by Rico et al. [88] but we have assessed it taking into consideration several important elements.

For the expression derived from a linear regression, intended to estimate a mean value, the regression coefficients r and the coefficient of determination r² related to the linear regression line are:

$$r = 0.75 \ et \ r^2 = 0.57$$

The regression is based on 27 cases drawn from the initial list and the number of degrees of freedom is therefore 25. In this case, for a 95% confidence level, the Pearson coefficient is equal to 0.381. The regression coefficient r is greater than this value and is therefore significant. In other words, the hypothesis of a linear correlation between $\ln(HxV_{mob})$ and ln(D) is valid on the sample. Nevertheless, the dispersion of the points around the line is important and the variance is only explained at 57% (r² value) by the linear regression model. In practical terms, this means that the distance can be estimated from the expression but the uncertainty can be significant. On the other hand, since the exponential function is applied to the linear relationship, the deviations will be even larger. For these reasons, we have judged the quality of the estimate to be low using this expression.

For the expression from a majoring line, intended to estimate a maximum value, you can expect to obtain very large envelope values when applying this formula because the exponential function is applied to the linear relationship. In the end, we judged the quality of the estimate to be average using this expression.

Synthesis of the relationships proposed by Rico et al.

Using a similar approach to the one explained earlier, Rico et al. [88] suggest four relationships and four envelope curves for the following pairs of parameters:

1. distance travelled by the flood wave *D (in km)* / height of the dyke *H (in m)*;
2. distance travelled by the flood wave *D (in km)* / volume of mobilised residue V_{mob} *(in* $10^6 m^3$*)*;
3. distance travelled by the flood wave *D (in km)* / height of the dyke x volume of tailings mobilised HxV_{mob} *(in* $km.10^6m^3$*);*

4. volume of mobilised tailings V_{mob} *in* $(10^6 m^3)$ / total volume of tailings in the reservoir *V in* $(10^6 m^3)$.

The expressions for the four curves are given in Table 21. For the pair of mobilised tailings volume V_{mob} *in* $(10^6\ m^3)$ / total tailings volume contained in the tank *V in* $(10^6\ m^3)$, the envelope curve is not defined from a graph. Instead, Rico et al. [88] proposed in their paper that *Vmob* should be at most equal to *V*. We have evaluated the quality of each expression as a forecasting model according to the method presented earlier.

Table 21: Relationships proposed by Rico et al. [88] obtained from linear regressions.

N°	Expression obtained from the linear regression Correlation coefficient r and determination coefficient r²	Number of cases used Pearson coefficient at 95% confidence level	Quality of the estimate
1a	$D = 0.05\ H^{1.41}$ $r = 0.4$ $r^2 = 0.16$	N= 29 C_p=0.367	The correlation coefficient is borderline significant. The proposed linear model does not explain the spread of values.
2a	$D = 14.45\ V_{mob}{}^{0.76}$ $r = 0.75$ $r^2 = 0.56$	N= 26 C_p=0.388	The correlation coefficient is significant. The expected quality of the estimates from equation 2a is low.
3a	$D = 1.61\ (HV_{mob})^{0.66}$ $r = 0.75$ $r^2 = 0.57$	N= 27 C_p=0.381	The correlation coefficient is significant. The expected quality of the estimates from equation 3a is low.
4a	$V_{mob} = 0.354\ V^{1.01}$ $r = 0.93$ $r^2 = 0.86$	N= 21 C_p=0.433	The correlation coefficient is significant. The expected quality of the estimates from equation 4a is average

Table 22: Expressions of the envelope curves proposed by Rico et al. [88]

N°	Expression of the envelope curve	Quality of the estimate
1b	$D = 0.01\ H^{3.23}$	Average
2b	$D = 112.61\ V_{mob}{}^{0.81}$	Average
3b	$D = 12.46\ (HV_{mob})^{0.79}$	Average
4b	$V_{mob} = V$	Good

Presentation of Costa's model

Costa [23] studied samples of constructed dam failures and natural dams formed during landslides or by glaciers. The variables listed are:

1. Height of the dam *H (in m);*
2. the total volume of water in reservoir *V (in* $10^6\ m^3$*);*
3. the maximum measured discharge *Q (in* $m^3.s^{-1}$*).*

For each type of dam, Costa [23] put forward three relationships between the following pairs of parameters, using a method similar to that used by Rico et al. [88]:

1. maximum flow *Q (in* $m^3.s^{-1}$*)* / height of the dam *H (in m)*;
2. maximum flow rate *Q (in* $m^3.s^{-1}$*)* / reservoir volume V_{tot} *(in* $10^6 m^3$*);*
3. maximum flow rate *Q (in* $m^3.s^{-1}$*)* / dam height x mobilised tailings volume *Hx* V_{tot} *(in km.*$10^6 m^3$*)* (see Figure 57).

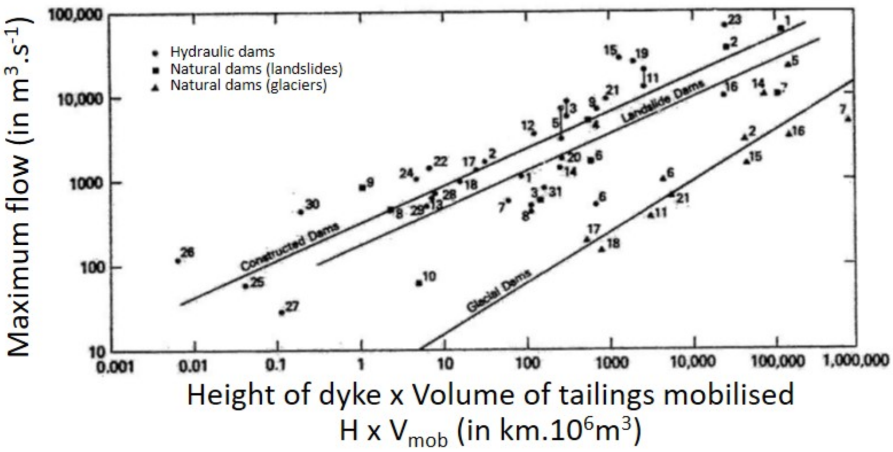

Figure 57: Graphs in logarithmic scales where the different pairs of values (HxV_{mob} , H; Q) are plotted according to the type of dams, as well as the linear regressions obtained (Costa [23])

Rico et al. [88] compared two breaches of retention dykes to the regression lines obtained by Costa [23]. Both cases were preferentially in the context of constructed dams and those created as a result of landslides. The sample of constructed dams is richer as it consists of 31 cases, compared to the 10 cases for landslide dams. The regression lines from the constructed dams increase those obtained for the natural dams. We have therefore chosen to reproduce in Table 23 the three expressions for built dams obtained by Costa [23]. We have evaluated the quality of each expression as a forecasting model according to the method presented in this annex [23].

Table 23: Linear regression relationships proposed by Costa [23]

N°	Expression obtained from the linear regression Correlation coefficient r and determination coefficient r²	Number of cases used Pearson coefficient at 95% confidence level	Quality of the estimate
5	$Q = 10.5\ H^{1.87}$ $r = 0.89$ $r^2 = 0.80$	N= 31 C_p=0.355	The correlation coefficient is significant. The expected quality of the estimates from equation 5 is average.
6	$Q = 961\ V^{0.48}$ $r = 0.81$ $r^2 = 0.65$	N= 29 C_p=0.367	The correlation coefficient is significant. The expected quality of the estimates from equation 6 is average.
7	$Q = 325\ (HV)^{0.42}$ $r = 0.86$ $r^2 = 0.75$	N= 29 C_p=0.367	The correlation coefficient is significant. The expected quality of the estimates from equation 7 is average.

Practical use of the relationships proposed by Rico and Costa

We suggest using the relationships described above to estimate the following two variables:

- the distance travelled by the flood wave D (in km), using the expressions in
-
- Table 21 and Table 22 ;
- the maximum discharge *Q (in m^3s^{-1})* using the expressions in Table 23.

Both variables are physical maxima but as random variables they have a range of variation that is important to estimate.

Establishing synthetic relationships

The relationships proposed by Rico et al. [88] can be used to estimate a mean value of the distance and the envelope curves can be used to estimate a high value. Finally, we have chosen to estimate the distance travelled by the flood wave through:

- estimating an average value of D through expressions 2a, 3a and 4a. We chose to keep the arithmetic mean of expressions 2a and 3a after injection of expression 4a[21] to have as input the total volume of stored tailings and not the volume of mobilised tailings;
- the estimation of a high value of D thanks to equations 2b, 3b and 4b. We chose to keep the maximum of expressions 2b and 3b after injecting expression 4b.

The considerations regarding the accuracy of the estimates given in this appendix do not allow us to expect a good quality estimate.

The relationships proposed by Costa [23] can be used to estimate an average value of the maximum flow rate Q. Only expressions 5 and 7 have been kept and the arithmetic mean of these two expressions has been considered. The considerations regarding the accuracy of the estimates given in this appendix do not allow us to expect a good quality estimate.

The three synthetic relationships obtained, labelled 8, 9 and 10, are summarised in Table 24.

Table 24: Synthetic expressions for the estimation of the distance travelled by the flood wave D and the maximum discharge Q from the relationships obtained by Rico et al. [88] and Costa [23]

N°	Purpose of the estimation	Expression	Quality of the estimate
8	*High value D in km*	$\max\ (112.61\ V^{0.81}; 12.46\ (HV)^{0.79})$	Low
9	*Average value D in km*	$3.28\ V^{0.76} + 0.40\ (HV)^{0.66}$	Average
10	*Average value Q in m^3s^{-1}*	$5.25\ \mathrm{H}^{1.87} + 162.50\ (\mathrm{HV})^{0.42}$	Low
H is the height of the retention dyke in m and V is the total volume of the deposit in 10^6 m^3			

Example of applying synthetic formulas

Table 25 shows the results obtained by applying the formulas from Table 24 in the case of a 10 m high retention dyke behind which 20,000 m^3 of tailings are stored.

Table 25: Example of applying synthetic relationships from Table 24

H en m	*V en $10^6 m^3$*	*High value D in km*	*Average value D in km*	*Average value in $m^3.s^{-1}$*
10	0.02	4.7	0.3	472

[21] The relationship 4a was approximated to the affine relationship: $V_{mob} = 0.354\ V$

Conclusions on the statistical models presented

The statistical models proposed by Rico et al. and Costa are simple models based on linear regressions between two variables. The analysis of these models showed that estimates could be made from these models but that the quality of the estimate was a priori low.

More complex models could be envisaged to take into account several variables (multiple regression for example) but the construction of the models would be limited a priori by the historical values available. Indeed, the predominant random variables of the flow phenomenon need to be collected downstream of the statistical analysis. Without this prior step, the improvements brought by more complex models will probably not be significant.

On the other hand, the results obtained by the statistical models presented are not satisfactory since they do not concern the height or the speed of the flood wave. In order to incorporate these random variables into the statistical models, it would be necessary to collect these values, which may be difficult.

Nevertheless, the appeal of the synthetic expressions presented in Table 24 remains undeniable in terms of how simple the expressions are to use and how accessible the input data is. Expressions 7 and 8, leading to an estimate of the distance travelled by the flow, could allow a first sorting among the retention dykes, in relation to the issues located in the estimated perimeter of influence.

Annex 3: Estimation of slope and distance travelled. Model of Lucia et al. [66] in the framework of deformable solid mechanics (extract from the Ineris report, 2009, [44])

This section discusses the basics of the model described by Lucia et al. [66], namely the general assumptions and the equation. In general, the approach used to build the model is not explained in detail. We have therefore chosen to repeat it in full, establishing the various hypotheses formulated or implied by Lucia et al. [66] and clearly explaining the system of equations to be solved.

General assumptions on the model

Lucia et al. put forward a model developed within the framework of deformable solid mechanics in which they consider the final equilibrium in two dimensions (Figure 58).

The proposed geometrical configuration of the final state of the flow is the first general assumption of the model. The schematic section is shown in Figure 59. A front (or levee) is considered at the downstream end of the flow. On the other hand, the slope formed by the tailings is assumed to be straight. The balance of forces in two dimensions on the medium considered in the final configuration constitutes the second element of the model. The balance of forces in two dimensions envisaged by Lucia et al. is shown in Figure 60. Only three forces are considered:

- the weight of the mobilised tailings;
- the frictional force at the interface between the natural terrain and the tailings;
- the thrust force exerted by the tailings upstream of the initial vertical axis of the dyke.

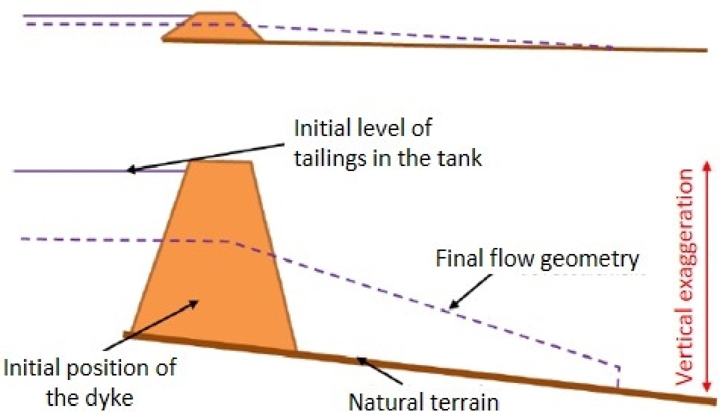

Figure 58: Schematic cross-section showing the initial and final states envisaged by Lucia et al. [66]

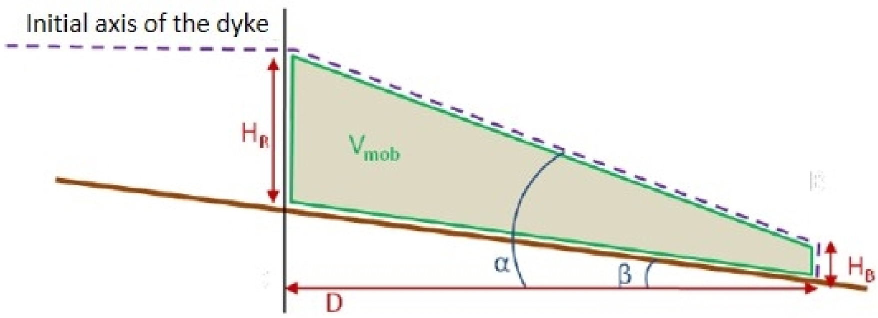

Figure 59: Typical cross-section of the final state of the flow and notations of geometric quantities

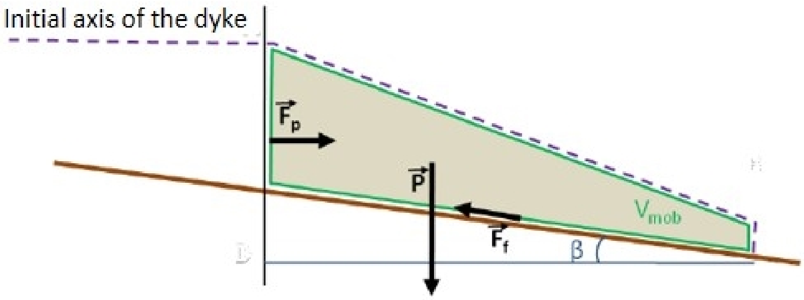

Figure 60: Balance of 2D forces on the mass of tailings mobilised in the final state of the flow, according to the assumptions of Lucia et al. [66]

The geometric and mechanical variables taken into account are listed in Table 26 and it is also specified whether they are inputs or outputs of the model. The geometric variables are marked on the drawing Figure 59.

Table 26: List of geometric and mechanical variables considered by Lucia et al.

Variable	Description	Input data	Result
	Geometric parameters		
β	Slope of the natural terrain	X	
V_{MOB}	Volume of tailings mobilised in the flow (actually a 2D surface)	X	
α	Slope of the flow in the final static equilibrium X		X
H_B	Levee height downstream of the flow X		X
H_R	Residual height at the initial location of the dyke		X
D	Distance travelled by the flow (actually the projection of this distance in the horizontal plane) X		X
	Mechanical parameters		
γ	Density of the tailings	X	
S_u	Shear stress of the tailings after flow X	X	
K_0	Earth pressure coefficient at rest X	X	

Equation setting

The problem has four unknowns (α, H_B, H_R and D) listed in Table 26, which can be related by the system of four equations shown in Table 27:

- Equation 1 comes from the expression of WBV as a function of the unknowns H_R, H_B and α;
- Equation 2 is the expression of D as a function of the unknowns H_R, H_B and α;
- Equation 3 is the projection of the force balance onto the slope axis;
- Equation 4 is a boundary condition on the stability of the downstream levee.

Equations 1 and 2 are derived from geometric considerations and are not based on any particular assumptions. Instead, assumptions are made about the thrust force exerted by the tailings upstream of the initial dyke axis and the frictional force at the interface:

- The frictional force is explained by considering S_u to be the boundary stress between the natural terrain and the tailings at the interface between the two. This assumption is moderately satisfactory since S_u is defined as an internal characteristic of the residual material;
- the thrust force is assumed to be horizontal and has two components, one of which corresponds to the thrust of a powdered soil and the other is a cohesive force again expressed with S_u. The latter assumption is moderately satisfactory since S_u is a shear stress and not a tensile one.

Similarly, the boundary condition on the stability of the downstream embankment again uses S_u as the boundary stress between the natural terrain and the tailings at the interface between the two. Improvements could be considered to clarify the role of the S_u variable.

Table 27: System of equations to solve

N°	Equation
1	$H_R = \sqrt{H_B^2 + 2 \times V_{MOB}(\tan\alpha - \tan\beta)}$
2	$D = \dfrac{H_R - H_B}{\tan\alpha - \tan\beta}$
3	$V_{MOB}\,\gamma\,\sin\beta - \dfrac{D \times S_u}{\cos\beta} + \dfrac{1}{2}K_0\gamma H_R^2\cos\beta - H_R \times S_u\cos\beta = 0$
4	$H_B = \dfrac{2S_u}{\gamma}$
Annex A specifies some intermediate calculation points.	

Observations of tailings flows in the field have allowed Lucia et al. to conclude that an equilibrium is difficult to envisage for natural slopes greater than 9°. Therefore Lucia et al. suggest using their model only for natural slopes of less than 4°.

Using the Lucia model

The analytical resolution of the system is not, a priori, easy due to the presence of non-linear relationships. Lucia et al. proposed a practical use of their method based on a graph. We preferred to solve the system of equations numerically in Visual Basic to be able to run on Excel.

Input data

The model's input data are presented in Table 28. Among these inputs, the mobilised volume V_{MOB} and the shear stress of the tailings after flow S_u seem to be the two most difficult variables to estimate.

Table 28: Model input variables.

Variable	Description	Result parameters
β	Slope of the natural terrain	
V_{MOB}	Volume of tailings mobilised in the flow (actually a 2D surface)	X
γ	Density of the tailings	
S_u	Shear stress of the tailings after flow X	X
K_0	Earth pressure coefficient at rest X	

Mobilised volume V_{MOB}

The mobilised volume V_{MOB} can be defined as a function of the total volume V_{TOT} which is a simpler input to calibrate. According to the statistical model of Rico et al. [88], V_{MOB} can be estimated to be about one third of V_{TOT}, but it seems preferable to keep the ratio V_{MOB} / V_{TOT} as a parameter of the result. The V_{TOT} input data becomes the new input data to be entered. Several methods can be used to estimate VTOT, which is a quantity in m2 in the two-dimensional geometric model, considering the two configurations in Figure 61:

- In the case of a valley dam, V_{TOT} can be estimated by V/l or by H x L_{max}. The latter estimate is safer;
- In the case of an ring dyke, V_{TOT} can be estimated by V/D_{max}.

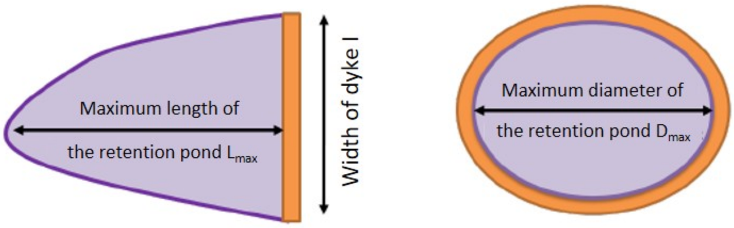

Figure 61: Plan views of a valley dam (left) and a ring dyke (right).

Ultimate shear stress S_u

The shear stress limit of the tailings after flow S_u is a difficult quantity to assess, especially as it is used in many equations. Lucia et al. have proposed values, calculated from real cases, which are reproduced in Table 29. The definition of S_u also allows this parameter to be considered similar to the threshold stress of rheological laws such as the Bingham model. Nevertheless, it seemed preferable to consider S_u as a parameter of the result.

Table 29: Feedback from 14 cases and estimation of the residual shear stress after flow (S_u), according to Lucia et al. [66].

N°	Type of residue	α (°)	S_u (kPa)
1	Copper processing tailings	1.5	2.4
2	Platinum processing tailings	1.3	0.7
3	Gypsum waste	1	1
4	Gold processing tailings	4 to 5	10.1
5	Coal waste	12	18
6	Coal waste	12	15.8
7	Coal waste	12	21.6
8	Tailings from porcelain manufacture	7	6.7
9	Tailings from porcelain manufacture	7	16.3
10	Tailings from carbide processing	1.5	2.5
11	Clay-fine sand	2.5	12
12	Fine sand	4	1
13	Fine sand	4	1.2
14	Fine sand	4	1.7

Example of the presentation of results

This section presents the results obtained using the model with the input data presented in Table 30.

Table 30: Input data used to create chart in Figure 62.

Variable	Description	Value
β	Slope of the natural terrain	2°
γ	Density of the tailings	$20kN.m^{-3}$
K_0	Earth pressure coefficient at rest X	0.5
V_{TOT}	Total volume of tailings stored behind the dyke (2D surface)	$1000m^2$

The result is provided in the form of a chart provided in Figure 62, on which it is possible to determine a value for the distance travelled by the flow as a function of the shear stress limit of the residue after flow and the ratio of the volume mobilised by the flow to the total volume.

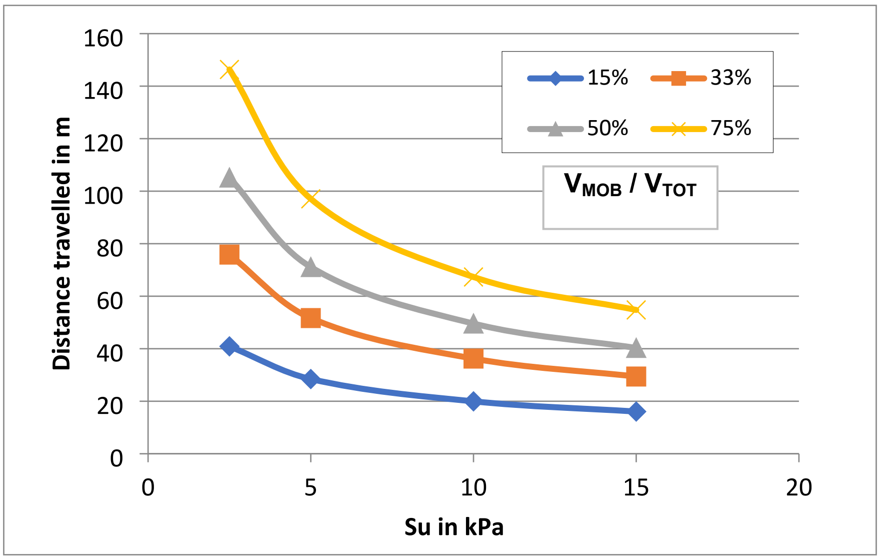

Figure 62: Chart providing the distance travelled as a function of the shear stress S_u, the ratio of mobilised volume to total volume and the input variables in Table 30.

Conclusions on the models developed in the context of deformable solid mechanics

The model presented, based on the work of Lucia et al, makes it possible to estimate the maximum distance travelled by the flood wave. The theoretical foundations of this model are satisfactory even if some assumptions could be reviewed and improved. In particular, the definition of the parameters concerning the mechanical behaviour of the tailings is important and cannot be considered as complete. The various possible improvements would probably lead to more accurate results, even if this macroscopic approach remains very rough.

The use of the model can be made simple through an implementation in Excel for example with a call to a macro in Visual Basic.

However, the output of the model presented is not entirely satisfactory as it only provides information on the distance travelled and the final height of the tailings. As already mentioned, this type of model does not allow access to the variables used in the hazard criterion since it does not address the transient regime. This is an inherent limitation of the model, which, like the statistical models presented in the previous chapter, could nevertheless be used to perform an initial sorting among the retention dykes, according to the issues located within the defined perimeter of influence.

Annex 4: Models developed in the context of fluid mechanics (extract from the Ineris report, 2009, [44])

The third category of models presented uses the framework of fluid mechanics. The moving tailings, mixed with the water initially present, can indeed under certain assumptions be assimilated to a fluid whose flow is governed by the Navier-Stokes equations. These equations describe the flow at any point in space and time and therefore allow access to the variables used in the hazard criterion. Contrary to the methods presented above, the correct equation of the problem requires more complex concepts. The theoretical aspects are recalled in the text.

First of all, the tailings-water mixture is complex and cannot be considered as a Newtonian fluid. In the context of a flood wave linked to a dyke failure, its flow regime is not known a priori either. These physical concepts are discussed below.

Secondly, the expected flood wave is a free-surface flow that has a priori a shallow depth compared to the other dimensions. The shallow area estimate, well known in hydraulics, can be used. The resulting equations are reiterated in this annex in the case of a two dimensional flow.

Finally, the equations obtained can be simplified again to have as only variables the time and the abscissa by integrating on the vertical. This approach implies new assumptions which are different depending on whether the fluid is Newtonian or not and whether the flow regime is laminar or turbulent. Several authors have finally proposed vertically integrated models based on hypotheses which constitute the specificity of their model and which are presented in this annex

Behavioural models and flow characterisation of the tailings-water mixture

The two points discussed in this section are the behavioural models used to characterise the tailings-water mixture and the laminar or turbulent nature of the flows.

Behavioural model of the tailings-water mixture

It is relatively difficult to characterise the behaviour of the tailings-water mixture which, depending on the flow velocity, can take on any state between a solid-liquid two-phase state and a visco-plastic homogeneous flow, as shown in Figure 63. The scheme is specific to tailings transport by pipe and in the case of free flow, the assumption of a homogeneous or pseudo-homogeneous flow seems relevant. In the remainder of the report, the term tailings-water fluid will therefore be used preferentially.

On the other hand, the fact that a minimum shear stress must be applied to set the tailings-water fluid in motion needs to be taken into account. The Newtonian approximation does not describe this fluid well and visco-plastic threshold laws of behaviour are therefore mainly used to describe it. The Herschel-Bulkley model relates the shear stress τ to the strain rate $\dot{\gamma}$ according to the model:

$$\tau = \tau_{seuil} + k\dot{\gamma}^{n}$$

where $\tau_{threshold}$, k and n are three parameters. The Bingham model corresponds to the special case where the power n is equal to 1, i.e. the fluid has Newtonian behaviour after the threshold. It is clear that these laws need to be calibrated in typical configurations and that, for example, the water content of the mixture probably influences the model parameters.

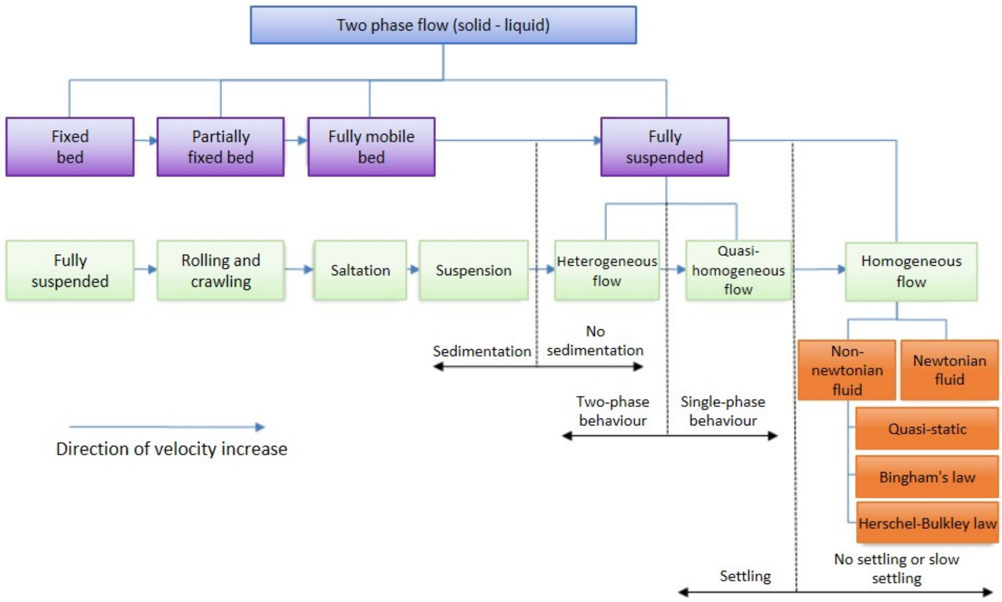

Figure 63: Classification of liquefied tailings, according to ICOLD [115].

Laminar or turbulent flow state

It is not straightforward to define, a priori, whether the flow of the tailings-water fluid will be laminar or turbulent following the dyke failure. Various observations of flows and current knowledge have led some authors to consider tailings flows as laminar even if turbulent systems have also been observed. Therefore, Jeyapalan et al. [56] differentiate in this way between phosphate tailings which, unlike other tailings, have a turbulent flow. This distinction is criticised by Vick [101] who believes that it is not straightforward to predict the nature of the flow regime for different types of tailings. For example, water content is a parameter to be taken into account and its influence could be more important than that of the type of tailings. This is essential because turbulent flow is likely to move at a much higher velocity than laminar flow, and velocity is one of the variables used in the hazard criterion. Finally, it is important to note that most of the scientific developments in fluid dynamics concern the failure of hydraulic dams and that in the case of water, the flood wave generated is a turbulent flow.

To conclude this section, it appears that both types of flow must be considered and that, to our knowledge, there are no criteria for judging, a priori, the turbulent or laminar nature of the tailings-water fluid. The water content of the material stored behind the dyke should be one of the most influential parameters in the nature of the flow, as well as the abrupt or gradual nature of the failure.

Shallow area approximations

In the case of flows with a free surface, the shallow area approximations (or Saint Venant approximation, see Thual [130]) is suitable for flows where the depth is small compared to other dimensions. Considering a two-dimensional problem defined with the variables z on the vertical and x on the horizontal, and the Saint Venant approximation, the Navier Stokes equations for an incompressible fluid become:

$conservation\ de\ la\ masse$

$$\frac{\partial u}{\partial x} + \frac{\partial w}{\partial z} = 0$$

$conservation\ de\ la\ quantité\ de\ mouvement$

$$\frac{\partial u}{\partial t} + u\frac{\partial u}{\partial x} + w\frac{\partial u}{\partial z} = -g\cos\beta\frac{\partial h}{\partial x} + g\sin\beta + v^*\frac{\partial^2 u}{\partial z^2}$$

where u and w are speeds according to x and z respectively, g is gravity and β is the terrain slope. The parameter v * is different depending on whether the type of flow studied is laminar or turbulent. In the case of turbulent flow, v* is the non-physical turbulent viscosity, which is much higher than the kinematic viscosity of the fluid. The introduction of this artificial viscosity integrates the viscosity induced by the vortices and makes it possible to consider a homogeneous velocity profile on a vertical to model the turbulent flow. This turbulent viscosity makes it easier to solve the equations in the turbulent regime. In the laminar case, the parameter v* represents the kinematic viscosity.

Integration of the equations on the vertical

The aim of the integration on the vertical is to have only two variables, the abscissa (x) and the time (t) in the equations. The solutions sought are U the average velocity on the vertical and h the fluid height. First, we will present the particular case of water, then we will look at the particular case of the tailings-water fluid and the differences induced on the integrated equations on the vertical.

The case of water, turbulent flow of a Newtonian fluid

In the case of water, the vertical integration of the simplified Navier Stokes equations according to the shallow area approximation gives the so-called 1D Saint Venant equations (see Thual [130]):

$conservation\ de\ la\ masse$

$$\frac{\partial h}{\partial t} + U\frac{\partial h}{\partial x} + h\frac{\partial U}{\partial x} = 0$$

$conservation\ de\ la\ quantité\ de\ mouvement$

$$\frac{\partial U}{\partial t} + U\frac{\partial U}{\partial x} + g\cos\beta\frac{\partial h}{\partial x} = g\sin\beta - \frac{C_f}{2}\frac{U|U|}{h}$$

where U is the average velocity on the vertical at an abscissa x and C_f is a coefficient depending on the variables U and h. The following two assumptions are required to verify the law of conservation of momentum:

1. the first assumption is that the flow velocity u is constant along the vertical and that we can therefore reason with mean U (U=u) which no longer depends on z;
2. the second assumption concerns the friction term in which the viscosity is initially involved. In the case of water, in turbulent flow, it is the turbulent viscosity that is used. Rather than determining this calculation artefact, it is entered in the coefficient C_f. Several expressions of this coefficient are described in the literature.

The analytical solution of these equations is not easy, especially because of the friction term involving the square of the mean velocity. Nevertheless, implicit relationships between the parameters can be established, if the expression chosen for the coefficient C_f is not too complicated.

Before examining the differences implied by the consideration of a non-Newtonian fluid, it is useful to recall that explicit analytical solutions exist for the simple case of turbulent flow of a Newtonian fluid in a ***frictionless channel***. These solutions, called Ritter solutions, are presented in the next two sections.

Ritter model for zero slope

The exact solutions, quoted in Chanson [20], for the velocity U and height h are as follows:

$$h = \frac{H}{9}\left(2 - \frac{x}{t\sqrt{gH}}\right)^2$$

$$U = \frac{2\sqrt{gH}}{3}\left(1 + \frac{x}{t\sqrt{gD}}\right)$$

$$avec\ -1 \leq \frac{x}{t\sqrt{gD}} \leq 2$$

with g being the gravity and H the initial height of the dyke.

When t tends to infinity, the function U(x,t) tends to $2\sqrt{gH}/3$ in the definition interval. This value is also the minimum of the U(x,t) function for t greater than 1 second. A calculation based on this limit value shows that all dykes with a height of more than 5.7cm are therefore likely to generate a flood wave with a velocity greater than $0.5 m.s^{-1}$, which is the velocity threshold used in the hazard criterion proposed by the administration. This result reflects the fact that the assumptions of a Newtonian fluid in a frictionless flow are particularly safe.

When t tends to infinity, the function h(x,t) tends to $4H/9$ in the definition interval. A calculation based on this limit value shows that all dykes with a height of more than 1.6m are therefore likely to generate a flood wave of more than 0.7m in height, which is the height threshold used in the hazard criterion proposed by the administration. This result is based on two assumptions in the model:

- the reservoir upstream of the dam is considered infinite and therefore the volume likely to flow is infinite;
- the fluid is Newtonian and therefore stability is obtained when the fluid surface is horizontal.

These two limitations are illustrated below in the case of a 10m high dyke with a 100m long reservoir (perpendicular to the dyke).

Ritter's solution for this dyke at different times after failure is shown in Figure 64. We note that 10 seconds after the rupture, the upstream edge of the reservoir is already reached and the Ritter solution is therefore no longer adequate afterwards. The time during which the solution is valid is noted t_v and the distances and heights will, a priori, be overestimated for times greater than t_v.

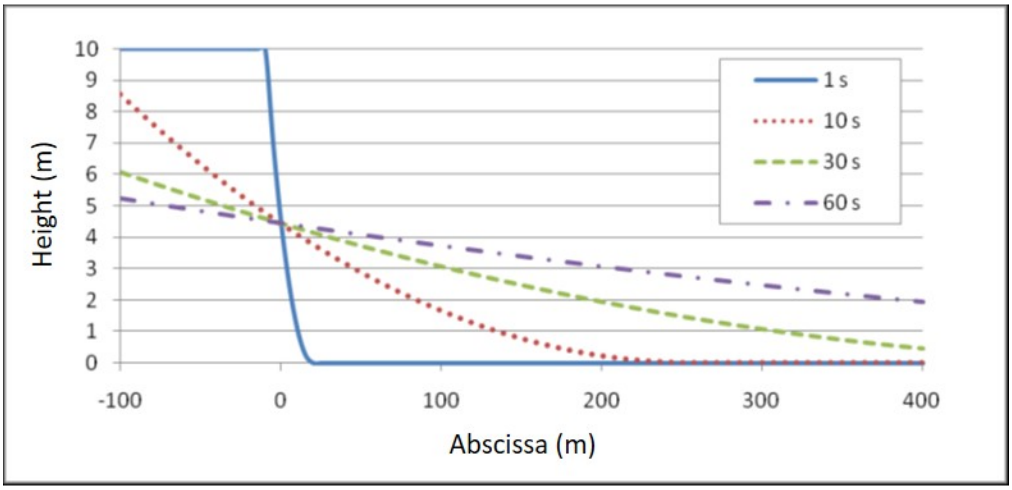

Figure 64: Ritter's solutions for a 10 m high dyke (placed at x=0) at different times after failure

The perfect character of the fluid implies a final horizontal equilibrium state. In the case of the water-residue fluid, it is conceivable that an equilibrium will form from a certain slope and time. Lucia et al. [66] have for example identified several slope values, reported in Table 15 in the main body of the report, which have been observed in tailings flows. On the basis of these values, an equilibrium slope of 1° can be considered as a minimum.

In the following, we will make the very strong assumption that the tailings-water fluid will initially flow like water but will stabilise in an equilibrium position as soon as the 1° slope criterion is exceeded[22]. The graph in Figure 65 plots the maximum slope as a function of time for a geometric configuration identical to that in Figure 65, i.e. a dyke 10m high and 100m long. The maximum slope of the flow is assessed over the interval [-100, infinity] and the time t_e where equilibrium is assumed can be estimated at 30 seconds in the example.

[22]This assumption is open to criticism as the slope is a direct result of the shape of the flow which is likely to be different in the case of a non-Newtonian fluid compared to a Newtonian fluid.

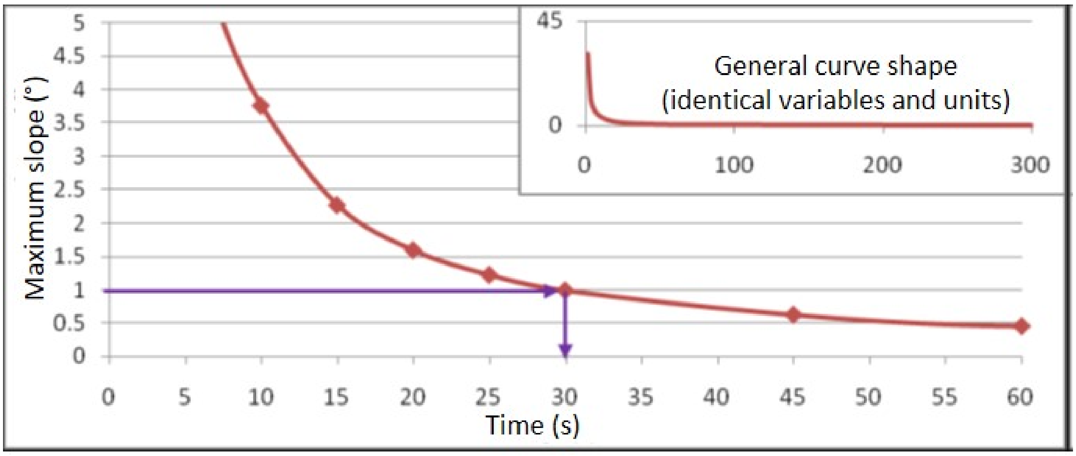

Figure 65: Maximum slope of the flow as a function of time after the failure.

It is then possible to determine for t_e how far a wave of more than 0.7m height travels, in order to take into account the danger criterion. In the example, this distance can be read from the graph in Figure 66, i.e. 358m for t_e equal to 30 seconds.

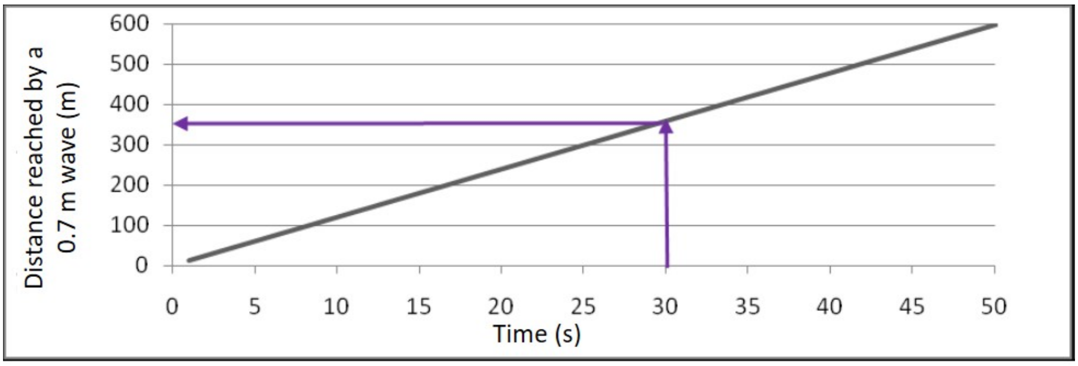

Figure 66: Maximum distance travelled by a wave of height greater than 0.7 m as a function of time.

In conclusion, if we consider a retention dyke on horizontal natural ground, Ritter's solution can be used to apply the hazard criterion concerning the water height. Even if after a very short time (10 seconds, in the example evaluated), the solution is no longer valid because the upstream edge has already been reached, it is, a priori, a major factor for the future. Contrary to a perfect fluid, it is possible to use for the residual-water fluid a stopping criterion relative to the maximum slope of the deposit. This criterion makes it possible to estimate the stopping time (30 seconds in the example for an equilibrium slope of 1°). The distance travelled by a wave of more than 0.7m in height can then be determined.

However, it is not possible to use Ritter's approach for the evaluation of the hazard criterion based on the fluid velocity since the assumptions of a perfect fluid on a frictionless ground directly lead to a velocity that is too high for realistic dyke heights.

Finally, another limitation of the approach concerns the slope of the natural terrain, which can have a significant influence. Lucia et al. [66] consider that stability cannot be achieved if the natural slope exceeds 9°. Ritter's solutions for a non-zero slope are given in the following section.

Ritter's model for a non-zero slope

The solutions, with the Ritter assumptions already mentioned in the previous sections and for an average slope of angle β are (Chanson [20]):

$$h = \frac{H}{9}\left(2 - \frac{x}{t\sqrt{gH}} + \frac{1}{2}\sin\beta\sqrt{\frac{g}{D}}t\right)^2$$

$$U = \frac{2\sqrt{gH}}{3}\left(1 + \frac{x}{t\sqrt{gD}} + \sin\beta\sqrt{\frac{g}{D}}t\right)$$

$$avec \ -1 + \frac{1}{2}\sin\beta\sqrt{\frac{g}{D}} \leq \ \frac{x}{t\sqrt{gD}} \leq 2 + \frac{1}{2}\sin\beta\sqrt{\frac{g}{D}}t$$

The method proposed in the previous section using an equilibrium criterion related to the slope of the tailings can also be considered. Using the example of a 10m high dyke with a natural slope of 2% and an equilibrium slope of 2.5%, the critical time t_e is 75 seconds and the distance over which the wave is greater than 0.7m is estimated at 1860 m.

Scenario of residual water fluid, laminar or turbulent flow of a non-Newtonian fluid

The Navier-Stokes equations as well as those obtained with the shallow media approximation are also valid for the residual-water fluid. However, different assumptions are needed to integrate correctly over the vertical:

1. in the case of turbulent flow, the assumption of a constant flow velocity along the vertical is maintained. On the other hand, in the case of a laminar flow the velocity profile is parabolic and even if it is still possible to reason with the average velocity U, this change has consequences in the mathematical expression of the problem;
2. in the case of a non-Newtonian fluid, the viscosity is not constant and it is therefore necessary to take these variations into account in the coefficient C_f which includes the notion of viscosity.

In the end, different equations can be obtained by integrating over the vertical. The different models stand out by the differences in these assumptions.

Jeyapalan et al. model

Jeyapalan et al. [56] and [57] have incorporated a Bingham model into the friction term:

$$\tau = \tau_B + \ \nu_B\dot{\gamma}$$

where τ_B and ν_B are parameters.

The approach uses Fanning's (or even Darcy's) coefficient of friction to finally express the friction term as a function of U, h and the Bingham model parameters, τ_B and ν_B, as follows:

$$\frac{C_f}{2}\frac{U|U|}{h} = g(\frac{2\nu_B\,U}{\gamma h^2} + \frac{\tau_B}{\gamma h})$$

Although the authors present their approach for a laminar flow case, the 1D equations used are those for a turbulent case. The solutions of these equations are analytical but the authors do not consider them valid for the wavefront and define specific ones. Moreover, from the moment when the maximum velocity is located upstream of the dyke axis, the authors consider that the residual water fluid solidifies. In the end, the proposed solution is not explicit and difficult to use in a simple way. Jeyapalan et al. [56] and [57] have drawn up charts that give access to the distance travelled by the flood wave.

On the other hand, one of the problems encountered by the authors is the determination of the parameters of the Bingham model. A formula is proposed linking the water content to ν_B and the term τ_B is determined from a slope stability analysis.

Chanson's model

Chanson [20] put forward implicit analytical solutions for turbulent and laminar flows. He considered a turbulent flow of a perfect fluid of the Ritter's solution type presented above with a different treatment for the front zone as illustrated in Figure 67. Different assumptions are made at the wavefront depending on whether the flow is assumed to be laminar or turbulent. These assumptions are included in the friction term.

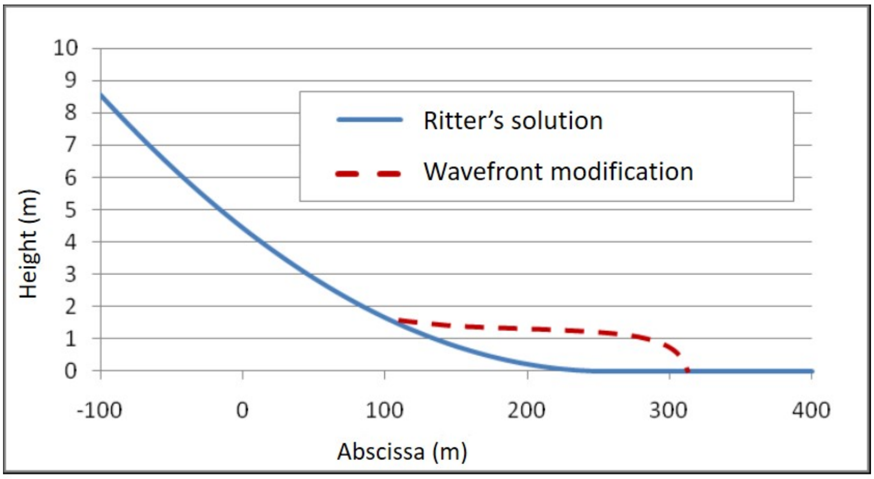

Figure 67: Principle of wavefront modification

Conclusions on the models developed in the context of fluid mechanics

To the best of our knowledge, there does not seem to be a simple model that satisfactorily predicts the flood wave of the tailings-water fluid generated by the failure of a retention dyke. Ritter's solutions, which apply to the case of a Newtonian fluid, ignoring friction, are easy and convenient to use but overestimate the speed and height. In the case of no or low slope, these equations can nevertheless give, a priori, a safe estimate of the area where the height of the tailings-water fluid is likely to be greater than 0.7m. The general approach to achieving this result is given in the flow chart in Figure 68. On the other hand, the velocity values calculated using this model are greater than the value of $0.5 m.s^{-1}$ put forward in the hazard criterion, whatever the dyke height considered. This result is induced by the hypothesis of a Newtonian fluid in a turbulent regime and the fact that friction is not taken into account.

Some ideas have been posited by different authors to take into account the laminar regime and the non-Newtonian character of the fluid in a simple way, as well as the shape of the wave front. These ideas have not led to robust and easy-to-use models.

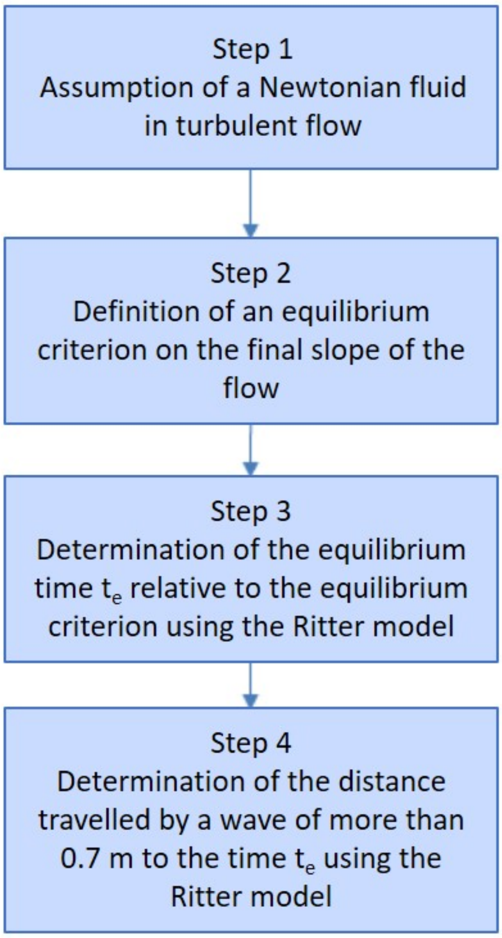

Figure 68: Flow chart showing the proposed approach to using the Ritter model

Institut national de l'environnement industriel et des risques [National Institute for the Industrial Environment and Risks]
Parc technologique Alata • BP 2 • F-60550 Verneuil-en-Halatte
03 44 55 66 77 • ineris@ineris.fr • www.ineris.fr

maîtriser le risque
pour un développement durable